Geological Survey of Israel
Ministry of Energy

Tectono-sedimentary evolution of the eastern Mediterranean after the Messinian salinity crisis: giant delta on a salt giant

Elchanan Zucker

Thesis for the degree of "Doctor of Philosophy" Submitted to the Senate of the Hebrew University of Jerusalem

This work was carried out under the supervision of:

Prof. Zohar Gvirtzman Geological Survey of Israel, Jerusalem.

Prof. Yehouda Enzel Hebrew University of Jerusalem

Report GSI/15/2023 December 2023

Acknowledgments

I would like to thank my advisors, Prof. Yehouda Enzel, Prof. Zohar Gvirtzman, and Dr. Josh Steinberg. It was a privilege to learn from their diverse set of experiences and from their honed research skills. I am thankful for the time they invested in my personal development as well as my research. Their supportive mentoring spurred my growth as a person and as a researcher. For this I am truly grateful.

My sincere gratitude goes to my lead advisor, Zohar Gvirtzman, for his advice, and true friendship throughout this entire project. He provided a wonderful learning experience in the office, in the lab, at conferences and around the globe. His passion for geology and incredible teaching methods continue to inspire me.

I would like to thank Dr. Didier Granjeon for his help with the DionisosFlow model presented here, and for always greeting me with a smile when I came to visit in Paris. His assistance and devotion to the project was phenomenal and much appreciated. I share my gratitude with Shimon Feinstein and Kul Karcz for their valuable advice and guidance during the work on this thesis. I also wish to thank Amotz Agnon, Ari Matmon, Amos Frumkin, Ronit Kessel, Nadav Lanski, Yizhaq Makovsky, Uri Schattner and Rami Weinberger, for their constructive meetings and helpful discussions along the way.

This research was supported by the Israeli Ministry of National Infrastructures, Energy and Water Resources and by the Mediterranean Research Center of Israel (MERCI).

I would like to thank my friends from the Institute of Earth Sciences at the Hebrew University and from the Geological Survey of Israel for their friendship, assistance, and counsel as well as providing me with many enjoyable hours together. They were always available to share advice or answer questions. Their friendship and support were an important part of my work.

I am also grateful to the administrative staff of the Institute of Earth Sciences at the Hebrew University. Their hard work enables the research that is led from that building while always being kind and helpful. As well, I'd like to thank the technical staff at the Geological Survey of Israel who support the research with a loving smile.

I am deeply grateful to my family and in-laws for their endless support and constant interest.

My most heartfelt gratitude goes to my loving wife, Tammi, who has stood by my side during this wonderful journey. No matter the ups and downs, she always supported my decisions and pushed me to be the best I could be. Tammi has shown me the true meaning of happiness and in doing so gave me wonderful children who are daily reminders of the power of love. To our wonderful children I give thanks for teaching me the true meaning of life through sharing valuable family experiences, love and exceptional moments of joy.

This work is dedicated to my mother who taught me that
I can do anything I put my mind to.

To my wife and children.

We are all given the same twenty-four hours in a day, it’s what
you decide to do with them that defines you

Abstract

Under the seafloor of the Mediterranean Sea lies one of Earth's salt giants deposited during the Messinian salinity crisis (MSC, 5.97-5.3 Ma) that occurred at the latest Miocene. Since its accumulation this salt giant has been buried by Pliocene-Quaternary sediments, but compared to other salt giants it is young and relatively shallow. Therefore, the Mediterranean Sea is a preferred location for studying the early stage of deformation in salt basins, which is difficult to reconstruct in older and usually highly deformed salt basins.

This study focuses on the Eastern Mediterranean with an emphasis on the Levant Basin, offshore Israel. The objective is to explore the evolution of the basin in the past 5 million years in order to understand three tectono-stratigraphic processes: the formation of a continental shelf (Levant) alongside a river delta (Nile); the interaction of a giant river delta (Nile) with an underlying salt giant (Messinian); and the interaction between turbitidy channels with salt tectonics obstacles at the present day seabed. The unique settings of the study area that contains a giant salt body, a giant river delta, and a continental shelf that is a few hundred kilometers away, but still fed by the giant delta, provides the opportunity to understand these fundamental processes which are relevant worldwide.

To study the accretion of the Levant continental shelf alongside the Nile delta I use a 3D diffusion-based, stratigraphic modeling tool (DionisosFlow) with a new module specially programmed for this study. I reexamine the existing paradigm about sediment transport and shelf-delta connection showing that alongshore sand transport is just a small part of a much larger process termed here margin-parallel sediment transport (MPST). I establish this concept and clarify its components. Sand is transported in a nearshore shallow water belt where marine currents are highly energetic. At the same time shale is transported at greater depths over the deeper shelf and the continental slope where marine currents are weaker. The modeling results show that without margin-parallel transport of silt and clay in the deeper waters, deposition offshore Israel probably would have been negligible, and the Levant shelf never would have developed. Moreover, though MPST has begun coevally with delta formation massive accretion of the Levant shelf occurred only 2-3 my later. Initially, a continental shelf formed offshore Sinai, then offshore Israel, and most recently along the Lebanon coast. The model also demonstrates a

significant lithological difference between sedimentation in front of the river's mouth and along adjacent continental margin. High energy down slope sediment transport carries sand, silt and clay, whereas margin-parallel currents are relatively weak and carry mainly silt and clay. One exception within the margin-parallel system is the highly energetic nearshore current that transport sand. Thus, I point out, MPST is an efficient differentiator between shale and sand. These modeling results contribute to the basic understanding of sediment transport, distribution, and deposition along continental margins and particularly to the connection between river deltas and adjacent shelves.

To study the interaction between the Nile Delta and the regional salt tectonics, I focused on the circum-Nile deformation belt (CNDB). The semi-radial shape of the CNDB was interpreted in previous studies as forming by salt squeezing out from under the thick Nile delta/cone. Following a synthesis of the available geophysical and drilled data and the construction of regional structural and isopach maps, I demonstrate that, in fact, the thickest part of the delta overlies a quite thin original salt section. i.e., the squeezing of salt would have had less impact on the regional deformation pattern than previously thought. Our data indicates that the squeeze-out model works only at the easternmost side of the delta, towards the Levant basin. There, differential loading over a few hundred meters thick salt, can produce the needed pressure gradient, sufficient to promote salt flow, even upslope against gradient. On the western side of the delta, towards the Herodotus basin, downslope gliding of the sediment-salt sequence is driven by pronounced gradients, enforcing contraction in the deepest part of the basin.

Following of the understanding of aspects of this salt tectonics, I focused on the influence of seabed obstacles (particularly expressions of salt tectonic ridges) on the present-day submarine channels that transport sediments on the seafloor toward the deeps of the Levant basin. In the Levant basin, numerous submarine channels around the Nile deep sea fan (NDSF) are affected by salt tectonics related to the Messinian salt giant. Initially, I applied methods developed for terrestrial morphological analysis and quantified channel sinuosity, width and slope in search for consistent relationships between these parameters and channel response to salt-tectonic obstacles. This traditional analysis did not yield robust patterns but led to other observations. To quantify these observations, I developed two new parameters characterizing the regional and local distortion of channel direction by the cumulative effect of the many obstacles generated by the salt tectonics. (a) The incident angle (α), defined as the acute angle between the regionally influenced channel direction and the strike of the individual tectonic obstacles. (b) The diversion angle (Ω), defined as the angle between the slope direction of the regional bathymetry and the average direction of the channel following its diversion by the obstacles. The values of these parameters along the channels illustrate the influence of the regional-scale basin geometry and the superimposed, tectonically influenced seabed patterns, on channel development. Hyperbolic relationships exist between incident angle (α) and diversion angle (Ω). Channels flowing approximately parallel ($\alpha \approx 0°$) to tectonic folds are (obviously) not diverted; channels nearly orthogonal ($\alpha \approx 90°$) to obstacles, cut at a point along them, right through and, again, not diverted by much. In contrast, channels with a general direction diagonal to the obstacles ($\alpha \approx 40°$), are diverted by ca. ten degrees ($\Omega \approx 10°$). Over long distances, this diversion accumulates and affects the regional development of channels around the NDSF. Noteworthy, this phenomenon of channel diversion, indirectly deteriorate normal slope-sinuosity relationships, known from terrestrial studies. These parameters can be quite easily applied in other basins, where submarine channels interact with seabed obstacles.

In Summary, this PhD research demonstrates the accretion of a continental shelf alongside a forming delta due to margin-parallel sediment transport; the salt tectonics impact on the evolution of the basin since the early Pliocene; and how salt tectonics affects the submarine transport systems that distributed sediments within the basin.

Letter of contribution

This thesis is comprised of five chapters. Chapters 1 and 5 are introduction and synthesis and conclusions, respectively. Chapters 3 & 4 were already published as peer-reviewed journal papers and Chapter 2 will be submitted with the completion of this thesis. The content of these papers and the rest of the chapters comprise this PhD dissertation, which is the result of the research done by me and the co-authors.

I am the main scientific contributor of every one of the chapters. All the formulation of research questions, literature survey, data acquisition, data analysis, processing, interpretation, conclusion, graphical and manuscript production were conducted by me under the supervision and in collaboration with my advisors and our co-authors. I am also the first author of every one of the chapters included in this work.

Dr. Josh Steinberg, who works in the industry, is a co-author in the publications of chapters 3 & 4 in which he closely advised me together with my two academic advisors.

My work on the DionisisFlow model in Chapter 2, was in collaboration with Dr. Didier Granjeon, who is the sole creator of the program and works at the IFP, France. Together we implemented new features and processes into the program. This collaboration was essential and fruitful. It assisted in developing more functions in this software, which is already preforming within the gas and oil industry. The results of our joint efforts in formulating these new models assist in answering a basic research question raised as part of my dissertation. Now it is Chapter 2, which processes, interprets, and provides valuable new insights on the evolution of the southeastern Mediterranean; it is written up by me as part of my research.

Elchanan Zucker *Zohar Gvirtzman* *Yehouda Enzel*

Table of contents

Chapter 1

Introduction

Introduction

During the late Miocene, the Atlantic-Mediterranean gateway was narrowed leading to deposition of 2-3-km-thick evaporite sequences across the Mediterranean Sea (e.g., Hsü et al., 1973; Ryan, 1973). This event, termed the Messinian Salinity Crisis (MSC), is dated to 5.97–5.33 Ma (for a review see Roveri et al., 2014 and references therein). During subsequent ~5 million years, the Messinian salt was buried by a Pliocene-Quaternary sequence and salt tectonics was initiated coeval with sedimentation. Compared with other salt giants that are deeper and older, the Mediterranean Sea is an ideal natural laboratory for exploring the early stage deformation in salt basins, which is difficult to reconstruct elsewhere (Hübscher et al., 2007).

The Eastern part of the Mediterranean Sea provides research opportunities to study three key tectono-stratigraphic processes:

(1) The interaction of a giant river delta (Nile) with an underlying salt giant. This process relates to fundamental issues concerning the forces driving salt tectonics.

(2) The formation of a continental shelf (Levant) alongside a river delta (Nile). This process relates to fundamental processes of sediment transport along continental margins.

(3) The interaction between turbitidy channels with salt tectonics obstacles. This process, observed on the present-day seabed, is a key for understanding the ancient development of such environments.

The objective of this research is to explore the evolution of the eastern Mediterranean in the past ~5 million years and shed new light on these three fundamental processes.

Geologic setting

The Levant Basin

The Levant Basin, located in the most southeastern corner of the Mediterranean Sea, is an extensional basin formed at the margins of the Neotethys Ocean during the late Paleozoic and early Mesozoic (Garfunkel, 1998; Robertson, 1998). During the Oligo-Miocene, a thick sedimentary section accumulated in the deep Levant Basin while only minor deposition occurred along its edges at the Levant continental margin (Steinberg et al., 2011; Macgregor, 2012; Bar et al., 2013; Gvirtzman et al., 2014).

Approximately 6 million years ago, towards the end of the Miocene (the Messinian stage), the Mediterranean transformed into a giant saline basin and a few km-thick salt layer was deposited on its deep seafloor (Hsü et al., 1973; Ryan, 1973, reviewed by 2009; Roveri et al., 2014). During this MSC the level of the Mediterranean Sea dropped. One of the major responses to this drop was the formation of canyons around the margins of the sea, including the 1.5 km deep gorge/canyon (termed also EoNile, Said, 1981, 1993; Abdelsalam, 2018) at the Egyptian continental margin. When normal marine conditions resumed in the early Pliocene, sediments quickly filled the Eonile canyon and propagated seaward forming the present day Nile delta and cone, which reaches a thickness of nearly 4 km (Said, 1981; Loncke et al., 2006; Mascle et al., 2006; Segev et al., 2006). The role of delta propagation in promoting salt tectonics is studied in chapter 3 of this thesis.

Alongside delta development, a continental shelf was built along the Sinai-Israel continental margin (the Levant shelf). The width of this shelf varies from 50, to 30, and to ~15 kilometers offshore Sinai, central Israel, and northern Israel, respectively, and then, narrowing to only a few km offshore Lebanon (e.g., Gvirtzman and Buchbinder, 1978; Mart et al., 1978; Almagor and Garfunkel, 1979; Goldsmith and

Golik, 1980; Ben-Avraham and Mart, 1981; Mart, 1982; Buchbinder and Zilberman, 1997; Ben-Gai et al., 2005). The relations between the Levant shelf and the Nile delta is studied in Chapter 2 of this thesis.

Salt tectonics in the Eastern Mediterranean

The unique mechanical behavior of salt that at a geological time scale behaves as a fluid (Jackson and Talbot, 1991 and references therein; Weijermars et al., 1993), greatly affected overlying sediments, and vice versa, coeval sedimentation promotes salt deformation (Gemmer et al., 2004; Brun and Fort, 2011). This produces a positive feedback, i.e., sediment loading induces subsurface salt flow, which, in turn, deforms the overlying rocks. Subsequent deposition is affected by such repeated load-controlled, near-surface deformation and so forth.

In the Levant Basin, salt tectonics was documented in numerous studies over the past four decades (Neev et al., 1976; Ben-Avraham, 1978; Ryan and Cita, 1978; Mart, 1982; Almagor and Hall, 1983; Tibor et al., 1992; Frey Martinez et al., 2005; Schattner et al., 2006; Hübscher et al., 2009; Cartwright et al., 2012; Lazar et al., 2012; Gvirtzman et al., 2013; Eruteya et al., 2016; Safadi et al., 2017; Elfassi et al., 2019; Lawal et al., 2019).

At the end of the Pliocene (~2.5 Ma), approximately 2.5 million years after the end of the MSC, highly noticeable deformation related to the subsurface salt motion has commenced (Almagor, 1984; Garfunkel and Almagor, 1984; Cartwright et al., 2012; Elfassi et al., 2019). The salt motion, over the past 2.5 million years, developed into a complex circum-Nile radial contraction domain of folds and faults (Gaullier et al., 2000; Loncke et al., 2006; Gvirtzman et al., 2015). The surface expression of the folds is quite subtle. They are tens of meters in amplitude, hundreds of meters wide, and a few kilometers long. They form a pattern of elongated obstacles on the sea floor, spacing 1.5-6 km apart. The connection between the development of the Nile delta and the circume-Nile deformation belt is studied in Chapter 3 and the interaction between salt-tectonics obstacles and turbidite channels is the focus of Chapter 4.

Dissertation outline

Chapters 1 and 5 are introduction and summary of the research, respectively.

Chapter 2 focuses on the development of the Levant continental shelf alongside the development of the Nile Delta. This chapter develops the concept of margin-parallel sediment transport (MPST) showing that alongshore sand transport at shallow waters is a small part of a larger process that transports huge amounts of clays and silts at deeper waters on and off the shelf. The model results demonstrate that the formation of the delta with properties similar to observations is possible, but with a failure to form a shelf. To form a continental shelf coevally with the evolution of the delta, we add a new MPST to the model, which then successfully generates a continental shelf with characteristics similar to observations. By doing so, this chapter aims to help understand sediment accumulation at the end of the Pliocene and up to the present-day accumulation; i.e., from sedimentation forming a delta/cone to margin-parallel sediment accumulation and Levant continental shelf formation.

Chapter 3 focuses on improving understanding and causes of salt tectonics at the circum-Nile deformation belt. The impact of salt tectonics on an evolving sedimentary basin leaves its marks. These marks can provide insights of identifying controlling mechanisms in the region. A prime example is the emphasis in previous studies of the salt squeeze-out mechanism as the dominant driver of salt tectonics in the Eastern Mediterranean. In this chapter, following the amassing of data into a much better map of the location of the salt giant and its association with the thickness of post-MSC sediments, I demonstrate that this simple squeeze-out mechanism cannot explain the distribution and asymmetry of the deformation in the Eastern Mediterranean. Therefore, the question remained (and raised here) is what can drive salt tectonics around the Nile deep sea fan? I show that, in the Eastern Mediterranean, the role of salt squeezing was overestimated. This may have been the case in other salt basins as well.

Chapter 4 focuses on the geomorphology of the submarine channels detected on the present seabed and the potential impact of salt tectonics on their courses. In the past decade, due to the expansion to the deep sea of oil and gas exploration and the importance of buried submarine channel as sediment conduits and reservoirs becoming clearer, the study of such modern channels became eminent. This study focuses on the submarine channels of the Eastern Mediterranean Sea and their relationships with the adjacent Nile deep sea fan. We show that in some cases, these channels are affected by salt tectonics that occurs within the basin.

The final chapter of this dissertation (Synthesis and Conclusions, Chapter 5) shows how each of these three chapters (Chapters 2-4) that use different approaches and the three combined, offer a regional synthesis demonstrating mutual sedimentation and salt tectonics impacts and assist in understanding the evolution of the Eastern Mediterranean since ~5 Ma.

Methods

The various issues studied here require several methods and tools. For modeling the Levant continental shelf alongside the Nile delta (Chapter 2) I used a state-of-the-art 3-D stratigraphic modeling tool, DionisosFlow that produces synthetic stratigraphy according to prescribed subsidence history, sea-level variations, sediment supply, water discharge, and sediment distribution by diffusion. Cooperation with the developer of this software at Beicip-Franlab, French Institute of Petroleum, we added a new module considering continental margin sediment transport.

For understanding the relationship between delta development and the circum-Nile deformation belt (Chapter 3) I prepared a structural map of the base Pliocene (~top salt) in the entire Eastern Mediterranean. This required compilation of published and unpublished data of thickness and depth, seismic profiles and well logs, maps and sections partly presented in TWT (sec) and partly in length units.

For analyzing the relationships between seabed obstacles and direction of turbidite channels (Chapter 4) I suggest a new morphometric analysis expressing the diversion of channel direction as a result of direction of the obstacles.

References

Abdelsalam, M.G., 2018, The Nile's journey through space and time: A geological perspective: Earth-Science Reviews, v. 177, p. 742–773, doi:10.1016/J.EARSCIREV.2018.01.010.

Almagor, G., 1984, Salt-controlled slumping on the Mediterranean slope of central Israel: Marine Geophysical Researches, v. 6, p. 227–243, doi:10.1007/BF00286527.

Almagor, G., and Garfunkel, Z., 1979, Submarine slumping in continental margin of Israel and northern Sinai: AAPG Bull, v. 63, p. 324–340, http://www.scopus.com/inward/record.url?eid=2-s2.0-0018440203&partnerID=tZOtx3y1.

Almagor, G., and Hall, J.K., 1983, Morphology of the continental margin off north central Israel: Israel Journal of Earth Sciences, v. 32, p. 75–82.

Bar, O., Gvirtzman, Z., Feinstein, S., and Zilberman, E., 2013, Accelerated subsidence and sedimentation in the Levant Basin during the Late Tertiary and concurrent uplift of the Arabian platform: Tectonic versus counteracting sedimentary loading effects: Tectonics, v. 32, p. 334–350, doi:10.1002/tect.20026.

Ben-Avraham, Z., 1978, The structure and tectonic setting of the levant continental margin, Eastern Mediterranean: Tectonophysics, v. 46, p. 313–331, doi:10.1016/0040-1951(78)90210-X.

Ben-Avraham, Z., and Mart, Y., 1981, Late Tertiary structure and stratigraphy of North Sinai continental margin: AAPG Bulletin, v. 65, p. 1135–1145.

Ben-Gai, Y., Ben-Avraham, Z., Buchbinder, B., and Kendall, C.G.S.C., 2005, Post-Messinian evolution of the Southeastern Levant Basin based on two-dimensional stratigraphic simulation: Marine Geology, v. 221, p. 359–379, doi:10.1016/j.margeo.2005.03.003.

Brun, J.P., and Fort, X., 2011, Salt tectonics at passive margins: Geology versus models: Marine and Petroleum Geology, v. 28, p. 1123–1145, doi:10.1016/J.MARPETGEO.2011.03.004.

Buchbinder, B., and Zilberman, E., 1997, Sequence stratigraphy of Miocene-Pliocene carbonate-siliciclastic shelf deposits in the eastern Mediterranean margin (Israel): effects of eustasy and tectonics: Sedimentary Geology, v. 112, p. 7–32, doi:10.1016/S0037-0738(97)00034-1.

Cartwright, J., Jackson, M.P.A., Dooley, T., and Higgins, S., 2012, Strain partitioning in gravity-driven shortening of a thick, multilayered evaporite sequence: Geological Society, London, Special Publications, v. 363, p. 449–470, doi:10.1144/SP363.21.

Elfassi, Y., Gvirtzman, Z., Katz, O., and Aharonov, E., 2019, Chronology of post-Messinian faulting along the Levant continental margin and its implications for salt tectonics: Marine and Petroleum Geology, v. 109, p. 574–588, doi:10.1016/J.MARPETGEO.2019.05.032.

Eruteya, O.E., Safadi, M., Waldmann, N., Makovsky, Y., and Ben-Avraham, Z., 2016, Seismic Geomorphology of the Israel Slump Complex in the Levant Basin (SE Mediterranean), *in* Springer, Cham, p. 39–47, doi:10.1007/978-3-319-20979-1_4.

Frey Martinez, J., Cartwright, J., and Hall, B., 2005, 3D seismic interpretation of slump complexes: examples from the continental margin of Israel: Basin Research, v. 17, p. 83–108, doi:10.1111/j.1365-2117.2005.00255.x.

Garfunkel, Z., 1998, Constrains on the origin and history of the Eastern Mediterranean basin: Tectonophysics, v. 298, p. 5–35, doi:10.1016/S0040-1951(98)00176-0.

Garfunkel, Z., and Almagor, G., 1984, Geology and structure of the continental margin off northern Israel and the adjacent part of the Levantine Basin: Marine Geology, v. 62, p. 105–131, doi:10.1016/0025-3227(84)90057-4.

Gaullier, V., Mart, Y., Bellaiche, G., Mascle, J., Vendeville, B.C., and Zitter, T., 2000, Salt tectonics in and around the Nile deep-sea fan: insights from the PRISMED II cruise: Geological Society, London, Special Publications, v. 174, p. 111–129, doi:10.1144/GSL.SP.1999.174.01.07.

Gemmer, L., Ings, S.J., Medvedev, S., and Beaumont, C., 2004, Salt tectonics driven by differential sediment loading: Stability analysis and finite-element experiments: Basin Research, v. 16, p. 199–218, doi:10.1111/j.1365-2117.2004.00229.x.

Goldsmith, V., and Golik, A., 1980, Sediment transport model of the southeastern Mediterranean coast: Marine Geology, v. 37, p. 147–175, doi:10.1016/0025-

3227(80)90015-8.

Gvirtzman, G., and Buchbinder, B., 1978, The Late Tertiary of the coastal plain and continental shelf of Israel and its bearing on the history of the Eastern Mediterranean:, file:///F:/Ph.D/Literature/Gvirtzman G. & B. Buchbinder-1978-The Late Tertiary of the coastal plain and continental shelf of Israel and its bearing on the history of the Eastern Mediterranean Initial reports of the deep sea drilling project.pdf.

Gvirtzman, Z., Csato, I., and Granjeon, D., 2014, Constraining sediment transport to deep marine basins through submarine channels : The Levant margin in the Late Cenozoic: Marine Geology, v. 347, p. 12–26, http://ac.els-cdn.com/S0025322713002296/1-s2.0-S0025322713002296-main.pdf?_tid=b3ca25b0-8f4f-11e4-9e6e-00000aab0f02&acdnat=1419853501_e004fd045a7011899e868cc54df9cc55.

Gvirtzman, Z., Reshef, M., Buch-Leviatan, O., and Ben-Avraham, Z., 2013, Intense salt deformation in the Levant Basin in the middle of the Messinian Salinity Crisis: Earth and Planetary Science Letters, v. 379, p. 108–119, doi:10.1016/j.epsl.2013.07.018.

Gvirtzman, Z., Reshef, M., Buch-Leviatan, O., Groves-Gidney, G., Karcz, Z., Makovsky, Y., and Ben-Avraham, Z., 2015, Bathymetry of the Levant basin: interaction of salt-tectonics and surficial mass movements: Marine Geology, v. 360, p. 25–39, doi:10.1016/j.margeo.2014.12.001.

Hsü, K.J., Ryan, W.B.F., and Cita, M.B., 1973, Late Miocene dessication of the Mediterranean: Nature, v. 242, p. 240–244.

Hübscher, C., Cartwright, J., Cypionka, H., DeLange, G.J., Robertson, A., Suc, J.-P., and Urai, J.L., 2007, Global look at salt giants: Eos, Transactions American Geophysical Union, v. 88, p. 177–179, doi:10.1029/2007EO160002.

Hübscher, C., Tahchi, E., Klaucke, I., Maillard, A., and Sahling, H., 2009, Salt tectonics and mud volcanism in the Latakia and Cyprus Basins, eastern Mediterranean: Tectonophysics, v. 470, p. 173–182, doi:10.1016/J.TECTO.2008.08.019.

Jackson, M.P.A., and Talbot, C.J., 1991, A glossary of salt tectonics: Bureau of Economic Geology, University of Texas at Austin.

Lawal, M., Orv, B.M., Waldmann, N., and Makovsky, Y., 2019, Seafloor Seepage Features and Subsurface Expressions of Gas Accumulations in the SE of the Levant Basin, Offshore Israel, *in* AAPG Geoscience Technology Workshop,.

Lazar, M., Schattner, U., and Reshef, M., 2012, The great escape: An intra-Messinian gas system in the eastern Mediterranean: Geophysical Research Letters, v. 39, p. 2012GL053484, doi:10.1029/2012GL053484.

Loncke, L., Gaullier, V., Mascle, J., Vendeville, B., and Camera, L., 2006, The Nile deep-sea fan: An example of interacting sedimentation, salt tectonics, and inherited subsalt paleotopographic features: Marine and Petroleum Geology, v. 23, p. 297–315, doi:10.1016/j.marpetgeo.2006.01.001.

Macgregor, D.S., 2012, The development of the Nile drainage system: integration of onshore and offshore evidence: Petroleum Geoscience, v. 18, p. 417–431, doi:10.1144/petgeo2011-074.

Mart, Y., 1982, Quaternary tectonic patterns along the continental margin of the southeastern Mediterranean: Marine Geology, v. 49, p. 327–344, doi:10.1016/0025-3227(82)90047-0.

Mart, Y., Eisin, B., and Folkman, Y., 1978, The Palmahim structure - A model of continuous tectonic activity since the Upper Miocene in the Southeastern Mediterranean off Israel: Earth and Planetary Science Letters, v. 39, p. 328–334, doi:10.1016/0012-821X(78)90018-3.

Mascle, J., Sardou, O., Loncke, L., Migeon, S., Caméra, L., and Gaullier, V., 2006, Morphostructure of the Egyptian Continental Margin: Insights from Swath Bathymetry Surveys: Marine Geophysical Researches, v. 27, p. 49–59, doi:10.1007/s11001-005-1559-x.

Neev, D., Almagor, G., Arad, A., Ginzburg, A., and Hall, J., 1976, The geology of the southeastern Mediterranean Sea: Geological Survery of Israel, p. 51, http://www.getcited.org/pub/101826857.

Robertson, A., 1998, Mesozoic-Tertiary tectonic evolution of the easternmost Mediterranean area: integration of marine and land evidence.: Proceedings of the Ocean Drilling Program, Scientific results, v. 160, p. 723–782, https://www.era.lib.ed.ac.uk/handle/1842/559.

Roveri, M. et al., 2014, The Messinian Salinity Crisis: Past and future of a great challenge for marine sciences: Marine Geology, v. 352, p. 25–58, doi:10.1016/j.margeo.2014.02.002.

Ryan, W.B.F., 2009, Decoding the mediterranean salinity crisis: Sedimentology, v. 56, p. 95–136, doi:10.1111/j.1365-3091.2008.01031.x.

Ryan, W.B.F., 1973, Geodynamic implications of the Messinian crisis of salinity, *in* Messinian events in the Mediterranean, p. 26–38.

Ryan, W.B.F., and Cita, M.B., 1978, The nature and distribution of Messinian erosional surfaces — Indicators of a several-kilometer-deep Mediterranean in the Miocene: Marine Geology, v. 27, p. 193–230, doi:10.1016/0025-3227(78)90032-4.

Safadi, M., Meilijson, A., and Makovsky, Y., 2017, Internal deformation of the southeast Levant margin through continued activity of buried mass transport deposits: Tectonics, doi:10.1002/2016TC004342.

Said, R., 1981, The Geological Evolution of the River Nile: New York, NY, Springer Science & Business Media, 153 p., doi:10.1007/978-1-4612-5841-4_1.

Said, R., 1993, The River Nile: geology, hydrology and utilization: Elsevier, 319 p.

Schattner, U., Ben-Avraham, Z., Lazar, M., and Hüebscher, C., 2006, Tectonic isolation of the Levant basin offshore Galilee-Lebanon – effects of the Dead Sea fault plate boundary on the Levant continental margin, eastern Mediterranean: Journal of Structural Geology, v. 28, p. 2049–2066, doi:10.1016/J.JSG.2006.06.003.

Segev, A., Rybakov, M., Lyakhovsky, V., Hofstetter, A., Tibor, G., Goldshmidt, V., and Ben Avraham, Z., 2006, The structure, isostasy and gravity field of the Levant continental margin and the southeast Mediterranean area: Tectonophysics, v. 425, p. 137–157, doi:10.1016/J.TECTO.2006.07.010.

Steinberg, J., Gvirtzman, Z., Folkman, Y., and Garfunkel, Z., 2011, Origin and nature of the rapid late Tertiary filling of the Levant Basin: Geology, v. 39, p. 355–358, doi:10.1130/G31615.1.

Tibor, G., Ben-Avraham, Z., Steckler, M., and Fligelman, H., 1992, Late Tertiary subsidence history of the southern Levant Margin, eastern Mediterranean Sea, and its implications to the understanding of the Messinian Event: Journal of Geophysical Research, v. 97, p. 17593, doi:10.1029/92JB00978.

Weijermars, R., Jackson, M.P.A., and Vendeville, B., 1993, Rheological and tectonic modeling of salt provinces: Tectonophysics, v. 217, p. 143–174, doi:10.1016/0040-1951(93)90208-2.

Chapter 2

The accretion of the Levant continental shelf alongside the Nile Delta by immense margin-parallel sediment transport

Elchanan Zucker[1,2], Zohar Gvirtzman[1,2], Didier Granjeon[3], Yehouda Enzel[1]

[1] *The Fredy and Nadine Herrmann Institute of Earth Sciences, The Hebrew University of Jerusalem, Jerusalem 91904, Israel*

[2] *Geological Survey of Israel, Yesha'yahu Leibowitz 32, Jerusalem, Israel*

[3] *Department of Geology-Geophysics-Geochemistry, IFP Energies nouvelles, 1 à 4 avenue de Bois, Préau, 92852 Rueil-Malmaison, France*

Marine and Petroleum Geology 126 (2021) 104876

Contents lists available at ScienceDirect

Marine and Petroleum Geology

journal homepage: www.elsevier.com/locate/marpetgeo

Research paper

The accretion of the Levant continental shelf alongside the Nile Delta by immense margin-parallel sediment transport

Elchanan Zucker [a,b,*], Zohar Gvirtzman [b,a], Didier Granjeon [c], Daniel Garcia-Castellanos [d], Yehouda Enzel [a]

[a] *The Fredy and Nadine Herrmann Institute of Earth Sciences, The Hebrew University of Jerusalem, Jerusalem, 91904, Israel*
[b] *Geological Survey of Israel, Yesha'yahu Leibowitz 32, Jerusalem, Israel*
[c] *Department of Geology-Geophysics-Geochemistry, IFP Energies Nouvelles, 1 à 4 avenue de Bois, Préau, 92852, Rueil-Malmaison, France*
[d] *Instituto de Ciencias de la Tierra Jaume Almera, ICTJA-CSIC, Barcelona, Spain*

ARTICLE INFO

Keywords:
Nile delta
Levant continental shelf
Sediment transport
Stratigraphic modeling
Sedimentation
Eastern Mediterranean
Coastal geomorphology

ABSTRACT

Following the termination of the Messinian salinity crisis ~5.3 million years ago, massive sedimentation in the Eastern Mediterranean Sea formed the huge Nile Delta. Alongside delta propagation, a continental shelf was accreted along the Levant margin. For several decades it was assumed that these two sedimentary structures were closely connected. Levant shelf deposits are composed of Nile-derived sediments and present-day measurements show that sand is currently being transported alongshore from the Nile Delta to offshore Israel. This study reexamines the existing paradigm about sediment transport and shelf-delta connection. We show that longshore sand transport is just a small part of a much larger process termed here margin-parallel sediment transport (MPST). Sand is transported in a nearshore shallow-water belt where marine currents are highly energetic. At the same time, shale is transported at greater depths over the deeper shelf and the continental slope where marine currents are weaker. To model the accretion of the Levant shelf alongside the Nile Delta we use a 3D, diffusion-based, stratigraphic modeling tool (DionisosFlow) with a new module representing MPST. Our results show that margin-parallel transport of silt and clay in the deeper waters accounts for the bulk of deposition offshore Israel and is responsible for the development of the Levant shelf. Moreover, though MPST has begun coevally with delta formation, massive accretion of the Levant shelf was delayed by 2–3 My. Initially, a continental shelf formed offshore Sinai, then offshore Israel, and most recently along the Lebanon coast. Our model also demonstrates the significant lithological differences observed between sedimentation in front of the Nile River mouth and along adjacent continental margin. High energy down-slope sediment transport carries sand, silt, and clay, whereas margin-parallel currents are relatively weak and carry mainly silt and clay. One exception within the margin-parallel system is the highly energetic nearshore current that transports sand. Thus, we point out, MPST is an efficient separator between shale and sand.

1. Introduction

The Nile Delta and its associated sedimentary cone are the largest in the Mediterranean Sea and one of the largest worldwide (Fig. 1). Five and a half million years ago, during the Messinian salinity crisis (Hsü et al., 1973; Ryan and Cita, 1978), the Mediterranean sea-level dropped and an approximately 1.5-km deep canyon (EoNile) incised into the Egyptian continental margin of the Mediterranean (Barber, 1981; Said, 1981, Fig. 2A). After this crisis, at the beginning of the Pliocene (5.3 Ma), when normal marine conditions resumed, sediments quickly filled this EoNile canyon and prograded from the canyon mouth into the open sea (Said, 1981; Sestini, 1989; Stanley and Warne, 1998). Today, after 5.3 My of progradation, the modern Nile Delta and its deep-sea fan and sedimentary cone spread ~200 km northward from the ancient canyon mouth and ~400 km in an east-west direction (Fig. 1). The thickness of the Pliocene-Quaternary (PQ) sediments building the Nile Delta and cone reaches ~4000 m at its depocenter offshore Egypt (Fig. 2B).

Alongside this PQ delta development, a continental shelf was accreted in the southeastern Mediterranean, offshore Sinai and Israel (termed here the Levant shelf, Fig. 1). The shelf deposits offshore Israel

* Corresponding author. The Fredy and Nadine Herrmann Institute of Earth Sciences, The Hebrew University of Jerusalem, Jerusalem, 91904, Israel.
E-mail address: elchanan.zucker@mail.huji.ac.il (E. Zucker).

https://doi.org/10.1016/j.marpetgeo.2020.104876
Received 30 July 2020; Received in revised form 13 December 2020; Accepted 15 December 2020
Available online 8 January 2021
0264-8172/© 2020 Elsevier Ltd. All rights reserved.

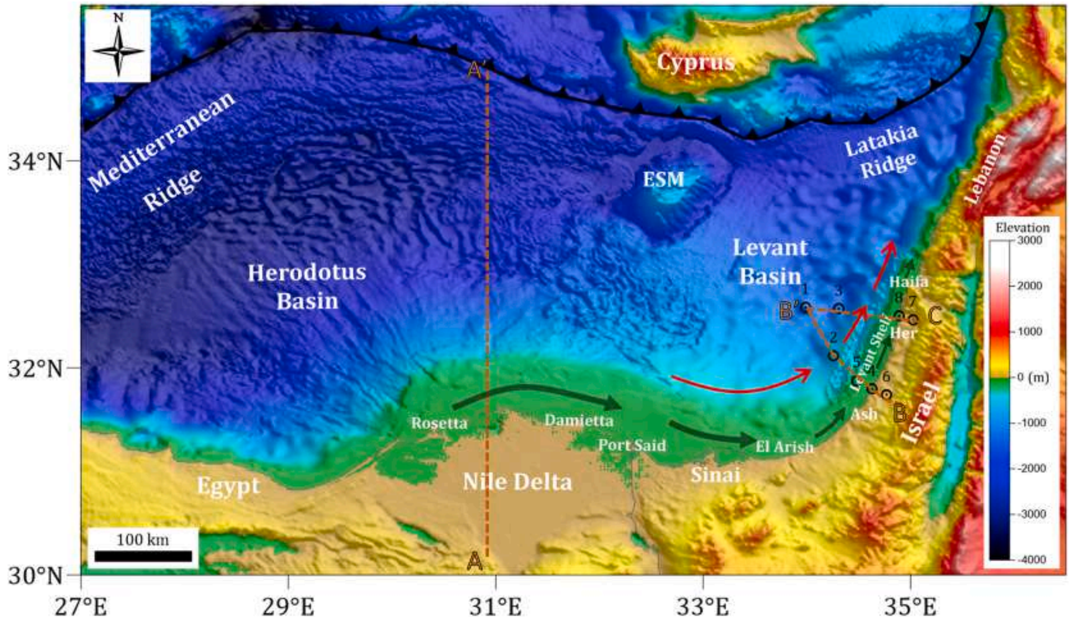

Fig. 1. Topography and bathymetry map of the Eastern Mediterranean. Her = Herzliya. Ash = Ashkelon. ESM = Eratosthenes Seamount. Black circles mark oil and gas wells: 1 = Mira, 2 = Hannah 01, 3 = Sara, 4 = Hof Ashdod 01, 5 = Yam 02, 6 = Yinnon, 7 = Maanit 01, 8 = Caesarea. Black line w/triangles mark the Hellenic–Cyprus subduction. Dashed brown lines = Locations of cross sections. Black arrows – longshore sand transport (after Inman and Jenkins, 1984). Red arrows – LJS (Levant Jet System, after Schattner et al., 2015). (For interpretation of the references to color in this figure legend, the reader is referred to the Web version of this article.)

are composed of Nile-derived sediments. It was hypothesized that the accretions of both these features are coeval (Buchbinder and Gvirtzman, 1976; Emery et al., 1960; Gvirtzman, 1970; Nachmias, 1969; Shukri, 1950; Shukri and Philip, 1960). Using sedimentological and seismic data, numerous studies support that sediment transport is in a coast-parallel direction (Buchbinder et al., 1993; Carmel et al., 1985; Davis et al., 2012; El Din and Mahar, 1997; Emery et al., 1960; Emery and Bentor, 1960; Goldsmith and Golik, 1980; Golik et al., 1999; Golik, 1993, 1997, 2002; Klein et al., 2007; Manohar, 1981; Perlin and Kit, 1999; Schattner et al., 2015; Schattner and Lazar, 2016; Shoshany et al., 1996; Stanley, 1989; Zaghloul et al., 1982; Zviely et al, 2006, 2007). In addition, present day measurements and estimations of sediment fluxes indicate that effective longshore transport delivers large amounts of sand mainly northwards along the Nile-Levant littoral cell (e.g., Rosentraub and Brenner, 2007; Zviely et al., 2007 and references within). These observations and summaries have focused most of the research for several decades on the near-shore sand transport (Fig. 1, Black arrows).

However, as new observations for the relative young age (mainly Pleistocene) of the Levant continental shelf become available (Bar, 2009; Bar et al., 2013; Ben Zeev and Gvirtzman, 2020; Elfassi et al., 2019), we question this existing view. If the Levant shelf coevolved alongside the Nile cone, why did its accretion start much later? The answer to this question presents major implications for understanding sediment transport along continental margins, in general, and particularly to the sedimentary source of the Levant shelf. Since current sediments moving over the Levant shelf do derive from the Nile Delta, what are the main controlling processes that transport sediments along the continental margin and what types of sediments are transported by these processes?

In what follows we develop, first the concept, and then the quantification of margin-parallel sediment transport (MPST) not limited to sand grain size and not limited to the nearshore belt. Earlier evidence regarding a mid-shelf mud-dominated belt shaped by oceanographic processes, were documented in the Gulf of Lions at the mouth of the Rhone River (Rabineau et al., 2005; and references therein) and suggested for the Levant margins by Schattner et al. (2015). Here, we further develop this concept exploring the hypothesis that deeper and distal currents first conveyed large amounts of clays and silts along the ancient continental margin and only then, after generating this clay and silt foundation, the shelf was established on top with sand transport, as we see it today. i.e., we hypothesize that only after filling the quite large accommodation space with the finer grains and generating the shallow water environment, sand could have started to accumulate as we observe today on the present-day shelf.

Here, we test this hypothesis using the stratigraphic simulation software DionisosFlow (Granjeon, 1997, 2014; Granjeon and Joseph, 1999). DionisosFlow is a state-of-the-art, 3-D stratigraphic modeling tool that produces synthetic stratigraphy according to prescribed subsidence history, sea-level variations, sediment supply, water discharge, and sediment distribution by diffusion. The problem is that to date, DionisosFlow has no module to simulate margin-parallel transport at shallow (alongshore) or deep (off shelf) waters. Therefore, we added to it a new module that may answer some of the above questions. The new module includes a simple advection law in which sediment flux is defined by the user, and deposition rate is calculated from this flux accounting for mass conservation. This volumetric exercise is constrained by ages and thicknesses of units. The sediment flux maps obtained by trial and error, indicate how much sediments pass through each point in the basin at various modeled time steps.

To account for lithological variations across the margin we also develop a depth-dependent function for the sand/shale ratio for the deposited sediments and the resulting stratigraphic section is calibrated by well data. Our results in terms of sediment flux and sand/shale ratio can be the basis for future physically based simulations that can better examine how surficial, intermediate, and deep marine currents transport sand and shale along various prescribed morphologies of continental margins.

2. Geological background

2.1. Sediment transport along the Nile littoral cell

The Nile littoral cell is one of the longest in the world with shorelines extending along ~700 km from the Nile Delta to northern Israel (Inman

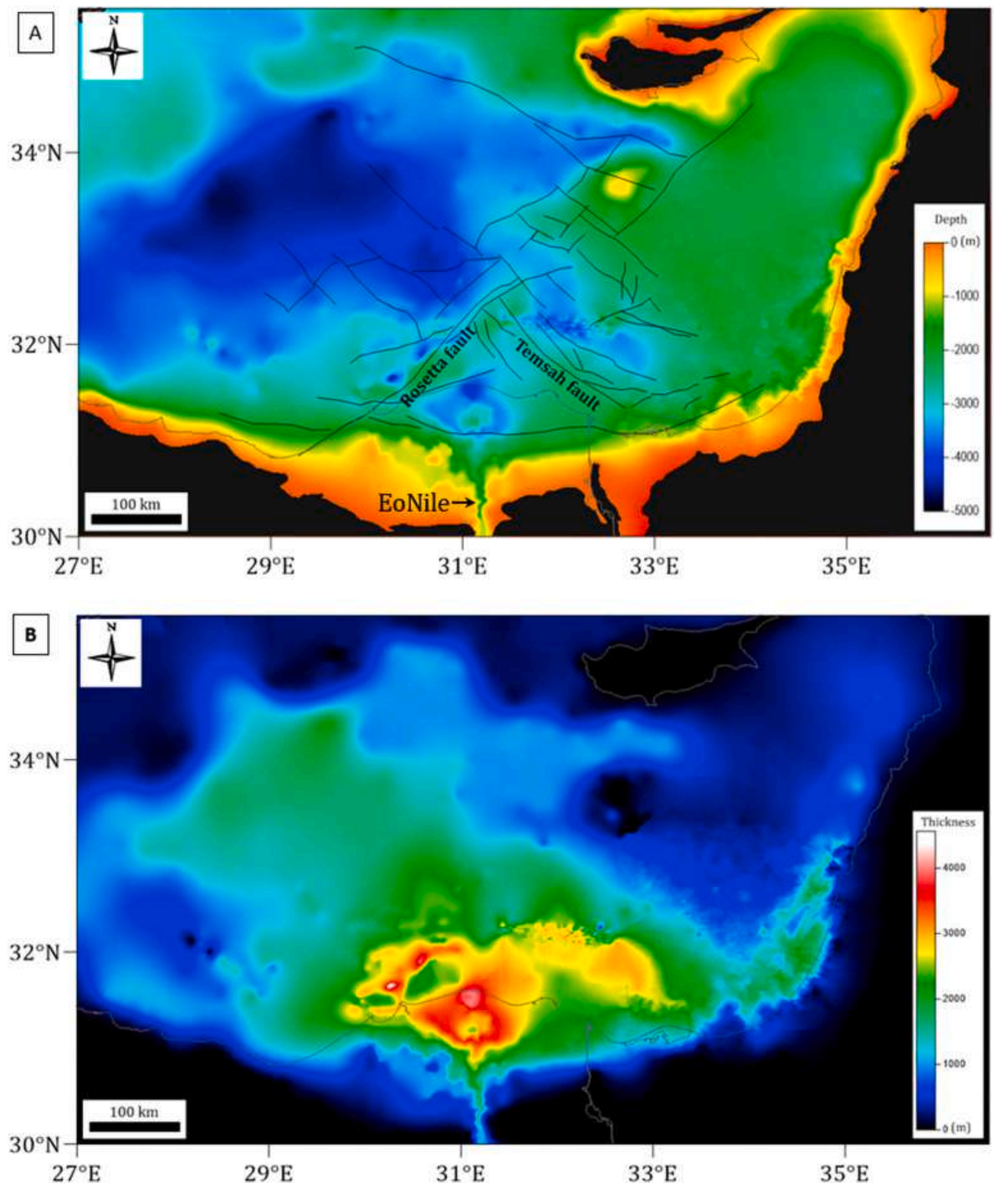

Fig. 2. (A) Structural map of the base of the Pliocene. Black lines are faults after Aal et al. (2000). (B) A map showing the thickness of the Plio-Quaternary sedimentary sequence. Present-day coastline (gray line) is shown for reference. Figure after (Zucker et al. (2019)).

and Brush, 1973; Inman and Jenkins, 1984). The source of this littoral cell is in the Nile River, it passes along the shallow (up to 30 m deep) nearshore water belt of the Levant, with current northernmost terminal deposition at the Haifa Bay (Buchbinder et al., 1993; Carmel et al., 1985; and the other references quoted in the above introduction). Some sediments that are transported northward turn west, fall off the shelf and then deposited along the continental slope of the Levant (Ben-Gai et al., 2005; Schattner et al., 2015; Schattner and Lazar, 2016; see data about Units 3–4 below). In addition to the nearshore transport, Woodward et al. (2007) showed that present-day Nile sediments extend across the Levant and Herodotus basins as far as Rhodes, Crete and north of Cyprus.

Longshore transport usually refers to the net movement of coastal and nearshore sand parallel to the shore (Seymour, 2005). This transport is either by currents carrying sand in suspension or by waves on the seabed (i.e., bedload transport). It is easier to measure concentration of suspended sediment, but quite difficult to measure the bedload component. Quantitative estimates of longshore transport, therefore, are based commonly on inferences from the suspended sediment concentrations indicating that longshore transport is at a maximum under the breaking waves and in the swash zone on the beach face (Seymour, 2005).

The annual longshore flux of sand from the Nile Delta (Fig. 1) eastward is estimated at about 10^6 m^3 yr^{-1} (Inman et al, 1976, 1993; Inman and Jenkins, 1984). Offshore Sinai, this flux slightly decreases to ~8.5 $\times$ 10^5 m^3 yr^{-1} and ~7 $\times$ 10^5 m^3 yr^{-1} off Port Said and off El Arish, respectively (Inman et al., 1976). This flux is estimated at 4.5 $\times$ 10^5 m^3 yr^{-1} and ~10^5 m^3 yr^{-1} at Ashkelon and Herzlia (Fig. 1), respectively (Perlin and Kit, 1999). Only a small portion (~8.5 $\times$ 10^4 m^3 yr^{-1}) of the initial sand flux reaches the currently considered final sink at Haifa Bay (Zviely et al., 2007).

2.2. *Different hypotheses*

An important point was raised by Schattner et al. (2015) who argued that longshore transport is limited to the shallow (<30 m depth) and narrow (350–400 m) near-shore belt and cannot explain the deposition at greater depths. In addition, we stress that longshore transport only moves sand and silt, whereas the PQ shelf is mainly composed of shales

(Yafo Formation) with only its topmost part composed of sand (Kurkar Group, e.g., Gvirtzman and Buchbinder, 1978).

Based on bathymetric, seismic, and oceanographic data, Schattner et al. (2015) suggest that since the Pleistocene-Holocene transition (~11 ka) fast water currents, termed the Levant Jet System (LJS; Fig. 1, red arrows), mobilizes sediments along the continental margin not only nearshore, but also in intermediate and deep waters (between 0 and 400 m water depths).

2.3. Timing of the Levant shelf accretion

A general PQ age was assigned for the continental shelf offshore Israel (e.g., Ben-Avraham, 1978; Ben-Gai et al., 2005; Gvirtzman and Buchbinder, 1978; Tibor et al., 1992). However, recent reexaminations of the biostratigraphy led Bar et al. (2009) to propose that most of the shelf was accreted later and that is composed primarily of Pleistocene sediments. This relatively young age is supported by Elfassi et al. (2019) and Ben Zeev and Gvirtzman (2020) who demonstrate that after the Pliocene the pattern of sedimentation in the Levant Basin changed drastically; from thicker accumulation in the deep basin to thicker accumulation along the continental margin. Particularly interesting and crucial is the observation that the preferred deposition along the margin was delayed by 2–3 My after the commencement of the Nile Delta formation offshore Egypt (Ben Zeev and Gvirtzman, 2020). This, once more, raises the question why did margin-parallel sediment transport and shelf accretion begun so late? Why were sediments not transported along the Sinai-Israel margin already during their initial supply in the Pliocene?

Hypothetically, this can be answered by proposing that external forcing such as climate or ocean circulation could have triggered margin-parallel marine currents only in the Pleistocene. Alternatively, we hypothesize here, sediment transport along continental margins is a strong depth-dependent process that becomes more effective under certain bathymetry conditions. In the case of the Nile, we hypothesize that only after 2–3 My of delta accretion, the continental margin offshore Sinai could have become an effective conduit for sediment transport and large amounts of sediments started arriving to offshore Israel.

3. Methods

3.1. Diffusion modeling in sediment transport

Since the early work of Culling (1960) and Young et al. (1973) and with the lack of specific information on the actual terms in physical sedimentology processes, diffusion laws have been used in geomorphology and geology to represent large-scale, spatially-averaged transport of sediment by creep, overland flow, and channel flow (e.g., Begin et al., 1981; Paola et al., 1992). Diffusive sediment transport states that the transport capacity of a water flow is proportional to the local basin slope and water discharge. It has been used in modeling sediment transport along alluvial fans, rivers and floodplains (Begin et al., 1981; Ben Moshe et al., 2008; Coulthard, 1999; Murray and Paola, 1994; Parker et al., 1998), mountains, foreland basins (Jordan and Flemings, 1991; Tucker and Slingerland, 1994) and passive margins (Rabineau et al., 2005).

Since the 1980s, when seabed morphology was shown to resemble lowland landscapes (e.g., Adams et al., 1998; Galloway, 1998; Mitchell and Huthnance, 2007; Schlager and Adams, 2001), laws of landscape evolution were extended to simulating progradation of deltas (Kenyon and Turcotte, 1985) and continental shelves (e.g., Granjeon, 1997; Jordan and Flemings, 1991; Kaufman et al., 1991; Mitchell and Huthnance, 2008; Rivenæs, 1997).

DionisosFlow is a 3D stratigraphic forward modeling tool aiming to simulate geometry and facies of sedimentary units on a scale of several tens to hundreds of kilometers and over geological intervals of 10^3–10^8 years (Granjeon, 2009; Granjeon and Joseph, 1999; Granjeon and Wolf, 2007); these are the scales of the problem at hand. At these spatial and temporal scales and the needed resolution, unfortunately, there is practically no way to apply physically based modeling. Using a diffusive approach for sediment transport (Gerber et al., 2009; Kaufman et al., 1991; Lai and Capart, 2007; Mitchell and Huthnance, 2008; Schlager and Adams, 2001; Spinewine et al., 2011; Steckler et al., 1999; Van Heijst et al., 2001), DionisosFlow averages the cumulative mass movement in time steps that combine many individual flows. In this way, DionisosFlow, for example, ignores individual turbidites, but considers their cumulative mass movement. Similarly, and important for our study, it does not account for the discontinuity between fluvial and submarine systems in cases that sediments temporarily settle down on the delta front or inner shelf and only later are transported downslope by gravity-driven processes. For simplicity, it assumes that flows continue seaward either directly by hyperpycnal flow or by slope failures.

DionisosFlow formulates two large-scale sedimentary processes: slow creep and fast transport driven by water discharge (Tucker and Slingerland, 1994; Willgoose et al., 1991). Creep is simulated by a linear, slope-driven diffusion equation (i.e., transport is proportional to gradient). Water-driven flow is simulated by a non-linear water- and slope-driven diffusion equation. Combining the driving equations of these transport laws (Granjeon, 2014; Granjeon and Joseph, 1999) leads to the sediment transport equation:

$$Q_s = -\left(K_s + K_w Q_w^n S^{m-1}\right)\vec{\nabla} h \tag{1}$$

where Q_s is sediment flux [km^2/yr]; h [m] is topographic elevation; K_s and K_w [km^2/yr] are the diffusion coefficient, respectively for slow creep transport and water flow process; Q_w is dimensionless local water discharge at the cell; S is local gradient of basin slope; n and m are constants, usually ranging between 1 and 2. Transport equation and mass conservation are applied to each grain size, leading to definition of local sedimentation or erosion. Sedimentation occurs where transport capacity decreases (by decreasing gradient or slower water flow) and erosion occurs where transport capacity increases.

The capability of DionisosFlow to simulate the production of large-scale systems such as deltas, fluvial plains, shelf plains, incised valleys, and deep water systems was tested and validated in several studies including, for example: (1) the XES 02 flume experiments designed to reproduce fluvial plain and incised valleys (Granjeon, 2014); (2) Synthetic case studies built to investigate the impact of millennial-scale climatic and eustatic cycles on the growth of a delta and the associated fluvial channel belts and incised valleys (Csato et al., 2014; Rabineau et al, 2005, 2006); (3) On modern delta, shelf, and deep-water turbiditic systems such as the Niger Delta (Laurent et al., 2020) and the Orinoco deep-sea fans (Deville et al., 2015).

3.2. Simulating margin-parallel sediment transport

The margin-parallel transport module developed here begins with a sediment flux map describing the intensity [km^2/My] of the flux transported through a given location in a coast-parallel, dynamically updated direction, which evolves with time. The flux obeys a simple user-defined advection law that accounts for mass conservation, i.e., when the flux decreases, sediments depart from the suspension plume and deposit. The rate of deposition, SED [km/My] is:

$$\begin{cases} \overrightarrow{q_{mp}} = Q_{mp}(x,y).\ \vec{n} \\ SED\ (x,y) = -div\ \left(\overrightarrow{q_{mp}}\right) \end{cases} \tag{2}$$

with q_{mp} the margin-parallel sediment flux [km^2/My], Q_{mp} the user-defined intensity of this flux, n a unit vector parallel to the closest shoreline [dimensionless], and SED [km/My] the sedimentation rate induced by this margin-parallel sediment transport.

The sand/shale ratio within the deposited sediment is computed

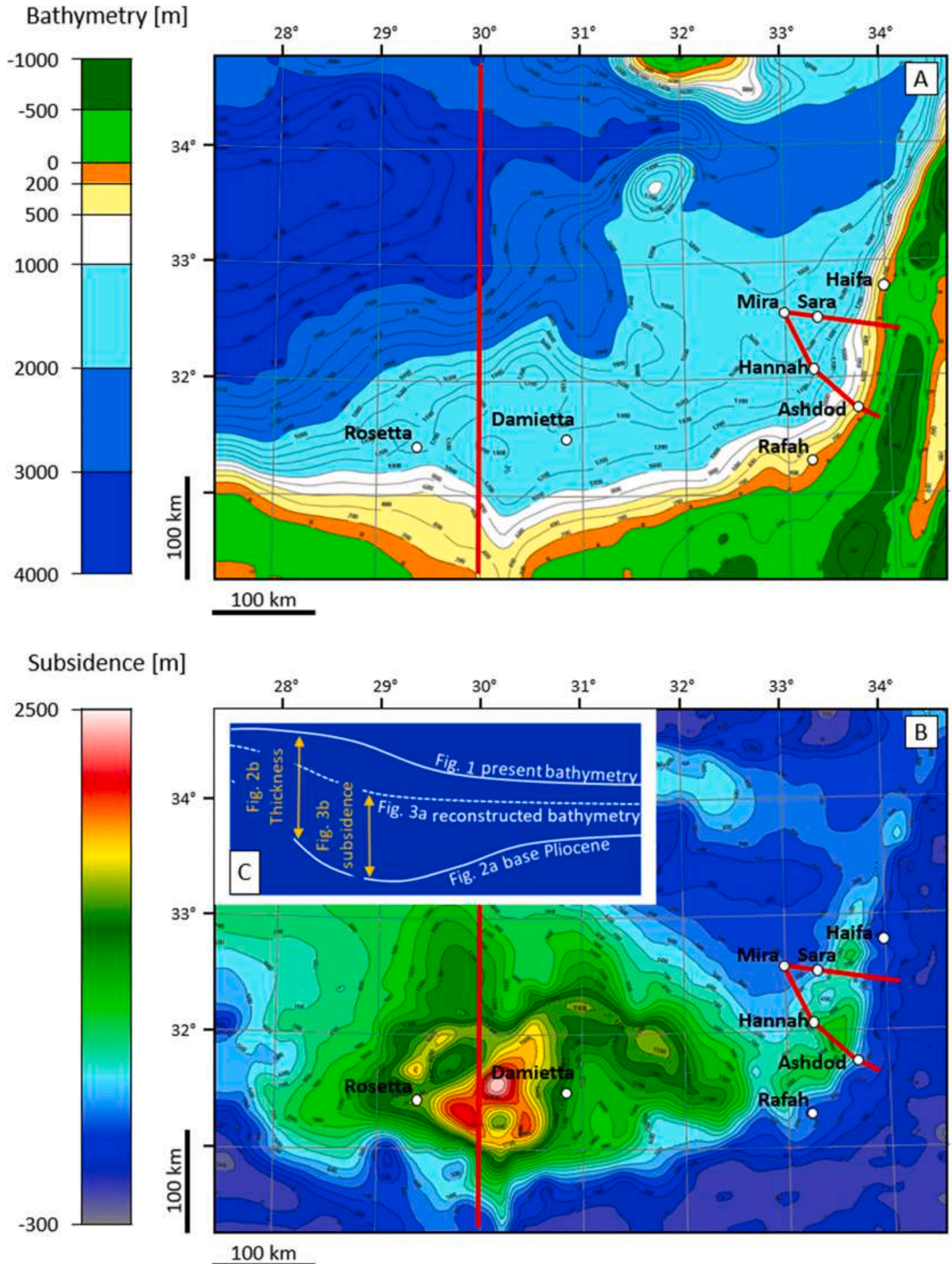

Fig. 3. (A) Reconstructed bathymetry for 5.3 Ma (obtained by flexural unloading of the PQ sediment from the base Pliocene map, see text). (B) Subsidence since the time of the base of the Pliocene sequence (5.3 Ma) until today. (C) 2D Illustration of the relationships between the data presented in Figs. 1–3.

from a given depth-dependent function, derived from observations. In addition to this deposition rule, we use the classical diffusion equations to transport sediments as soon as they reach the sea floor. By the end of this computation, we obtain a stratigraphic layer whose thickness is compared with observations. By trial-and-error (i.e., sensitivity over a range), the flux map is corrected, and simulations rerun until they satisfy borehole and geophysical data.

3.3. Data

3.3.1. Basin structure

The stratigraphic PQ sequence simulated here is bounded by the present-day bathymetry at its top and the base Pliocene surface at its base. Bathymetry (Fig. 1) is taken from ETOPO1 (Amante and Eakins, 2009). The base Pliocene structure map (Fig. 2A) is after Zucker et al. (2019). The PQ isopach (Fig. 2B), which is the subtraction of Fig. 2A from Fig. 1, defines the major depocenter under the Nile Delta and cone (reaching a thickness of 4 km) and a secondary and connected, local depocenter under the Israeli coastal plain and shelf (reaching a thickness

Table 1
Model parameters from the literature and this study.

Diffusion Coefficient [km2/ky]					
		K gravity terrestrial [km^2/ky]	K gravity marine [km^2/ky]	K water terrestrial [km^2/ky]	K water marine [km^2/ky]
Sand					
Csato et al.(2014)	Delta	0.001	0.001	250	5
Zhang et al., 2018	Delta	0.05	0.005	50	0.01
Csato et al.(2013)	Margin			2000	0.4
Harris et al.(2016)	Margin	0.001	0.001	250	1
Gvirtzmann et al. (2014)	Turbidites				2
Hawie et al.(2017)	Turbidites				0.3
Hawie et al.(2018)	Turbidites		0.007		20
range		0.001–0.05	0.001–0.005	50–2000	0.01 - 20
Levant 103 (best fit)		0.001	0.001	100	0.5
Shale					
Csato et al.(2014)	Delta	0.001	0.001	1000	5
Zhang et al., 2018	Delta	0.1	0.05	100	0.1
Csato et al.(2013)	Margin			4000	10
Harris et al.(2016)	Margin	0.001	0.001	1000	5
Gvirtzmann et al. (2014)	Turbidites				10
Hawie et al.(2017)	Turbidites				0.063
Hawie et al.(2018)	Turbidites		0.001		100
range		0.001–0.1	0.001–0.05	100–4000	0.063 - 100
Levant 103 (best fit)		0.01	0.01	500	2.5

of 2 km). Resolving these two depocenters - a delta and an adjacent continental shelf - are the targets of this simulation.

3.3.2. Paleo-bathymetry

For the paleo-bathymetry at 5.3 Ma (Fig. 3A), which is the surface on which we begin to model deposition, we used the base Pliocene map corrected for the load of the overlying sediments (PQ section). For this flexural backstripping procedure, we assumed an average density of 2000 kg/m^3 for unloaded sediments, adopting a pure elastic thin plate approach to isostasy and an elastic thickness of 30 km, a relatively large value consistent with the old tectonothermal age of the northeast African margin. For the decompaction of the underlying sediments, we considered an approximately 10-km thick pre-Pliocene section. The decompaction results are very insensitive to the depth of the base of this layer because only the upper ~2 km retains a significant porosity. Details about this pseudo-3D (planform) flexural backstripping procedure are described in Garcia-Castellanos et al. (2003) and in Amadori et al. (2018). To correct for post-Miocene tectonics, the sediment-unloaded map was smoothed in the area of the Rosetta and Temsah faults (Fig. 2A), which were active in the PQ (Aal et al., 2000). In addition, the northern Levant Basin that subsided towards the Cyprus Arc during the Plio-Quaternary (Ben-Avraham, 1978; Kempler, 1998; Robertson, 1998; Schattner, 2010) was uplifted by ~200 m. The uncertainty of post Miocene tectonics is discussed below.

3.3.3. Subsidence

Subsidence (Fig. 3B) is calculated in the model by taking the difference between the paleobathymetry at 5.3 Ma (Fig. 3A) and the present-day base Pliocene surface (Fig. 2A), the surface which should be obtained at the end of simulation. Average subsidence rate for the entire simulation is taken as the total calculated subsidence divided by 5.3 My. This assures that at the end of the simulation, the modeled and observed bases of Pliocene surfaces will coincide to allow comparing the modeled and observed bathymetries (Fig. 3C).

3.3.4. Sediment supply

A first order approximation for sediment supply is derived from the total volume of the PQ isopach (Fig. 2B) divided by 5 million years (i.e., 70,330 km^3/My). From this number we subtract biogenic carbonates produced in the water column. Well samples and logs from the Israeli coastal plain indicate that the Plio-Quaternary Yafo Formation contains ~10% calcite in the form of micro- and nano-fossils (Gvirtzman, 1970). Considering that 10% of the total PQ volume did not arrive from the clastic feeders, we initially applied 90% of the total deposited volume. After a set of trials constrained by the sediment thickness maps, we applied an average value of 64,417 km^3/My (~91.5%) to represent sediment supply by the Nile River for the entire duration of the model. It is interesting to note that this average value obtained from sediment volume is on the same order of magnitude as the sediment yield presently measured at the mouth of the Nile River (60,000 km^3/My, Syvitski and Milliman, 2007). Sand/shale ratio for Nile sediments was taken as 20% and carbonate production was taken as 5910 km^3/My.

3.3.5. Margin-parallel transport

Regarding present-day measurements of longshore transport (references above), it should be noted that they refer only to the sand fraction (1000 km^3/My from Nile Delta to Sinai; 850 km^3/My at Port Said, 700 km^3/My at El Arish; 450 km^3/My at Ashkelon; 100 km^3/My at Herzlia; and 85 km^3/My arrive to Haifa Bay). The big unknown in our simulation is the total amount of sediments (sand to clay) moving along the continental margin nearshore, on and off the shelf.

A lower limit for the total sediment flux along the Levant continental margin is obtained from the average deposition rate along the Israeli margin since the early Pliocene. Considering a rectangular 200 km (Rafah to Southern Lebanon) by 20 km (approximately the mean width of shelf) by 2 km (thickness of PQ section offshore Tel Aviv), the total volume of the Israeli shelf is about 8000 km^3. Dividing this by 5.3 million years, yields ~1500 km^3/My. This set a minimal constraint for the flux that entered the Israeli margin from offshore Sinai, because the actual flux includes sediments that continued northward to offshore Lebanon. No siliclastic sediments can enter the shelf from the onshore carbonate platform of the Levant. It is interesting to note that this estimated minimum value of total sediment flux triples the sand flux (~500 km^3/My) currently entering to Israeli margins at Rafah (the southern boundary of the Gaza strip between El Arish and Ashkelon). Below, the unknown flux of sediments along the Levant continental margin is modeled by trial-and-error.

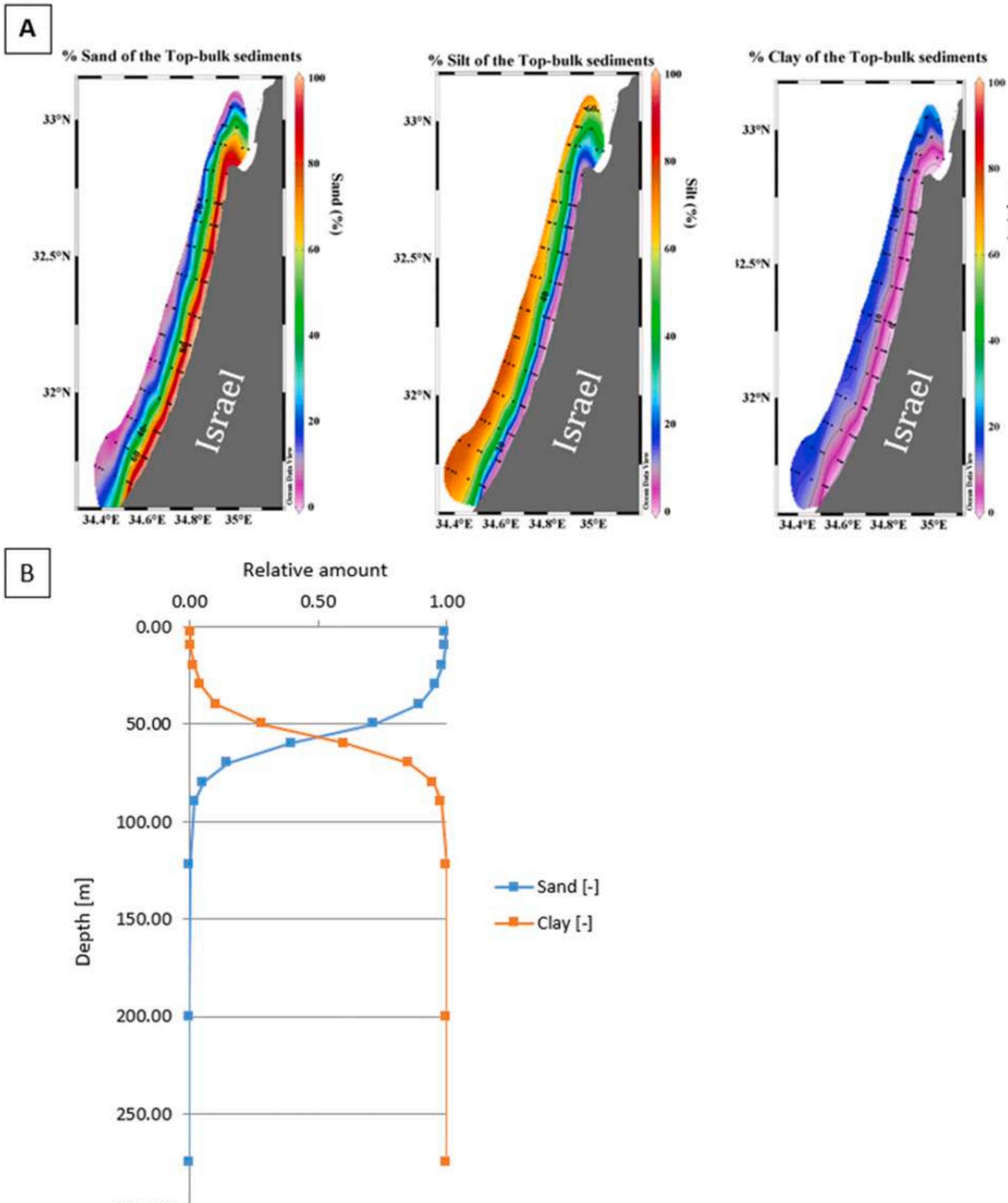

Fig. 4. (A) Sediment grain size as documented on the present-day seabed offshore Israel (after Almogi-Labin et al., 2012); the data indicate the coast-parallel distribution of the sand, silt, and clay belts. (B) Depth dependent sand/shale ratio parameters introduced in the model. Generated following Almogi-Labin et al. (2012).

3.3.6. *Water discharge*

Present day water discharge of the Nile River is 2830 m^3/s (Milliman and Syvitski, 1992). The paleo-discharge of the ancient Nile River can be further, but only roughly, constrained by paleogeographic (drainage area) and paleoclimatic (rain) considerations and compared with modern rivers worldwide that have similar drainage areas (Dai and Trenberth, 2002; Milliman and Syvitski, 1992; Syvitski and Milliman, 2007). Although we are aware of the impact of Quaternary climatic changes on the Nile discharge, for the lack of data and for the sake of simplicity, we took the present-day value as a constant throughout the entire duration of the model.

3.3.7. *Diffusion coefficients*

Efficiency of sediment transport depends on difficult-to-quantify

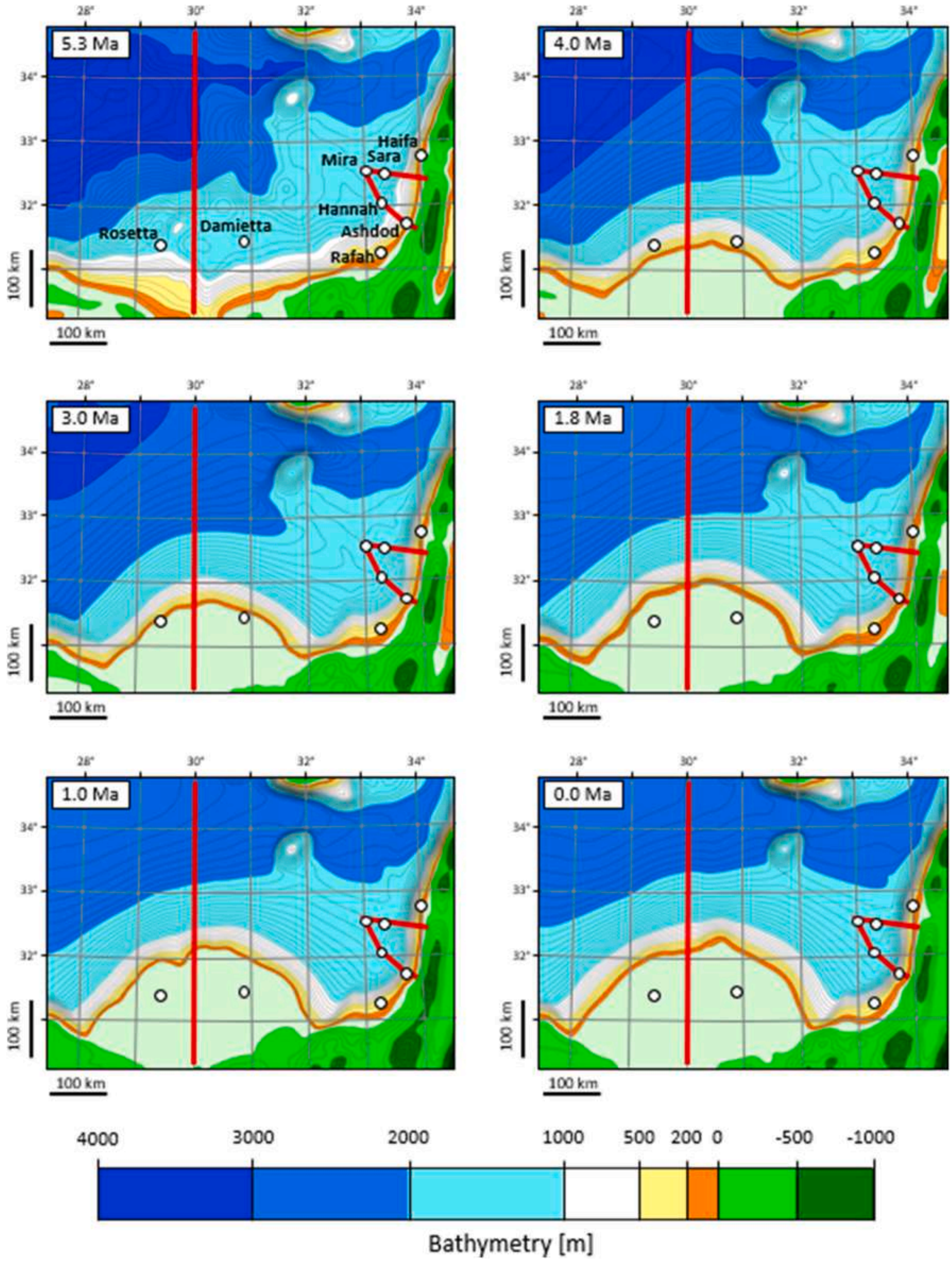

Fig. 5. Maps illustrating the evolution of the bathymetry through time as modeled by DionisosFlow using the basic sediment transport model without the MPST (see text). Red lines show locations of cross sections. Top left is the same as Fig. 3A. (For interpretation of the references to color in this figure legend, the reader is referred to the Web version of this article.)

factors such as grain size, lithology, roundness, water depth, water discharge, vegetation, river type and more. In practice, coefficients used to model various basins do not always express the same factors and their values vary greatly from case to case. One reason for this large range is that efficiency of diffusion can be controlled either by the diffusion coefficient or by the amount of water pushing the sediments (Equation(1)). Accordingly, Gvirtzman et al. (2014) and Hawie et al. (2015) showed that by constraining water discharge, the range of possible diffusion coefficients is narrowed. Recent stratigraphic forward models run at a basin scale, using diffusion laws to simulate slow creep and water flow processes, and calibrated on seismic and well log data suggested the following range of values (Table 1): Ks (slow creep) is about 0.001–0.05 km^2/ky for sand, and 0.001 and 0.1 km^2/ky for shale; while Kw (water flow process) is about 50 to 2000 km^2/ky for sand in terrestrial

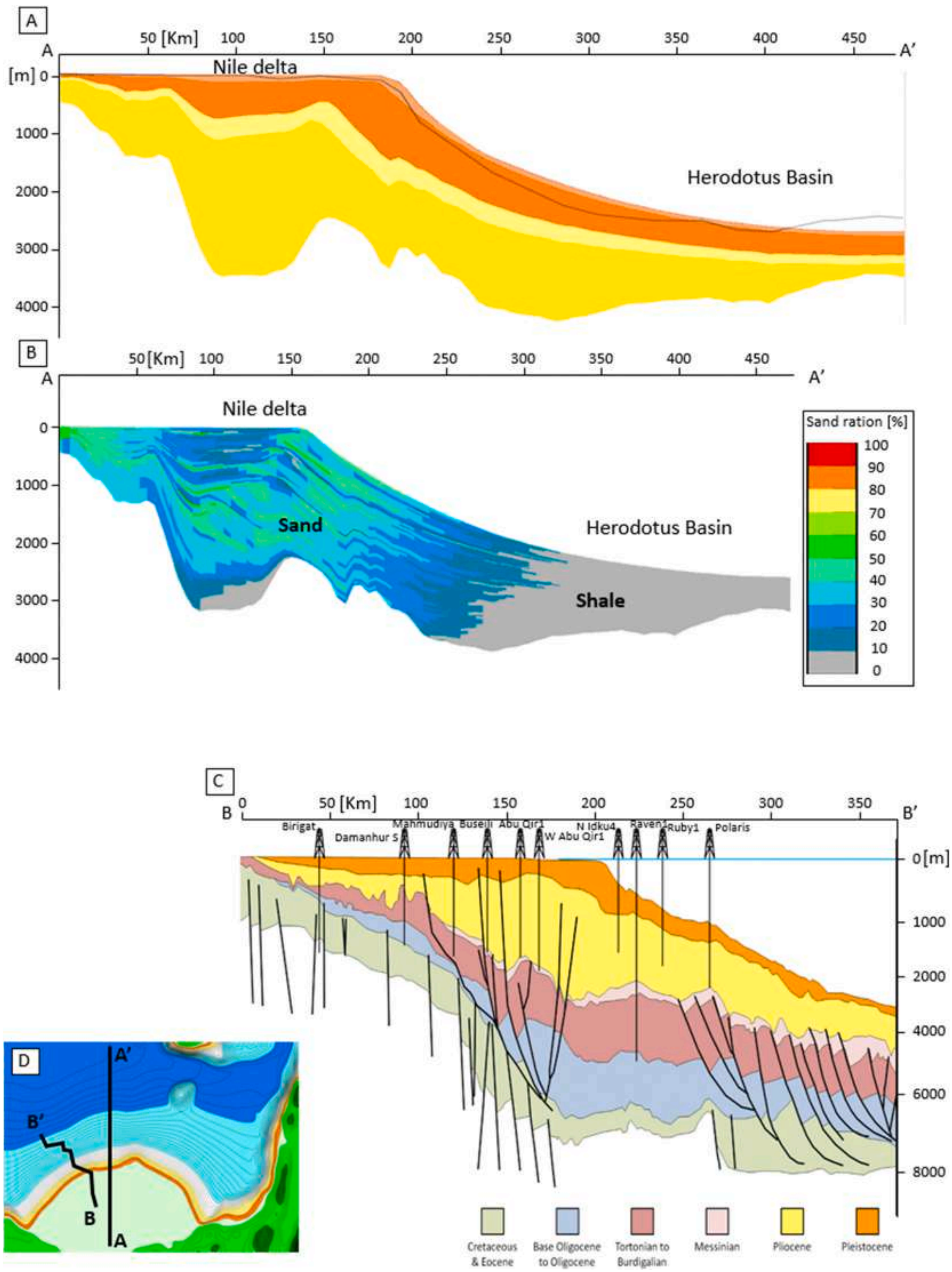

Fig. 6. (A) Model results using a basic sediment transport that show a good fit with a cross section (B–B′, see 6D for location) after Kellner et al. (2009) across the Nile Delta. (B) Cross section A-A' (see D for location) of the Nile Delta sand [%] that builds the delta at the end of the model that includes MPST (see text). (C) Interpreted seismic composite line across the Nile Delta (Kellner et al., 2009). (D) Location map of cross sections B–B′, and A-A'. Dashed black line in cross section A-A′, shows present-day bathymetry. Color bar is the same for Fig. 6A and C. (For interpretation of the references to color in this figure legend, the reader is referred to the Web version of this article.)

environments, 100 to 4000 km^2/ky for shale in terrestrial environments, 0.01–20 km^2/ky for sand in marine environments, and 0.063–100 km^2/ky for shale in marine environments (Csato et al, 2013, 2014; Gvirtzman et al., 2014; Harris et al., 2016; Hawie et al, 2017, 2018; Zhang et al., 2019). Here we take the present-day water discharge of the Nile as a starting point and identify the best-fit diffusion coefficients of shale and sand inside these ranges by trial and error.

3.3.8. *Sand/shale ratio*

Present-day measurements of sediment composition at the seabed offshore Israel (Almogi-Labin et al., 2012) indicate the presence of three coast-parallel belts (Fig. 4A): (a) An almost pure, well-sorted sand belt from the shoreline to a water depth of 35 m. (b) A silt-dominated belt from water depths of 35–100 m in which the amount of silt gradually grows from a few percent at a depth of 35 m–85% at depths of 60–100 m. The rest is shale; this shale represents only a few percent of the total

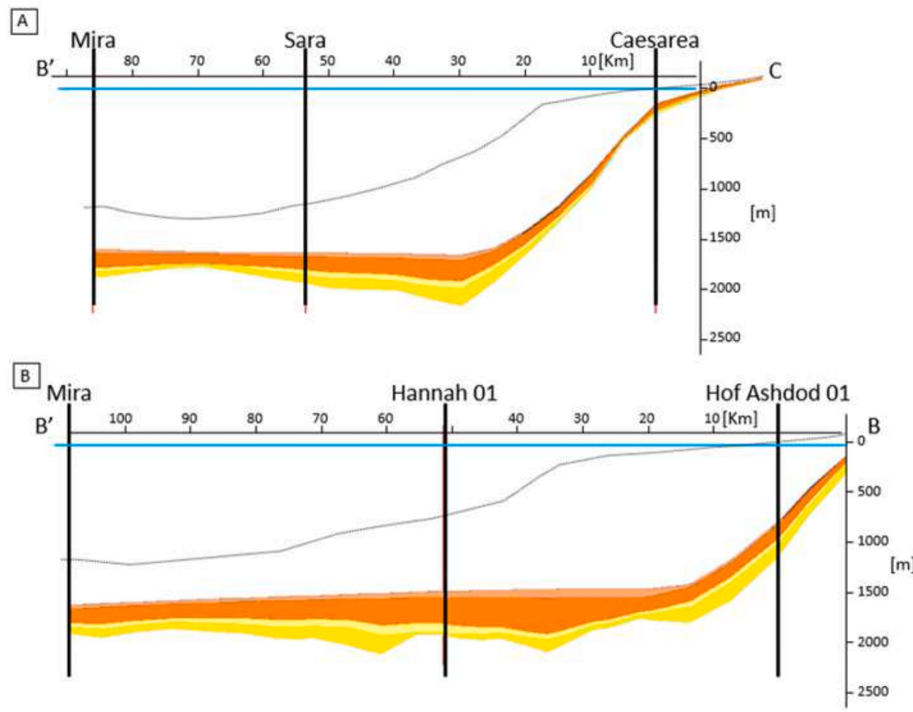

Fig. 7. (A and B) Results of chronostratigraphic model using basic sediment transport that indicate a bad fit to the observed present-day bathymetry reference (gray line) across the Levant continental margin. Black vertical lines mark locations of oil and gas wells with their names written above (see wells and cross section locations in Fig. 1).

sediment volume near the coast and 10–15% at depths of 60–100 m. (c) A shale dominated belt at depths >100 m, where sand is negligible. For modeling we simplified these observations to only two components (sand and shale) with a depth-dependent ratio shown in Fig. 4B.

3.4. Modeling strategy

The first objective of this modeling study is to obtain the diffusion parameters that explain the Nile Delta formation with the given values of water discharge and sediment supply. For this, we first use DionisosFlow without the added new module of MPST. Considering that the base of the simulated PQ package is forced to coincide with the observed base Pliocene surface (see above constraints for subsidence), testing the model is carried out by comparing the modeled and observed bathymetries. If bathymetry fits, sediment thickness also fits. This stage of the modeling is expected to provide a rough fit between the model and observations at the delta area, but not at the Levant margin.

The second objective is to simulate the formation of the Levant shelf. For this, we apply all model parameters realized in the first stage (and particularly the diffusion coefficients) and rerun DionisosFlow; this time the runs include the upgraded module for margin-parallel transport. By numerous trial-and-error runs, we identify the sediment flux maps that yield the better fit between model and observation. For calibration of the lithostratigraphy, we use a published lithostratigraphic section that distinguishes the sandy Kurkar Group from the shales of the Yafo Formation (data from Gvirtzman and Buchbinder, 1978). For chronostratigraphic calibration, we use the subdivision of the PQ section offshore Israel identified for four dated seismic units (Ben Zeev and Gvirtzman, 2020; Elfassi et al., 2019).

4. Results

Stage 1: basic model without the margin-parallel sediment transport (MPST).

Fig. 5 presents the simulated bathymetry from 5.3 Ma to the present, using the basic model without the MPST. The parameters for sediment distribution that generate this model are listed in Table 1. These results demonstrate that the model successfully produces the Nile Delta, but essentially fails to produce the Levant shelf. The general fit between model and present-day observations in bathymetry and thickness (Fig. 6A) is evident in section AA' crossing the Nile Delta. Moreover, a comparison with a published geological section in that area from Kellner et al. (2009) indicates that even the subdivision between Pliocene and Quaternary is modeled quite well (Fig. 6C). On the other hand, offshore Israel there is only a poor fit between model and observations (Fig. 7A and B). This discrepancy in the east-west cross sections is primarily because the model produces, by far, too little deposition offshore Israel (Fig. 8A). The map presenting the discrepancy in thickness between model and observations (Fig. 8B) further indicates that the sediment, unaccounted for at the Levant margin (~2 km, blue colors), is compensated by excess sediments in the Herodotus Basin (200–900 m, red); i.e., the sediments were delivered there. This discrepancy strengthens our hypothesis that without a large margin-parallel sediment supply, it is impossible to simulate the formation of the Levant continental shelf.

Except for this discrepancy, which is related to the lack of margin-parallel transport, the generally good agreement between model and observations offshore the Nile Delta (e.g., Fig. 6) indicates that (1) sediment distribution in the model functions quite well, and (2) average values of Qw, Qs for the entire simulated interval are suitable approximations. We therefore take model parameters obtained in the first modeling stage and continue to the next stage.

Stage 2: Adding the margin-parallel sediment transport (MPST) to the model.

Fig. 9 shows the simulated bathymetry from 5.3 Ma to the present, using the upgraded model, which includes the margin-parallel sediment transport (MPST) module. Unlike the basic model (Fig. 5), here with the addition of this module, a shallow continental shelf is produced (orange color) offshore Israel with nearly a 2-km-thick section deposited there (Fig. 10A). Throughout the studied area, the model produces a thickness

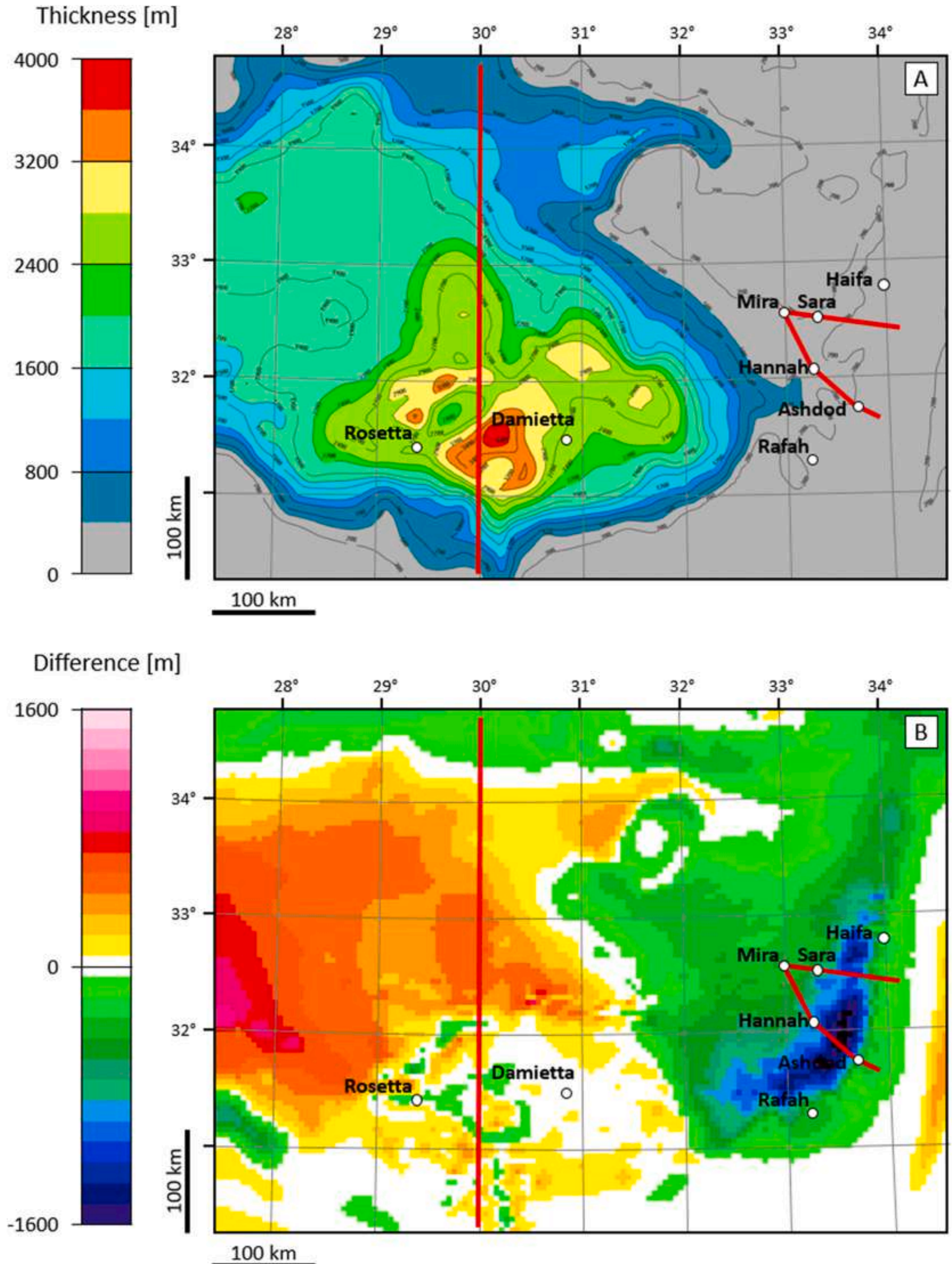

Fig. 8. (A) Total sediment thickness (from 5.3 to 0.0 Ma) as simulated without MPST (see text). (B) The difference in sequence thickness between simulated (A) and observed.

within <200 m from the observed thickness (Fig. 10B); this is quite a satisfactory result as this value is within <10% of the total observed thickness.

Two modeled chronostratigraphic cross sections offshore Caesarea and Ashdod demonstrate the good fit with observations (Fig. 11). Furthermore, Two lithological sections at the same location (Fig. 12) indicate that sand is accumulated only in the upper part of the section. This is also consistent with observations as the age of the Kurkar Group varies laterally, from Pliocene-Pleistocene inland to only Pleistocene at the coastline (Fig. 12C, Gvirtzman and Buchbinder, 1978). According to our model, farther west at the shelf area, the age of the sandy Kurkar Group is limited to a few hundred thousands of years and to only several tens of thousands of years near the shelf edge (Fig. 12). The noticeable sand intercalations into the shaly section represent intervals of eustatically low sea levels (Haq et al., 1987) used as part of the model input.

The successful simulation of sand deposition and its accretion in the shallow environment is the outcome of the depth-dependent sand/shale ratio (Fig. 4) that was fed to the model. This depth dependency is also expressed in Fig. 13 and indicates that more sand was deposited offshore Israel during the latter part of stratigraphic sequence accretion (1.8–0 Ma), when a shallow shelf was already developed.

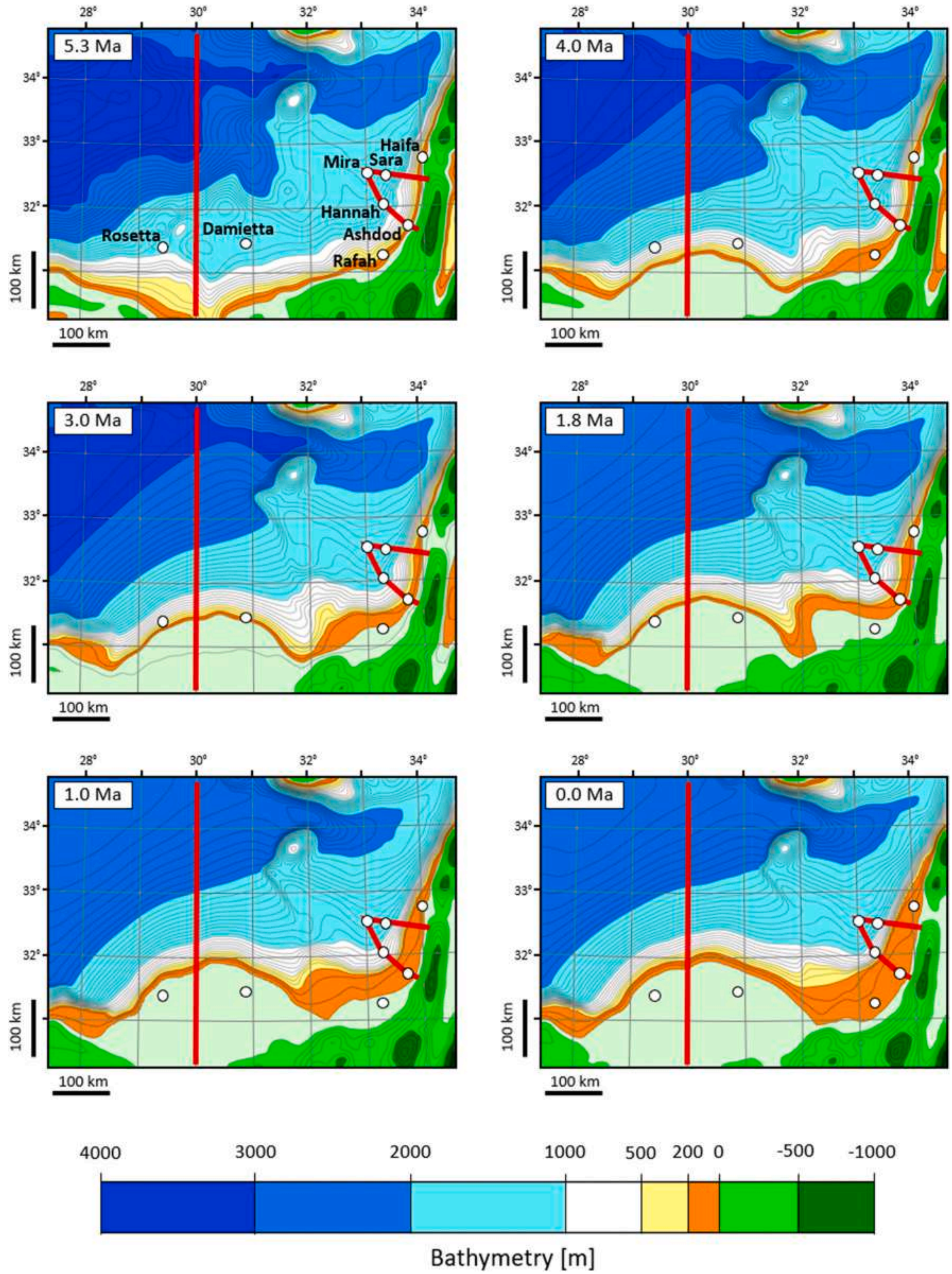

Fig. 9. Bathymetry evolution through time as modeled by DionisosFlow implementing MPST. Note the difference between this model, which produces the Levant shelf, and the basic model that does not (Fig. 5). Red lines show locations of cross sections. (For interpretation of the references to color in this figure legend, the reader is referred to the Web version of this article.)

4.1. Rates, accretion, and shelf buildup

To summarize our results, we compare modeled and observed sedimentation rates in the Levant Basin over the four time intervals of 5.3–2.6 Ma, 2.6–1.8 Ma, 1.8–0.35 Ma, and 0.35–0 Ma (i.e., interval durations of 2.7, 0.8, 1.45, and 0.35 My), which were defined as traceable chronostratigraphic zones by Elfassi et al. (2019) based on seismic- and bio-stratigraphy. These four stratigraphic units are the basis for the four thickness maps prepared by (Ben Zeev and Gvirtzman, 2020) and are the basis for the rates we use in the comparison with the modeling. The division of the thickness of the four units corresponds to the above interval durations.

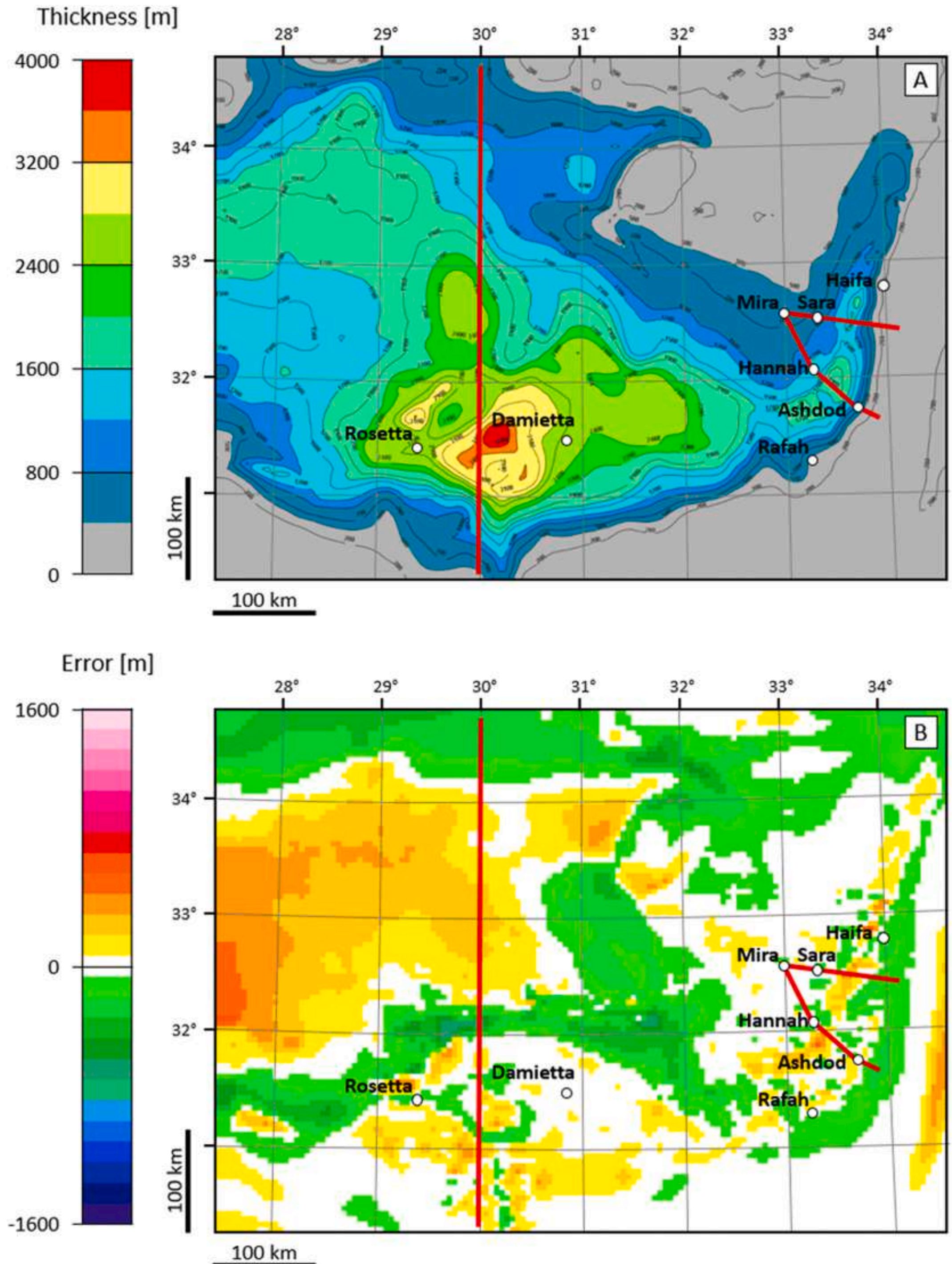

Fig. 10. (A) Total sediment thickness, from 5.3 to 0.0 Ma generated by simulation including MPST (see text). (B) Difference between simulated (A) and observed sediment thickness. Note the relatively small difference here in comparison with the basic, without MPST, model (Fig. 8b).

Deposition rates calculated for the basic model (without MPST), indicate that deposition was not sufficient to form a continental shelf in the Levant (Fig. 14). In the upgraded model that includes MPST, a continental shelf is gradually built; this buildup is observed in the model to occur first, offshore Sinai, then offshore Israel, and most recently offshore Lebanon. The calculated rates of accretion are consistent with observations but present some exceptions. Unit 2 (Gelasian) in the actual stratigraphy presents an increase in sedimentation rate both in the southwest, near the Nile Delta, and along the Levant margin (Fig. 14). This could have been an expression of a temporal increase of the Nile's sediment discharge, which we do not model. Furthermore, the Israel Slump Complex that provided ~1000 km^3 of sediments from the Levant slope to the basin (Frey Martinez et al., 2005) in a short episode, limited to Unit 2 (Elfassi et al., 2019) and is not modeled either. In addition, our model ignores other local sediment contribution that may have reached the basin from the east (e.g., the Yafo sand member, Druckman et al., 1995; Frey-Martınez et al., 2007; Frey Martinez et al., 2005; Gardosh et al., 2009).

The importance of the MPST is demonstrated by comparing (Fig. 15) sedimentation rates in the deep basin and at the continental margin (locations appear as white dots in Fig. 14). In the basic model, without MPST, the difference between these two localities is minor and the rate

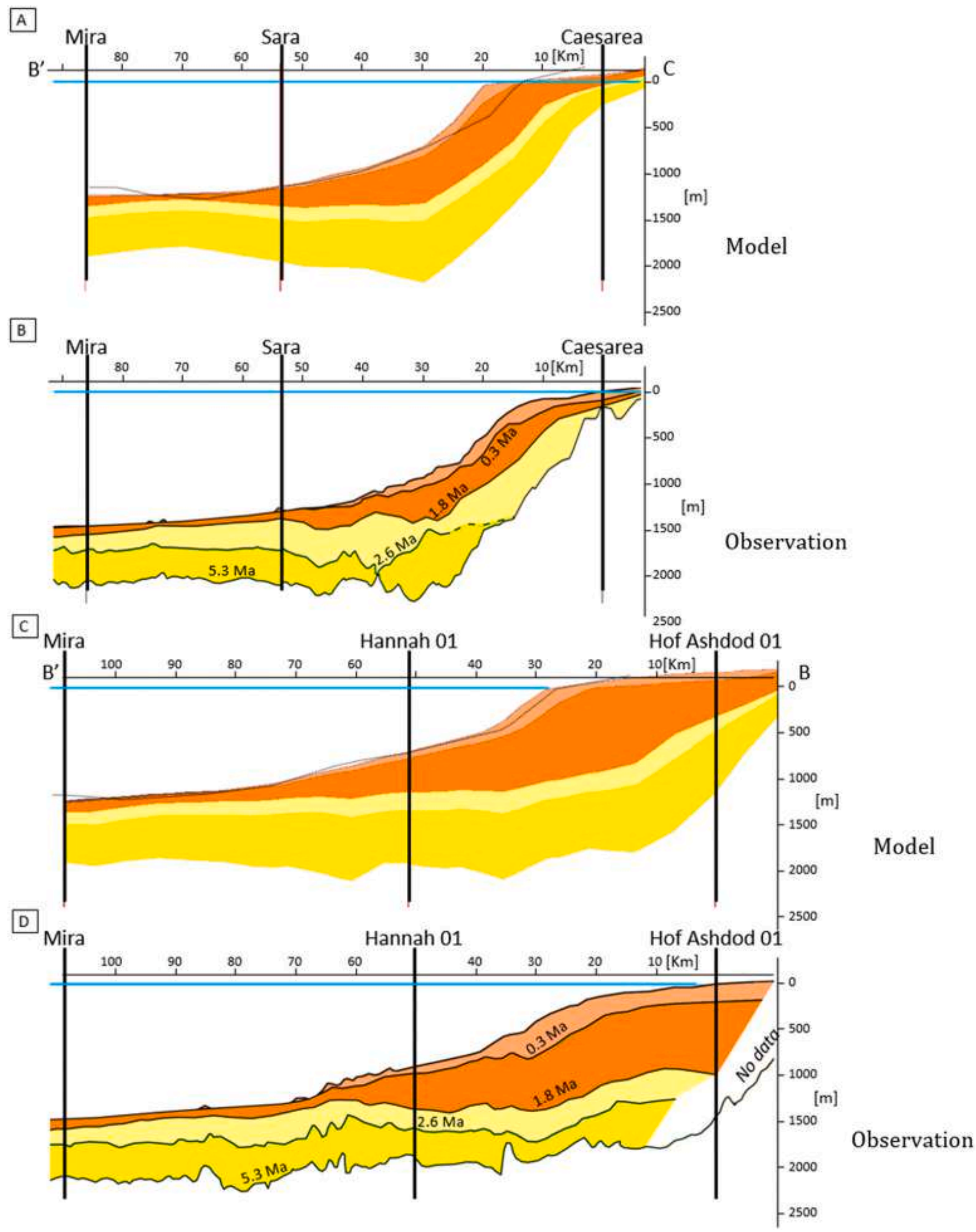

Fig. 11. (A and C) Chrono-stratigraphy of sections across the Levant margin derived from the model after adding the MPST. These sections show a good fit to observed sections based on seismic data (B and D). Black vertical lines in cross sections mark locations of oil and gas wells. Well names and cross section locations are in Fig. 1.

of sedimentation is relatively low in both. This is because the model depends almost entirely on slow and gradual diffusion of sediments from the Nile Delta through and into the deep basin. On the other hand, with the addition of the MPST, increasingly more sediments arrive and deposit along the continental margin of the Levant and as a result less sediments reach and deposit in the deep basin.

4.2. Margin-parallel sediment flux

Sediment flux maps obtained by trial-and-error are shown in Fig. 16A and B. In these maps each pixel represents a flux (km^2My^{-1}) in a coast-parallel direction (approximately to the northeast). Integrating the pixels along an east-to-west transect across the continental margin, provides the total northward sediment flux (km^3My^{-1}) through that transect line (Fig. 16C and D).

During the first modeled interval (5.3–1.8 Ma), calculated sediment flux offshore Rafah was ~2500 km^3My^{-1} (Fig. 16D, blue line). Most of these sediments were trapped and deposited offshore Israel while very little volume continued north of Haifa. This has changed during the 1.8–0 Ma interval with flux offshore Rafah reaching ~5300 km^3My^{-1} and the flux offshore Haifa increased to ~3000 km^3My^{-1} (Fig. 16D, red line). Subtracting the modeled flux north of Haifa from the flux offshore Rafah indicates that about 2300 km^3My^{-1} of sediments were trapped in the shelf south of Haifa; this is not very different from the volume deposited during the first interval (2500 km^3My^{-1}).

The modeled total sediment fluxes are difficult to compare with present-day observations that measure only the sand flux, but they do produce satisfactory results for deposition and the quite correct thickness. Sand fluxes are easier to compare (Fig. 16C). They show that during the early interval less than 100 km^3My^{-1} had entered the Israeli margin from the south (Rafah) and these were trapped almost immediately (Fig. 16C, blue line). During the 1.8–0 Ma interval nearly 350

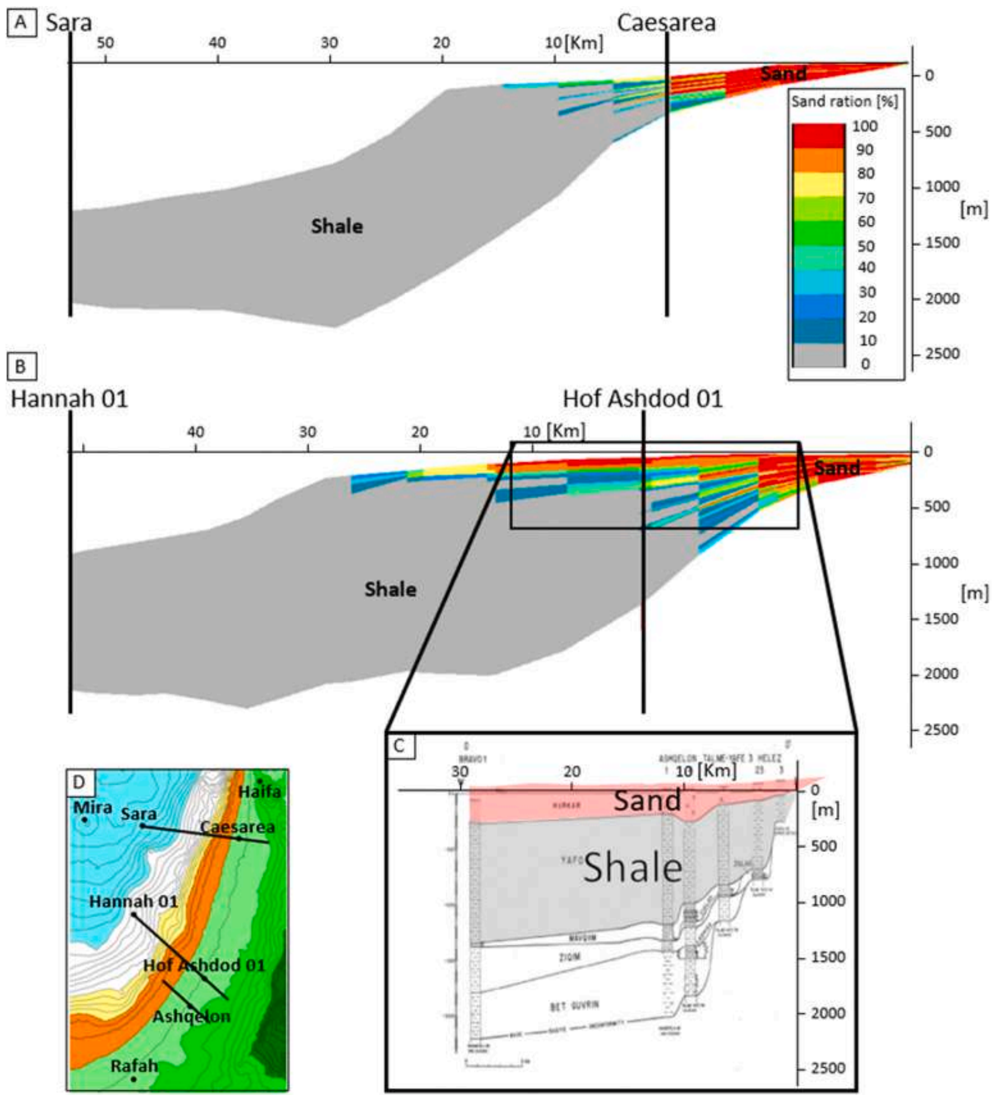

Fig. 12. Simulated MPST cross sections (A and B) showing the resulted Kurkar (mainly sand) and Yafo Formations (mainly shale); black rectangle in B shows the location of the enlarged cross section (C) (after Gvirtzman and Buchbinder, 1978). The sand fingers into the shaly section of Yafo Formation is the result of including the eustatic curve of Haq et al. (1987) in the model. (D) Location map. Color bar is the same for cross sections A and B. (For interpretation of the references to color in this figure legend, the reader is referred to the Web version of this article.)

km^3My^{-1} of sand entered from offshore Rafah, most of this volume was trapped before reaching Ashdod, and about 40 km^3My^{-1} of sand arrived at Haifa (Fig. 16C, red line). These results are slightly lower than the present-day observations and may be improved by a sensitivity analysis that will include changes in the sand/shale ratio considered in the model input. In general, approximately 6% of the modeled sediment flux offshore Israel is sand, concentrated in near coastal areas.

The two flux maps (Fig. 16A and B) indicate a northward shift of transport and alongshore deposition propagation between the first and second sequences. Initially sediments were primarily trapped offshore Sinai and only then offshore Israel. Moreover, during the first interval sediment transport offshore Israel occurred mainly at deep waters (i.e., west of the first isobath after isobath 0 m - isobaths 200 m in Fig. 16A), whereas during the second interval transport mostly occurred on the shelf (i.e., east of isobaths 200 m depth in Fig. 16B).

5. Discussion

5.1. Continental shelves and river deltas

Development of continental shelves adjacent to river deltas is quite common, but the dependency of the shelf evolution on sediment transport from the nearby delta is not fully resolved. Here we study the accretion of the Levant shelf alongside the Nile Delta, exploring coevality and the dependency of the Levant shelf on sediment transport from the Nile Delta. First, we show that longshore sand transport is only a small fraction of a much larger process, termed here MPST. In the Levant shelf, sand accumulation in the past 5 My comprises only about 6% of the total volume of sediments that arrived from the Nile Delta. Furthermore, without the large transport of silt and clay in the deeper waters, deposition offshore Israel probably would have been negligible, and the Levant shelf never would have developed (see Basic in Fig. 14).

Our observations and modeling results indicate that MPST has begun coevally with delta formation, but at first, developed quite slowly. Initially, a continental shelf formed offshore Sinai, then offshore Israel, and most recently along the Lebanon coast, where it is probably still in its initial buildup stage. Throughout this time, longshore sand transport and deposition has taken place near the coastline, but only recently (sometime in the last hundreds of thousands of years), when the shelf became shallow enough, sand transport and deposition expanded westward. We hypothesize that this westward expansion was more pronounced during eustatic sea-level drops.

Our results emphasize the importance of deep-water, margin-parallel currents for sediment transport (e.g., Rebesco, 2018, 2005; Rebesco et al., 2014; Rebesco and Camerlenghi, 2008; Schattner and Lazar, 2016 and references within), which is studied less than longshore sand transport (see introduction) and is still poorly understood. The argument that sand transport along the Levant margin occurs within a wide depth

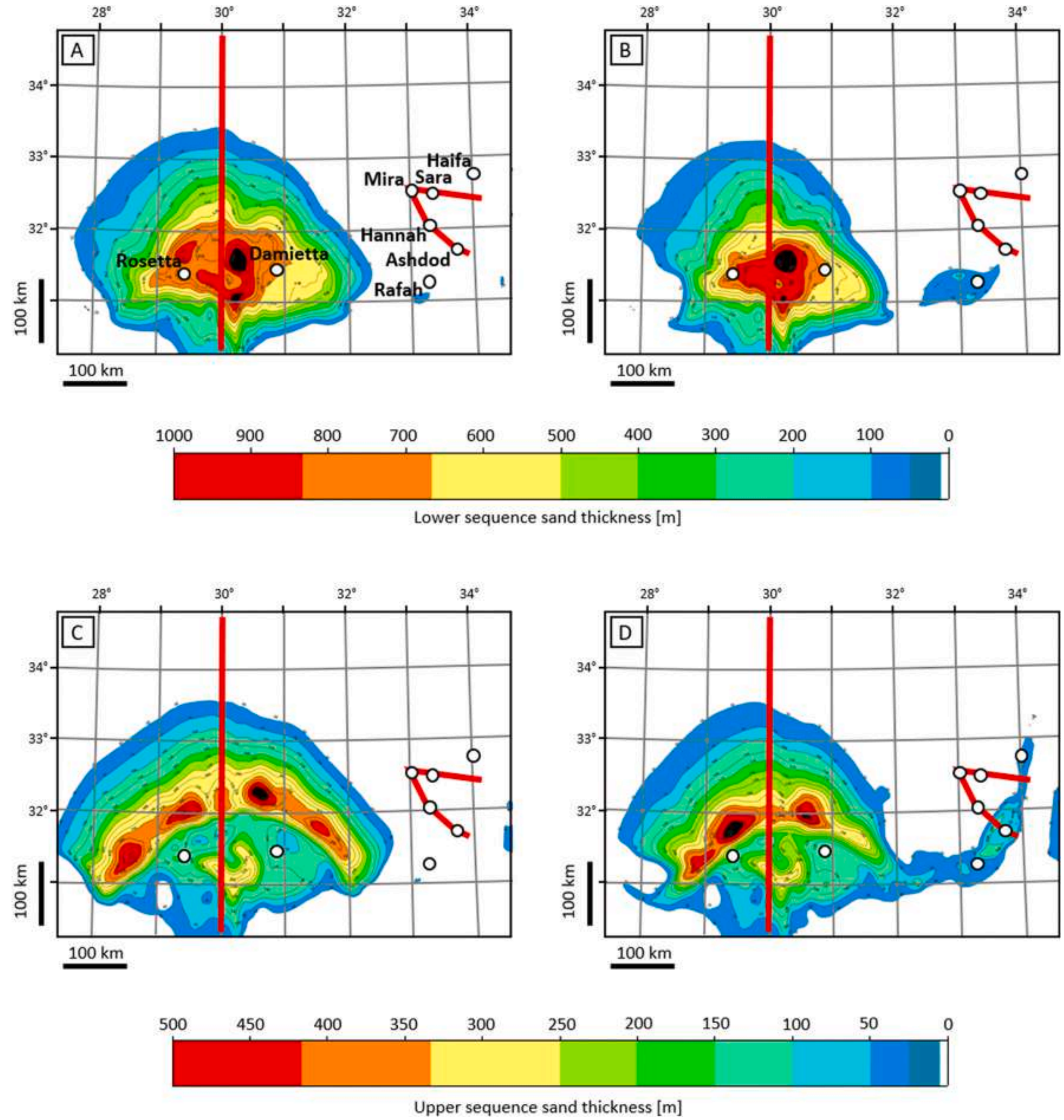

Fig. 13. The total sand thickness as simulated for the lower sequence (5.3–2.6 Ma) and for the upper sequence (2.6–0.0 Ma), using the model without and with the MPST laws. (A) Lower sequence, using the basic model. (B) Lower sequence, using the MPST model. (C) Upper sequence, using the basic model. (D) Upper sequence, using the MPST model.

range (0–400 m), was first proposed by Schattner et al. (2015), arguing that sediments are transported by the Levant jet system (LJS), which is a fast water current related to the present day thermohaline circulation in the Eastern Mediterranean. According to Schattner et al. (2015) this jet system initiated during the Pleistocene-Holocene transition (~11 ka), intensifying after the last glacial maximum (LGM). Our results show that MPST started coevally with the Nile Delta formation (5.3 Ma) and intensified at the beginning of the Pleistocene (2.6 Ma). We do not have any knowledge of the water circulation during the Pliocene and Pleistocene. However, based on our knowledge of the depositional history, we infer the paleo-sediment fluxes. These fluxes indicate margin-parallel transport much earlier than the Holocene, even at depths greater than 400 m. At the nearest shore environments, where they are dependent on eustatic sea levels, it is possible that the last emplacement of the jet occurred following the last glacial. If the current interglacial is a clue to the past, this could have been a cyclic occurrence during the Quaternary with early interglacials experiencing an increase in Nile River discharge and sediment supply to its delta accompanied by pronounced LJS that intensified the MPST. Such a cyclic process may have facilitated the construction of the Levant continental shelf.

Obviously, our model is not driven by physical processes. However, it presents a first step in transforming available data about sediment deposition in and on shelves (thickness and lithology) into sediment fluxes. This is essential for future physically based simulations that can examine how surficial, intermediate, and deep marine currents transport sediments along various morphologies of continental margins.

5.2. *Margin-parallel vs. margin-perpendicular sediment transport*

In the Levant margin, sand is forming a relatively thin sequence at the top of the shelf, reaching ~180 m at the coastline and wedging out landwards. Sand grains comprise 90–100% of this sequence (i.e., the Kurkar Group; Fig. 12). Conversely, sand is spread throughout the entire thickness (>3.5 km) of the PQ section of the Nile Delta, from its base to

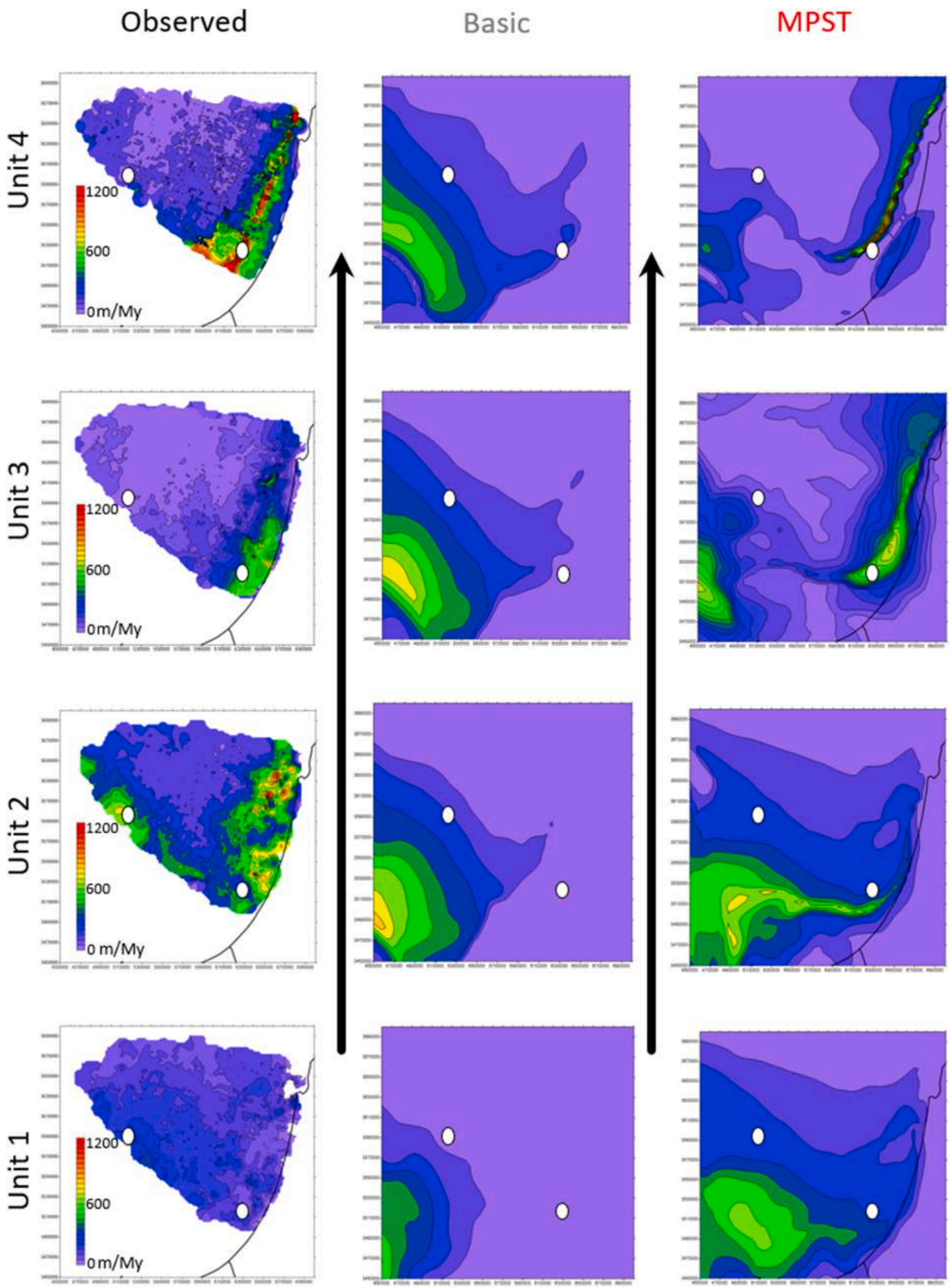

Fig. 14. Sedimentation rates generated by both modeled scenarios in comparison with the observed sedimentation, divided into the four chronostratigraphic units determined by Ben Zeev and Gvirtzman (2020). White dotes mark the locations points taken, one in the deep basin and a second at the continental margin, for calculating sedimentation rates measured in Fig.15.

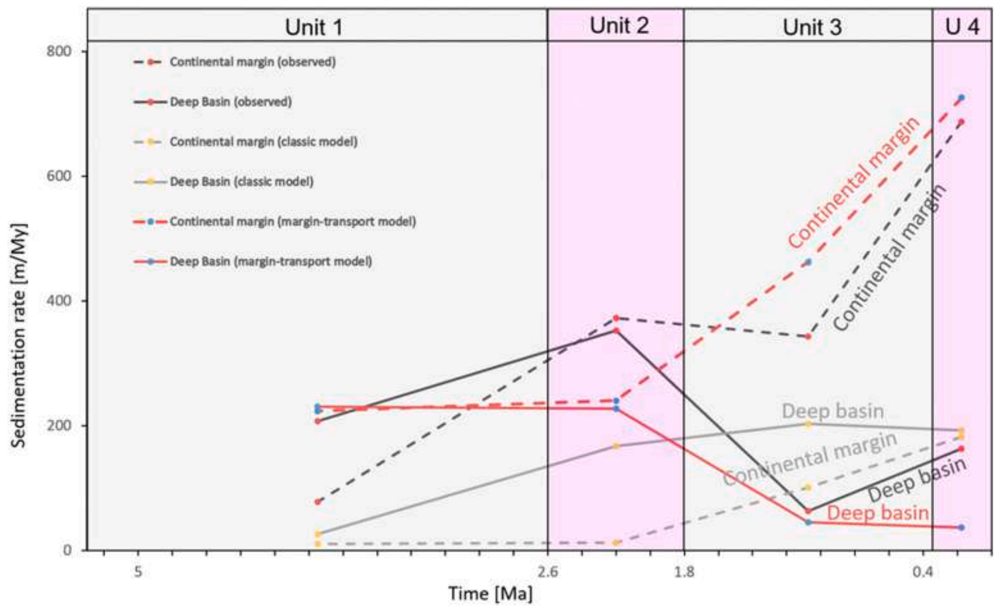

Fig. 15. Comparing sedimentation rates for the models without and MPST (red and gray, respectively) and the observed (black) sedimentation rate, in two locations (marked in Fig. 14): Deep basin (solid line) and continental margin (dashed line). (For interpretation of the references to color in this figure legend, the reader is referred to the Web version of this article.)

its top and from its eastern to western edges, comprising a maximum of 50% of the sequence (Fig. 6B). We propose that this profound difference in sand content is an expression of the available energy for transport. Sediment discharge from the river mouth down and straight to the deep basin is larger in comparison with margin-parallel discharge that keeps a nearly constant elevation. Accordingly, offshore the Nile River mouth, sand grains were transported straight downslope over large distances since the early Pliocene. On the other hand, the much weaker margin-parallel currents transported only fine grains that had built the shaly Levant shelf. One exception within the margin-parallel system is the highly energetic nearshore current that transported sand continuously since the Pliocene. This, however, is limited, here and probably elsewhere, to a very narrow zone and very shallow water depth. Thus, the combination of nearshore energetic currents and deeper weaker currents produce an efficient differentiation between shale and sand deposits, although they source at the same river mouth. Such differentiation characterizes margin-parallel sub-horizontal sediment transport in contrast with the margin-perpendicular steep-gradient transport.

An additional basin-wide expression of the margin-parallel vs. the common margin-perpendicular transport is deltas growing thicker towards the open sea more than they grow wider along the adjacent continental margins. The Nile Delta started developing immediately following the recovery from the Messinian salinity crisis (early Pliocene) and then it had propagated 150–200 km from the river mouth northward within about 1 My (Fig. 9). At the same time the Levant coast started receiving small amounts of sand (Pleshet Formation, Gvirtzman and Buchbinder, 1969). The shelf, which has existed earlier (probably was initially forming in the Miocene) presumably was very narrow (Buchbinder and Zilberman, 1997; Gvirtzman and Buchbinder, 1969). Only 2–3 My after the beginning of delta formation a notable shelf began developing in the Levant margin (Figs. 9and11).

5.3. Implications for shelf exposure during sea level drops

The youngest stage (hundreds of thousands of years) of delta development is the extension of sand deposition 10–20 km westward during eustatic lowstands (Fig. 13). These results are consistent with the proposal of Amit et al. (2011) that only around 180–200 ky, the Nile Delta has been accreted to levels that its surface could have been exposed during eustatic low stands. Only then, the sand surface and deposits of the delta and the northern Sinai shelf could have been subaerially exposed and initiate their eolian transport under the increasingly gusty glacial climate in northern Sinai. This gusty sand transport has generated the northern Sinai dune fields and abraded the sand grains into coarse silts that comprise the loess of the Negev (Amit et al., 2011; Crouvi et al., 2008). We hypothesize that some of the shelf sand was also exposed and was involved in the accretion of the Eastern Mediterranean coastal plain (Harel et al., 2017).

6. Conclusions

1. Longshore sand transport is a part of a much broader process termed here margin-parallel sediment transport (MPST). Sand is transported in a nearshore shallow water belt, where marine currents are highly energetic. Shale transport occurs at greater depths over the deeper shelf and the continental slope, where marine currents are weaker.
2. Without the large transport of silt and clay in the deeper waters, deposition offshore Israel probably would have been negligible, and the Levant shelf never would have developed.
3. The delay in the formation of the Levant continental shelf relative to the Nile Delta is not a result of external forcing. MPST has begun coevally with delta formation but developed slower. Initially, a continental shelf formed offshore Sinai, then offshore Israel, and most recently along the Lebanese coast.
4. Throughout this time, longshore sand transport and deposition has taken place very close to the coastline, but only recently (last hundreds of thousands of years), when the shelf became shallow enough, sand transport and deposition expanded 10–20 km westwards. This implies subaerial exposure of sandy landscape during recent eustatically low stands.
5. Down slope sediment transport into deep basins is relatively energetic and carries sand, silt, and clay, whereas margin-parallel currents are relatively weak and carry mainly silt and clay. One exception within the margin-parallel system is the highly energetic nearshore current that transport sand. Thus, MPST is an efficient differentiator between shale and sand.

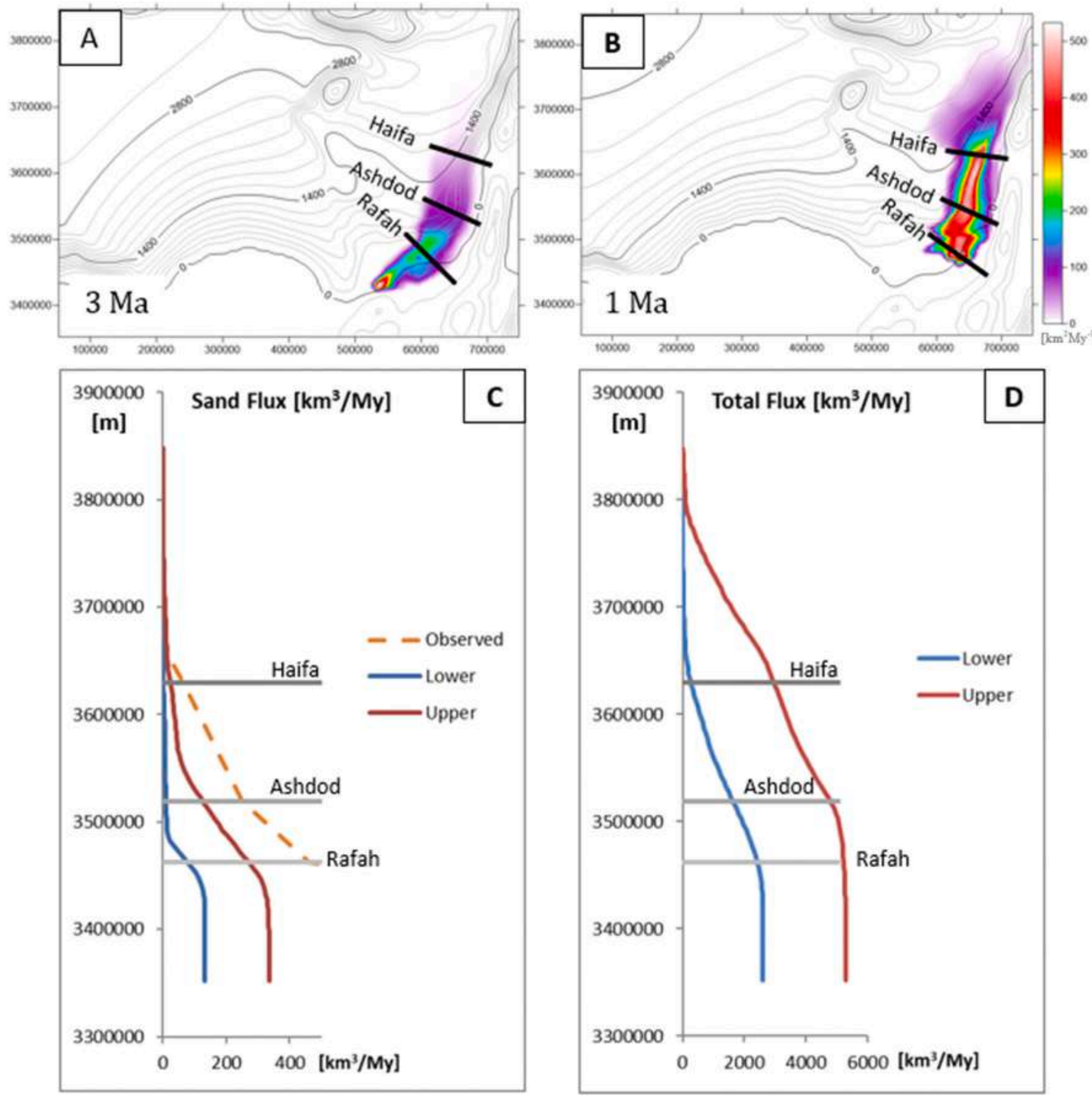

Fig. 16. Sediment flux maps obtained by trial and error for lower (A) and upper (B) sequences overprinted on isobaths representing 3 Ma and 1 Ma, respectively. Each pixel in the maps represents the flux (km^2My^{-1}) in a coast-parallel direction. Total sediment (D) and sand (C) fluxes crossing margin-perpendicular transects during deposition of lower and upper sequences. Curve representing the observed sand flux is based on references listed in the introduction.

Credit author statement

Elchanan Zucker: Conceptualization, Methodology, Formal analysis, Investigation, Resources, Writing - Original Draft, Visualization. **Zohar Gvirtzman**: Resources, Writing - Review & Editing, Supervision. **Didier Granjeon**: Software, Data Curation. **Daniel Garcia-Castellanos**: Software, Data Curation. **Yehouda Enzel**: Writing - Review & Editing, Supervision.

Declaration of competing interest

The authors declare that they have no known competing financial interests or personal relationships that could have appeared to influence the work reported in this paper.

Acknowledgments

This study was supported by the Israeli Ministry of Energy and by the Mediterranean Research Center of Israel (MERCI). The article is further based upon work of COST Action "Uncovering the Mediterranean salt giant" (MEDSALT) supported by the European Cooperation in Science and Technology.

Appendix A. Supplementary data

Supplementary data to this article can be found online at https://doi.org/10.1016/j.marpetgeo.2020.104876.

References

Aal, A.A., El Barkooky, A., Gerrits, M., Meyer, H., Schwander, M., Zaki, H., 2000. Tectonic evolution of the eastern mediterranean basin and its significance for hydrocarbon prospectivity in the ultradeepwater of the nile delta. The Leading Edge 19 (10), 1086–1102. https://doi.org/10.1190/1.1438485.

Adams, E.W., Schlager, W., Wattel, E., 1998. Submarine slopes with an exponential curvature. Sedimentary Geology 117 (3–4), 135–141.

Almogi-Labin, A., Calvo, R., Elyashiv, H., Amit, R., Harlavan, Y., Herut, B., 2012. ediment Characterization of the Israeli Mediterranean Shelf (10-100 m). Geological Survey Report 43.

Amadori, C., Garcia-Castellanos, D., Toscani, G., Sternai, P., Fantoni, R., Ghielmi, M., Di Giulio, A., 2018. Restored topography of the Po Plain-Northern Adriatic region during the Messinian base-level drop—implications for the physiography and

compartmentalization of the palaeo-Mediterranean basin. Basin Research 30 (6), 1247–1263.
Amante, C., Eakins, B.W., 2009. ETOPO1 Arc-Minute Global Relief Model: Procedures, Data Sources and Analysis.
Amit, R., Enzel, Y., Crouvi, O., Simhai, O., Matmon, A., Porat, N., McDonald, E., Gillespie, A.R., 2011. The role of the Nile in initiating a massive dust influx to the Negev late in the middle Pleistocene. Geol. Soc. Am. Bull. 123 (5–6), 873–889. https://doi.org/10.1130/B30241.1.
Bar, O., 2009. The shaping of the continental margin of central Israel since the Late Eocene—tectonics, morphology and stratigraphy. Geol. Surv. Isr. Rep. GSI/32/2009.
Bar, O., Gvirtzman, Z., Feinstein, S., Zilberman, E., 2013. Accelerated subsidence and sedimentation in the levant basin during the late tertiary and concurrent uplift of the arabian platform: tectonic versus counteracting sedimentary loading effects. Tectonics 32, 334–350. https://doi.org/10.1002/tect.20026.
Barber, P.M., 1981. Messinian subaerial erosion of the proto-Nile Delta. Mar. Geol. 44, 253–272. https://doi.org/10.1016/0025-3227(81)90053-0.
Begin, Z.B., Meyer, D.F., Schumm, S.A., 1981. Development of longitudinal profiles of alluvial channels in response to base-level lowering. Earth Surf. Process. Landforms 6, 49–68. https://doi.org/10.1002/esp.3290060106.
Ben-Avraham, Z., 1978. The structure and tectonic setting of the levant continental margin, Eastern Mediterranean. Tectonophysics 46, 313–331. https://doi.org/10.1016/0040-1951(78)90210-X.
Ben-Gai, Y., Ben-Avraham, Z., Buchbinder, B., Kendall, C.G.S.C., 2005. Post-Messinian evolution of the Southeastern Levant Basin based on two-dimensional stratigraphic simulation. Mar. Geol. 221, 359–379. https://doi.org/10.1016/j.margeo.2005.03.003.
Ben Moshe, L., Haviv, I., Enzel, Y., Zilberman, E., Matmon, A., 2008. Incision of alluvial channels in response to a continuous base level fall: field characterization, modeling, and validation along the Dead Sea. Geomorphology 93, 524–536. https://doi.org/10.1016/J.GEOMORPH.2007.03.014.
Ben Zeev, Y., Gvirtzman, Z., 2020. When two salt tectonics systems meet: gliding downslope the levant margin and salt out-squeezing from under the nile delta. Tectonics 39 (12), e2019TC005715. https://doi.org/10.1029/2019TC005715.
Buchbinder, B., Gvirtzman, G., 1976. The break-up of the tethys ocean into the Mediterranean sea, the red sea, and the mesopotamian basin during the Miocene: a sequence of fault movements and desiccation events. In: Abstract of the Fi Rst Congress Pacifi C Neog, pp. 32–35. Stratigr.
Buchbinder, B., Martinotti, G.M., Siman-Tov, R., Zilberman, E., 1993. Temporal and spatial relationships in Miocene reef carbonates in Israel. Palaeogeogr. Palaeoclimatol. Palaeoecol. 101, 97–116. https://doi.org/10.1016/0031-0182(93)90154-B.
Buchbinder, B., Zilberman, E., 1997. Sequence stratigraphy of Miocene-Pliocene carbonate-siliciclastic shelf deposits in the eastern Mediterranean margin (Israel): effects of eustasy and tectonics. Sediment. Geol. 112, 7–32. https://doi.org/10.1016/S0037-0738(97)00034-1.
Carmel, Z., Inman, D.L., Golik, A., 1985. Directional wave measurement at Haifa, Israel, and sediment transport along the Nile littoral cell. Coast. Eng. 9, 21–36. https://doi.org/10.1016/0378-3839(85)90025-0.
Coulthard, T.J., 1999. Modelling Upland Catchment Response to Holocene Environmental Change. (Doctoral dissertation, University of Leeds).
Crouvi, O., Amit, R., Enzel, Y., Porat, N., Sandler, A., 2008. Sand dunes as a major proximal dust source for late Pleistocene loess in the Negev Desert, Israel. Quat. Res. 70, 275–282. https://doi.org/10.1016/j.yqres.2008.04.011.
Csato, I., Catuneanu, O., Granjeon, D., 2014. Millennial-scale sequence stratigraphy: numerical simulation with dionisos. J. Sediment. Res. 84, 394–406. https://doi.org/10.2110/jsr.2014.36.
Csato, I., Granjeon, D., Catuneanu, O., Baum, G.R., 2013. A three-dimensional stratigraphic model for the Messinian crisis in the Pannonian Basin, eastern Hungary. Basin Res. 25, 121–148. https://doi.org/10.1111/j.1365-2117.2012.00553.x.
Culling, W.E.H., 1960. Analytical theory of erosion. J. Geol. 68, 336–344. https://doi.org/10.1086/626663.
Dai, A., Trenberth, K.E., 2002. Estimates of freshwater discharge from continents: latitudinal and seasonal variations. J. Hydrometeorol. 3, 660–687.
Davis, M., Matmon, A., Rood, D.H., Avnaim-Katav, S., 2012. Constant cosmogenic nuclide concentrations in sand supplied from the Nile River over the past 2.5 m.y. Geology 40, 359–362. https://doi.org/10.1130/G32574.1.
Deville, E., Mascle, A., Callec, Y., Huyghe, P., Lallemant, S., Lerat, O., Mathieu, X., Padron De Carillo, C., Patriat, M., Pichot, T., Loubrieux, B., Granjeon, D., 2015. Tectonics and sedimentation interactions in the east Caribbean subduction zone: an overview from the Orinoco delta and the Barbados accretionary prism. Mar. Petrol. Geol. 64, 76–103. https://doi.org/10.1016/j.marpetgeo.2014.12.015.
Druckman, Y., Buchbinder, B., Martinotti, G.M., Siman Tov, R., Aharon, P., 1995. The buried Afiq Canyon (eastern Mediterranean, Israel): a case study of a Tertiary submarine canyon exposed in Late Messinian times. Mar. Geol. 123, 167–185. https://doi.org/10.1016/0025-3227(94)00127-7.
El Din, S.H.S., Mahar, A.M., 1997. Evaluation of sediment transport along the Nile Delta coast, Egypt. J. Coast Res. 23–26.
Elfassi, Y., Gvirtzman, Z., Katz, O., Aharonov, E., 2019. Chronology of post-Messinian faulting along the Levant continental margin and its implications for salt tectonics. Mar. Petrol. Geol. 109, 574–588. https://doi.org/10.1016/J.MARPETGEO.2019.05.032.
Emery, K.O., Bentor, Y.K., 1960. The Continental Shelf of Israel. State of Israel. Ministry of Development, Geological Survey.
Emery, K.O., Neev, D., Bentor, Y.K., 1960. Mediterranean Beaches of Israel. State of Israel. Ministry of Agriculture, Division of Fisheries, the Sea Fisheries Research Station.
Frey-Martınez, J., Hall, B., Cartwright, J., Huuse, M., 2007. Clastic intrusion at the base of deep-water sands: a trap-forming mechanism in the eastern mediterranean. Am. Assoc. Pet. Geol. 49–63. https://doi.org/10.1306/1209849M873255.
Frey Martinez, J., Cartwright, J., Hall, B., 2005. 3D seismic interpretation of slump complexes: examples from the continental margin of Israel. Basin Res. 17, 83–108. https://doi.org/10.1111/j.1365-2117.2005.00255.x.
Galloway, W.E., 1998. Siliciclastic slope and base-of-slope depositional systems: component facies, stratigraphic architecture, and classification. Am. Assoc. Petrol. Geol. Bull. 82, 569–595.
Garcia-Castellanos, D., Vergés, J., Gaspar-Escribano, J., Cloetingh, S., 2003. Interplay between tectonics, climate, and fluvial transport during the Cenozoic evolution of the Ebro Basin (NE Iberia). J. Geophys. Res. Solid Earth 108 (B10). https://doi.org/10.1029/2002JB002073.
Gardosh, M.A., Druckman, Y., Buchbinder, B., 2009. The late tertiary deep-water siliciclastic system of the levant margin–an emerging play offshore Israel. Am. Assoc. Pet. Geol. Search Discov. Artic. 10211.
Gerber, T.P., Amblas, D., Wolinsky, M.A., Pratson, L.F., Canals, M., 2009. A model for the long-profile shape of submarine canyons. J. Geophys. Res. 114, F03002. https://doi.org/10.1029/2008JF001190.
Goldsmith, V., Golik, A., 1980. Sediment transport model of the southeastern Mediterranean coast. Mar. Geol. 37, 147–175. https://doi.org/10.1016/0025-3227(80)90015-8.
Golik, A., 2002. Pattern of sand transport along the Israeli coastline. Isr. J. Earth Sci. 51.
Golik, A., 1997. Dynamics and management of sand along the Israeli coastline. Bull. Oceanogr. MONACO-NUMERO Spec. 97–110.
Golik, A., 1993. Indirect evidence for sediment transport on the continental shelf off Israel. Geo Mar. Lett. 13, 159–164. https://doi.org/10.1007/BF01593189.
Golik, A., Rosen, D.S., Brachia, V., 1999. Management of the Israeli Coastal Sand Resources. CAMPIsrael, Mediterr. Action Plan, UNEP Isr. Minist. Environ. IOLR ReportH28/1999, Haifa.
Granjeon, D., 2014. 3D forward modelling of the impact of sediment transport and base level cycles on continental margins and incised valleys. In: From Depositional Systems to Sedimentary Successions on the Norwegian Continental Margin. John Wiley & Sons, Ltd, Chichester, UK, pp. 453–472. https://doi.org/10.1002/9781118920435.ch16.
Granjeon, D., 2009. Deterministic stratigraphic modeling: design and applications of a multilithological 3D diffusive model (Doctoral dissertation, Rennes 1). AAPG Search Discov (Artic).
Granjeon, D., 1997. Modélisation stratigraphique déterministe: Conception et application d'un modèle diffusif 3D multilithologique. Univ. of Rennes.
Granjeon, D., Joseph, P., 1999. Concepts and Applications of a 3-D Multiple Lithology, Diffusive Model in Stratigraphic Modeling.
Granjeon, D., Wolf, S., 2007. 3D stratigraphic modeling in complex tectonics area. In: Abstract of the AAPG Annual Convention and Exhibition. AAPG Search and Discovery Long Beach, California, USA.
Gvirtzman, G., 1970. Geological Survey of Israel Report OD/5/67, p.170.
Gvirtzman, G., Buchbinder, B., 1978. The Late Tertiary of the Coastal Plain and Continental Shelf of Israel and its Bearing on the History of the Eastern Mediterranean, Initial Reports of the Deep Sea Drilling Project.
Gvirtzman, G., Buchbinder, B., 1969. Outcrops of Neogene Formation in the Central and Southern Coastal Plain, Hashephela and Beer Sheva`Regions, Israel. Geological Survey.
Gvirtzman, Z., Csato, I., Granjeon, D., 2014. Constraining sediment transport to deep marine basins through submarine channels : the Levant margin in the Late Cenozoic. Mar. Geol. 347, 12–26.
Haq, B.U., Hardenbohl, J.A.N., Vail, P.R., 1987. Chronology of Fluctuating Sea Levels since the Triasic, , 4793rd235. Science, pp. 1156–1167.
Harel, M., Amit, R., Porat, N., Enzel, Y., 2017. Evolution in of the southeastern Mediterranean coastal plain. In: Enzel, Yehouda, Bar Yosef, Ofer (Eds.), Quaternary of the Levant: Environments, Climate Change, and Humans. Cambridge University Press, Cambridge, pp. 433–445.
Harris, A.D., Covault, J.A., Madof, A.S., Sun, T., Sylvester, Z., Granjeon, D., 2016. Three-Dimensional numerical modeling of eustatic control on continental-margin sand distribution. J. Sediment. Res. 86, 1434–1443. https://doi.org/10.2110/jsr.2016.85.
Hawie, N., Barrois, A., Marfisi, E., Murat, B., Hall, J., El-Wazir, Z., Al-Madani, N., Aillud, G., 2015. Forward stratigraphic modelling, deterministic approach to improve carbonate heterogeneity prediction; lower cretaceous, abu dhabi. In: Abu Dhabi International Petroleum Exhibition and Conference. Society of Petroleum Engineers. https://doi.org/10.2118/177519-MS.
Hawie, N., Covault, J.A., Dunlap, D., Sylvester, Z., 2018. Slope-fan depositional architecture from high-resolution forward stratigraphic models. Mar. Petrol. Geol. 91, 576–585. https://doi.org/10.1016/J.MARPETGEO.2017.12.033.
Hawie, N., Deschamps, R., Granjeon, D., Nader, F.H., Gorini, C., Müller, C., Montadert, L., Baudin, F., 2017. Multi-scale constraints of sediment source to sink systems in frontier basins: a forward stratigraphic modelling case study of the Levant region. Basin Res. 29, 418–445. https://doi.org/10.1111/bre.12156.
Hsü, K.J., Ryan, W.B.F., Cita, M.B., 1973. Late Miocene dessication of the mediterranean. Nature 242, 240–244.
Inman, D.L., Brush, B.M., 1973. The coastal challenge. Science 181 (4094), 20–32. https://doi.org/10.1126/science.181.4094.20.
Inman, D.L., Elwany, M.H.S., Khafagy, A.A., Golik, A., 1993. Nile Delta profiles and migrating sand blankets. In: Coastal Engineering 1992, pp. 3273–3284.

Inman, D.L., Jenkins, S.A., 1984. The Nile littoral cell and man's impact on the coastal littoral zone in the SE Mediterranean. In: Proceedings of the 17th International Coastal Engineering Conference. ASCE, Sydney, Australia, pp. 1600–1617.
Inman, D.L., Nordstrom, C.E., Flick, R.E., 1976. Currents in submarine canyons: an air-sea-land interaction. Annu. Rev. Fluid Mech. 8, 275–310.
Jordan, T.E., Flemings, P.B., 1991. Large-scale stratigraphic architecture, eustatic variation, and unsteady tectonism: a theoretical evaluation. J. Geophys. Res. Solid Earth 96, 6681–6699. https://doi.org/10.1029/90JB01399@10.1002/(ISSN)2169-9356.LTSLC1.
Kaufman, P., Grotzinger, J., McCormick, D., 1991. Depth-dependent diffusion algorithm for simulation of sedimentation in shallow marine deposition systems. Sediment. Model. Camputer Simulations Methods Improv. Param. Defin. 489–508.
Kellner, A., Khawaga, H. El, Brink, G., Brink-larsen, S., Hesham, M., Abu, H., Saad, E., Atef, A., Young, H., Finlayson, B., 2009. Depositional history of the west nile delta – upper oligocene to upper Pliocene. In: AAPG International Conference and Exhibition (Cape Town, South Africa).
Kempler, D., 1998. Eratosthenes Seamount: the possible spearhead of incipient continental collision in the eastern Mediterranean. Proc. Ocean Drill. Progr. Sci. Results 160, 709–722. https://doi.org/10.2973/odp.proc.sr.160.031.1998.
Kenyon, P.M., Turcotte, D.L., 1985. Morphology of a delta prograding by bulk sediment transport. Geological Society of America Bulletin 96 (11), 1457–1465. https://doi.org/10.1130/0016-7606(1985)96<1457:MOADPB>2.0.CO;2.
Klein, M., Zviely, D., Kit, E., Shteinman, B., 2007. Sediment transport along the coast of Israel: examination of fluorescent sand tracers. J. Coast Res. 1462–1470.
Lai, S.Y.J., Capart, H., 2007. Two-diffusion description of hyperpycnal deltas. Journal of Geophysical Research: Earth Surface 112 (F3). https://doi.org/10.1029/2006JF000617.
Laurent, D., Marsset, T., Droz, L., Granjeon, D., Molliex, S., Picot, M., Rabineau, M., 2020. 4D forward stratigraphic modelling of the Late Quaternary Congo deep-sea fan: role of climate/vegetation coupling in architectural evolution. Mar. Geol. 429, 106334.
Manohar, M., 1981. Coastal processes at the nile delta coast. Shore Beach 49, 8–15.
Milliman, J.D., Syvitski, J.P.M., 1992. Geomorphic/Tectonic control of sediment discharge to the ocean: the importance of small mountainous rivers. J. Geol. 100, 525–544. https://doi.org/10.1086/629606.
Mitchell, N.C., Huthnance, J.M., 2008. Oceanographic currents and the convexity of the uppermost continental slope. J. Sediment. Res. 78, 29–44. https://doi.org/10.2110/jsr.2008.006.
Mitchell, N.C., Huthnance, J.M., 2007. Comparing the smooth, parabolic shapes of interfluves in continental slopes to predictions of diffusion transport models. Mar. Geol. 236, 189–208. https://doi.org/10.1016/J.MARGEO.2006.10.028.
Murray, A.B., Paola, C., 1994. A cellular model of braided rivers. Nature 371 (6492), 54–57.
Nachmias, J., 1969. Source rocks of the Saqiye Group sediments in the coastal plain of Israel—a heavy mineral study. Isr. J. Earth-Sci. 18, 1–16.
Paola, C., Heller, P.L., Angevine, C.L., 1992. The large-scale dynamics of grain-size variation in alluvial basins, 1: Theory. Basin Res. 4, 73–90.
Parker, G., Paola, C., Whipple, K.X., Mohrig, D., 1998. Alluvial fans formed by channelized fluvial and sheet flow. I: Theory. J. Hydraul. Eng. 124, 985–995.
Perlin, A., Kit, E., 1999. Longshore sediment transport on Mediterranean coast of Israel. J. Waterw. Port, Coast. Ocean Eng. 125, 80–87.
Rabineau, M., Berné, S., Aslanian, D., Olivet, J.L., Joseph, P., Guillocheau, F., Bourillet, J. F., Ledrezen, E., Granjeon, D., 2005. Sedimentary sequences in the Gulf of Lion: a record of 100,000 years climatic cycles. Mar. Petrol. Geol. 22, 775–804.
Rabineau, M., Berné, S., Olivet, J.-L., Aslanian, D., Guillocheau, F., Joseph, P., 2006. Paleo sea levels reconsidered from direct observation of paleoshoreline position during Glacial Maxima (for the last 500,000 yr). Earth Planet Sci. Lett. 252, 119–137.
Rebesco, M., 2018. Sedimentary environments: contourites. Ref. Modul. Earth Syst. Environ. Sci. https://doi.org/10.1016/B978-0-12-409548-9.09094-1.
Rebesco, M., 2005. SEDIMENTARY ENVIRONMENTS | contourites. Encycl. Geol. 513–527. https://doi.org/10.1016/B0-12-369396-9/00497-4.
Rebesco, M., Camerlenghi, A., 2008. Contourites. Elsevier.
Rebesco, M., Hernández-Molina, F.J., Van Rooij, D., Wåhlin, A., 2014. Contourites and associated sediments controlled by deep-water circulation processes: state-of-the-art and future considerations. Mar. Geol. 352, 111–154. https://doi.org/10.1016/J.MARGEO.2014.03.011.
Rivenæs, J.C., 1997. Impact of sediment transport efficiency on large-scale sequence architecture: results from stratigraphic computer simulation. Basin Res. 9, 91–105. https://doi.org/10.1046/j.1365-2117.1997.00037.x.
Robertson, A.H.F., 1998. Tectonic significance of the Eratosthenes Seamount: a continental fragment in the process of collision with a subduction zone in the eastern Mediterranean (Ocean Drilling Program Leg 160). Tectonophysics 298, 63–82. https://doi.org/10.1016/S0040-1951(98)00178-4.
Rosentraub, Z., Brenner, S., 2007. Circulation over the southeastern continental shelf and slope of the Mediterranean Sea: direct current measurements, winds, and numerical model simulations. J. Geophys. Res. 112, C11001. https://doi.org/10.1029/2006JC003775.
Ryan, W.B.F., Cita, M.B., 1978. The nature and distribution of Messinian erosional surfaces — indicators of a several-kilometer-deep Mediterranean in the Miocene. Mar. Geol. 27, 193–230. https://doi.org/10.1016/0025-3227(78)90032-4.
Said, R., 1981. The Geological Evolution of the River Nile. Springer Science & Business Media, New York, NY.
Schattner, U., 2010. What triggered the early-to-mid Pleistocene tectonic transition across the entire eastern Mediterranean? Earth Planet Sci. Lett. 289, 539–548. https://doi.org/10.1016/J.EPSL.2009.11.048.
Schattner, U., Gurevich, M., Kanari, M., Lazar, M., 2015. Levant jet system-effect of post LGM seafloor currents on Nile sediment transport in the eastern Mediterranean. Sediment. Geol. 329, 28–39. https://doi.org/10.1016/j.sedgeo.2015.09.007.
Schattner, U., Lazar, M., 2016. Hierarchy of source-to-sink systems — example from the Nile distribution across the eastern Mediterranean. Sediment. Geol. 343, 119–131. https://doi.org/10.1016/j.sedgeo.2016.08.006.
Schlager, W., Adams, E.W., 2001. Model for the sigmoidal curvature of submarine slopes. Geology 29 (10), 883–886.
Sestini, G., 1989. Nile Delta: a review of depositional environments and geological history. Geol. Soc. London, Spec. Publ. 41, 99–127. https://doi.org/10.1144/GSL.SP.1989.041.01.09.
Seymour, R.J., 2005. Longshore sediment transport. The Encyclopedia of Coastal Science 600.
Shoshany, M., Golik, A., Degani, A., Lavee, H., Gvirtzman, G., 1996. New evidence for sand transport direction along the coastline of Israel. J. Coast Res. 311–325.
Shukri, N.M., 1950. The mineralogy of some Nile sediments. Q. J. Geol. Soc. 106, 466–467. https://doi.org/10.1144/GSL.JGS.1950.106.01-04.23.
Shukri, N.M., Philip, G., 1960. The mineralogy of some recent deposits in the Arish-Gaza area. Bull. Fac. Sci. Cairo Univ. 35, 73–85.
Spinewine, B., Sun, T., Babonneau, N., Parker, G., 2011. Self-similar long profiles of aggrading submarine leveed channels: analytical solution and its application to the Amazon channel. Journal of Geophysical Research: Earth Surface 116 (F3). https://doi.org/10.1029/2010JF001937.
Stanley, D.J., Warne, A.G., 1998. Nile delta in its destruction phase. J. Coast Res. 14, 794–825.
Stanley, J.D., 1989. Sediment transport on the coast and shelf between the nile delta and Israeli margin as determined by heavy minerals. J. Coast Res. 5, 813–828.
Steckler, M.S., Mountain, G.S., Miller, K.G., Christie-Blick, N., 1999. Reconstruction of Tertiary progradation and clinoform development on the New Jersey passive margin by 2-D backstripping. Mar. Geol. 154, 399–420. https://doi.org/10.1016/S0025-3227(98)00126-1.
Syvitski, J.P.M., Milliman, J.D., 2007. Geology, geography, and humans battle for dominance over the delivery of fluvial sediment to the coastal ocean. J. Geol. 115, 1–19.
Tibor, G., Ben-Avraham, Z., Steckler, M., Fligelman, H., 1992. Late tertiary subsidence history of the southern levant margin, eastern Mediterranean sea, and its implications to the understanding of the messinian event. Journal of Geophysical Research: Solid Earth 97 (B12), 17593–17614. https://doi.org/10.1029/92JB00978.
Tucker, G.E., Slingerland, R.L., 1994. Erosional dynamics, flexural isostasy, and long-lived escarpments: a numerical modeling study. Journal of Geophysical Research: Solid Earth 99 (B6), 12229–12243. https://doi.org/10.1029/94JB00320.
Van Heijst, M., Postma, G., Meijer, X.D., Snow, J.N., Anderson, J.B., 2001. Quantitative analogue flume-model study of river-shelf systems: principles and verification exemplified by the Late Quaternary Colorado river-delta evolution. Basin Res. 13, 243–268.
Willgoose, G., Bras, R.L., Rodriguez-Iturbe, I., 1991. Results from a new model of river basin evolution. Earth Surf. Process. Landforms 16, 237–254. https://doi.org/10.1002/esp.3290160305.
Woodward, J.C., Macklin, M.G., Krom, M.D., Williams, M.A.J., Gupta, A., 2007. The Nile: evolution, Quaternary river environments and material fluxes. Large rivers Geomorphol. Manag. 13, 712.
Young, A., Carson, M.A., Kirkby, M.J., 1973. Hillslope form and process. Geogr. J. 139, 140–141. https://doi.org/10.2307/1795822.
Zaghloul, Z.M., El-Nasharty, F.A., Isa, I.A., 1982. Post-aswan high dam changes of the nile delta coast, east of ras El bar, interpreted from aerial photographs. Remote Sens. Arid semi-arid lands 877–883.
Zhang, J., Burgess, P.M., Granjeon, D., Steel, R., 2019. Can sediment supply variations create sequences? Insights from stratigraphic forward modelling. Basin Res. 31, 274–289. https://doi.org/10.1111/bre.12320.
Zucker, E., Gvirtzman, Z., Steinberg, J., Enzel, Y., 2019. Salt tectonics in the Eastern Mediterranean Sea: where a giant delta meets a salt giant. Geology 48 (2), 134–138. https://doi.org/10.1130/G47031.1.
Zviely, D., Kit, E., Klein, M., 2007. Longshore sand transport estimates along the Mediterranean coast of Israel in the Holocene. Mar. Geol. 238, 61–73. https://doi.org/10.1016/J.MARGEO.2006.12.003.
Zviely, D., Sivan, D., Ecker, A., Bakler, N., Rohrlich, V., Galili, E., Boaretto, E., Klein, M., Kit, E., 2006. Holocene evolution of the Haifa Bay area, Israel, and its influence on ancient tell settlements. Holocene 16, 849–861.

Chapter 3

Salt tectonics in the Eastern Mediterranean Sea: Where a giant delta meets a salt giant

Published in an electronic format in Geology

Zucker, E., Gvirtzman, Z., Steinberg, J., Enzel, Y., 2019. Salt tectonics in the Eastern Mediterranean Sea: Where a giant delta meets a salt giant. Geology. https://doi.org/10.1130/G47031.1

GEOLOGY | THE GEOLOGICAL SOCIETY OF AMERICA®

https://doi.org/10.1130/G47031.1

Manuscript received 1 August 2019
Revised manuscript received 20 September 2019
Manuscript accepted 16 October 2019

© 2019 Geological Society of America. For permission to copy, contact editing@geosociety.org.

Salt tectonics in the Eastern Mediterranean Sea: Where a giant delta meets a salt giant

Elchanan Zucker[1,2], Zohar Gvirtzman[1,2], Josh Steinberg[3] and Yehouda Enzel[1]
[1]The Fredy and Nadine Herrmann Institute of Earth Sciences, The Hebrew University of Jerusalem, Jerusalem 9190401, Israel
[2]Geological Survey of Israel, Yesha'yahu Leibowitz 32, Jerusalem 9692100, Israel
[3]Ratio Oil Exploration, Tel Aviv 6579614, Israel

ABSTRACT

The circum-Nile deformation belt (CNDB) demonstrates the interaction between a giant delta and a giant salt body. The semi-radial shape of the CNDB is commonly interpreted as the product of salt squeezing out from under the Nile Delta. We demonstrate, however, that this is not the dominant process, because the delta and its deep-sea fan do not reach the deep-basin salt. The distal part of the deep-sea fan overlies the edge of the salt giant, but squeezing this edge (<150 m thickness) should have had only little effect on the regional salt tectonics. Only on the easternmost side of the deep-sea fan, toward the Levant Basin, does the squeeze-out model work. Here, the delta front reaches the thick salt layer and differential loading promotes basinward salt flow, even upslope. On the western side of the delta, downslope gliding of the sediment-salt sequence toward the Herodotus Basin is driven by the elevation gradient toward the deepest part of the basin. Our analysis shows that salt squeezing by differential loading was previously overestimated in the Eastern Mediterranean and raises the need to carefully map the boundary of salt basins prior to any interpretation. This conclusion is especially relevant in young basins where deltas and shelves have not propagated far enough into the basin.

INTRODUCTION

Giant salt bodies and giant deltas (here including the submarine cone) are key structures affecting sedimentary basins (Sestini, 1989; Hübscher et al., 2007). In particular, giant deltas evolving atop salt giants provide key locations for studying the positive feedback and interaction between sedimentation and deformation (Gemmer et al., 2004; Brun and Fort, 2011). Sediment loading induces subsurface salt flow, which, in turn, deforms the overlying rocks; subsequent deposition is affected by such repeated load-controlled, near-surface deformation, and so forth. These processes are well illustrated in the Eastern Mediterranean Sea, where the Nile deep-sea fan (NDSF) has been deposited over the Messinian salt giant since ca. 5 Ma (e.g., Gaullier et al., 2000; Loncke et al., 2006; Allen et al., 2016).

Because salt behaves as a fluid over geologic time scales (Jackson and Talbot, 1991, and references therein), salt tectonics is conveniently simplified by concepts of hydraulic head (Hudec and Jackson, 2007). Two end-member scenarios commonly describe these concepts:

(1) Differential loading due to lateral thickness variations of rocks overlying a horizontal salt layer. In this scenario, the pressure-head gradient within the salt drives salt flow ("salt squeeze-out").

(2) Basinward tilting of a salt-overburden sequence that is uniform in thickness. In this scenario, elevation-head gradient within the tilted salt layer initiates flow.

In both scenarios, overriding rocks, which are mechanically coupled to the salt, also move basinward, and a variety of deformation patterns form.

When the moving rock mass slips over a detachment surface (décollement) with minor internal deformation, the process is termed gravity gliding. When the moving mass deforms internally, the process is termed gravity spreading (Jackson, 1995; Schultz-Ela, 2001; Vendeville, 2005; Hudec and Jackson, 2007; Cartwright and Jackson, 2008; Brun and Fort, 2011; Peel, 2014; Allen et al., 2016; Jackson and Hudec, 2017). In reality, gravity spreading is dominant when salt basins are differentially loaded by sediments that produce a pressure-head gradient, whereas gravity gliding dominates in tilted basins that are associated with elevation-head gradients (Brun and Fort, 2011; Allen et al., 2016). It is noteworthy that in both cases, the basinward motion of the salt-overburden package produces updip extension (in the area from where rocks have moved) and downdip contraction (where allochthonous rocks are pushed against autochthonous rocks; e.g., Wu et al., 1990; Peel, 1995). Therefore, determining the driving force (pressure gradient or elevation gradient) only from the distribution of extension and contraction is not straightforward.

Bathymetric and subsurface observations around the NDSF indicate that the salt-overburden package is moving basinward, producing updip extension and downdip contraction (Fig. 1; e.g., Gaullier et al., 2000; Loncke et al., 2006; Allen et al., 2016). This basinward motion produces a semi-radial deformation pattern (Fig. 1A), which was termed by Gvirtzman et al. (2015) the circum-Nile deformation belt (CNDB). North of the Herodotus Basin, the thin-skinned folds of the CNDB merge with deep-seated folds of the Mediterranean Ridge (Fig. 1A), the accretionary complex surrounding the Hellenic subduction (Costa et al., 2004; Loncke et al., 2006). In the Levant Basin, contraction diminishes northward, forming a relatively flat seafloor offshore Lebanon. Only near the Latakia Ridge (Fig. 1) does deformation reappear due to subduction south of Cyprus (Hübscher et al., 2009; Maillard et al., 2011).

The CNDB is commonly interpreted as the outcome of salt being squeezed out from under the NDSF due to the thick Pliocene–Quaternary (PQ) overburden (Loncke et al., 2006, 2010; Netzeband et al., 2006; Cartwright et al., 2012; Gvirtzman et al., 2013, 2015). Consequently, salt remnants and welds are recognized where salt has been evacuated, and a thickened salt layer is observed where the flow was accommodated

CITATION: Zucker, E., Gvirtzman, Z., Steinberg, J., and Enzel, Y., 2020, Salt tectonics in the Eastern Mediterranean Sea: Where a giant delta meets a salt giant: Geology, v. 48, p. , https://doi.org/10.1130/G47031.1

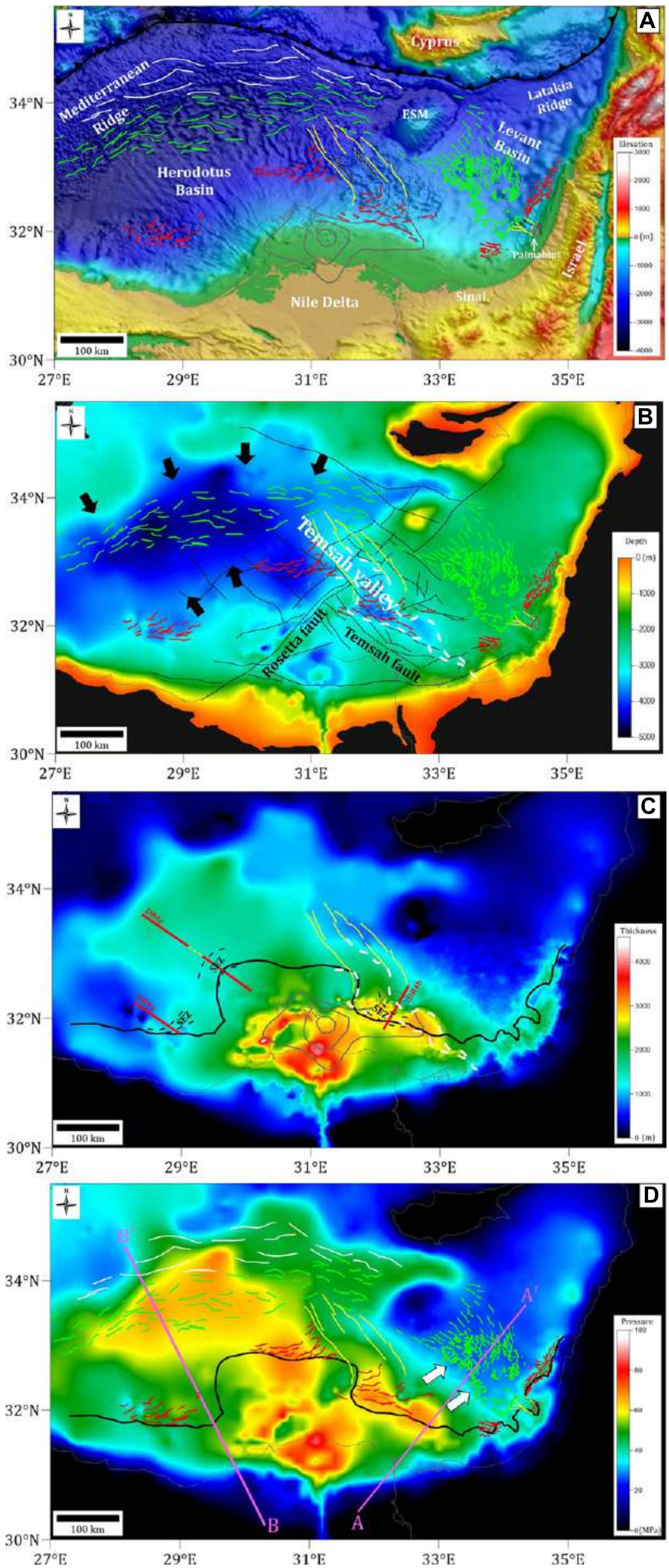

Figure 1. (A) Circum-Nile deformation belt shown on bathymetry-topography background. Red and green lines represent extension and contraction structures, respectively. Yellow lines mark strike-slip faults. These faults represent two strike-slip–bounded corridors: one southwest of the Eratosthenes Seamount (ESM), and a similar small one offshore of Israel (Palmahim disturbance). Data for the Levant Basin are from Gvirtzman et al. (2015); other parts are simplified from Loncke et al. (2006, 2010). Thickness contours (gray) represent Pliocene–Quaternary (PQ) sediments (after Segev et al., 2006). Thick black line with triangles marks the Hellenic-Cyprus subduction. (B) Base-Pliocene (approximate top of Messinian evaporites) structural map. Thin black lines are faults, after Aal et al. (2000). Dashed white contour outlines the Temsah valley approximately coinciding with the Temsah fault system and with the Temsah thin-skinned tectonic corridor. Present-day coastline (thin gray) is shown for reference. Black arrows indicate the direction of structural elevation gradients controlling salt tectonics in Herodotus Basin. (C) PQ thickness map and salt pinch-out line (black), showing that a huge PQ load overlies the area with thin salt. Salt pinch-out is the line from where salt thins rapidly (<150 m) landward (Bertoni and Cartwright, 2006; Loncke et al., 2006; Allen et al., 2016; Gvirtzman et al., 2017). Lines DR4a, DR4b, and DR4c (red) are seismic profiles provided in the Data Repository (see footnote 1). SEZ (salt evacuation zone) is the area from which salt has migrated as indicated by salt rollers, welds, and normal faults (see the Data Repository). Currently, the only place where the thick PQ section (~3 km) covers thick salt is Temsah valley (white dashed line). Note ~100 km shift between the depocenter mapped here and the depocenter (gray) mapped by Segev et al. (2006). (D) Map showing pressure exerted on top of Messinian evaporites by overlying sediments and seawater. White arrows indicate direction of high-pressure gradient separating extension from compression. AA′ and BB′ represent cross sections shown in Figure 2.

(Loncke et al., 2006; Allen et al., 2016). Here we stress the observation that the CNDB around the NDSF is asymmetric (Fig. 1A), first with respect to delta morphology; i.e., the distance from coastline to contraction fold belt is 200 km in the Levant Basin and 400 km in the Herodotus Basin. This asymmetry is also expressed in the pattern of turbidite channels surrounding the NDSF, which are disturbed and diverted by folds in the Levant Basin but not in the Herodotus Basin, where folds are located farther north (Zucker et al., 2017). The CNDB is asymmetric also with respect to the PQ depocenter (Fig. 1A), which would be somewhat surprising if the PQ overburden were the salt "squeezer". The 200-km-long and 50–100-km-wide deformation corridor (Fig. 1A) that obliquely crosses the NDSF (Loncke et al., 2006, 2010) further enhances the asymmetry of the CNDB. This unique corridor is moving basinward faster than its surroundings, as evident by the sense of motion along strike-slip faults (yellow lines in Fig. 1A) on its two sides (Loncke et al., 2010). Considering that a simple squeeze-out mechanism does not explain this asymmetry, the main question raised here is: what drives salt tectonics around the NDSF? Here we show that the role of salt squeezing has been overestimated in this case, and propose that this may have been the case in other salt basins as well.

DATA AND METHODS

To determine what drives salt tectonics, we quantify elevation and pressure gradients affecting the salt. We begin with the structure of the top of the Messinian evaporite surface, herein termed "top salt", which illustrates basin geometry and particularly elevation differences. Our compilation is based on published and unpublished data of thickness and depth, seismic profiles, well logs, maps, and sections, partly presented in two-way traveltime (in seconds) and partly in length units (for previous compilations, see Gennesseaux et al., 1998; Nashaat, 1998; Hall et al., 2005; Segev et al., 2006; Macgregor, 2012). Then, to quantify the pressure exerted on the top salt, we consider, jointly, the load of the PQ sequence and the seawater column (for data sources and calculations, see the GSA Data Repository[1]).

RESULTS

The top salt map (Fig. 1B) shows three key features. First, the contraction domain in the Herodotus Basin coincides with the deepest part of the basin, both in terms of depth to the top of the Messinian salt (~4500 m) and present-day bathymetry (~2500 m). This observation indicates that in the western NDSF, basinward motion can be simply explained by the elevation gradient; i.e, the salt-overburden package is gliding downslope. Second, the Herodotus Basin is separated from the Levant Basin by ~1 km of elevation difference across a zone that follows the northeast-trending Rosetta (Qattara-Eratosthenes) fault (Fig. 1B; Neev, 1977; Aal et al., 2000). This is related to a deep crustal structure (e.g., Sagy et al., 2015; Granot, 2016; Steinberg et al., 2018). Third, the Levant-Herodotus structural step is crosscut by a nearly orthogonal northwest-trending, >200-km-long and 50–100-km-wide valley (Fig. 1B), approximately tracing the Temsah fault (Fig. 1B; Aal et al., 2000; Dolson et al., 2005) and coinciding with the thin-skinned salt tectonic corridor detected on the seafloor (Loncke et al., 2006, 2010; Fig. 1A, yellow lines). We suggest that the close association between the tectonic valley, the deep-seated bounding faults, and the thin-skinned salt tectonic strike-slip faults indicates that the three phenomena are interconnected. A small canyon incised across the northern Sinai continental margin west of the El-Arish canyon, that is draining into this valley (Fig. DR2 in the Data Repository) indicates that the valley existed before the salt-related deformation. This is consistent with the suggested pre-Pliocene and even pre-Messinian age of this valley and its bounding faults (Aal et al., 2000; Mascle et al., 2000; Dolson et al., 2005; Loncke et al., 2010; Allen et al., 2016). Note that here we use the name "Temsah" for three related structures: (1) deep-seated faults, (2) a pre-salt tectonic valley, and (3) a post-salt thin-skinned tectonic corridor.

The PQ thickness map (Fig. 1C) shows a 4-km-thick depocenter located south of the salt pinch-out line (thick black line), a zone where salt thickness is <~150 m or absent. Originally, the edge of the salt basin extended further landward as evident by salt withdrawal structures (salt rollers, welds, and normal faults), but the width of the salt evacuation zone (SEZ, Fig. 1C) is only ~30 km (for seismic profiles supporting this conclusion, see Fig. DR4). We conclude that the thick Nile-derived overburden (delta and deep-sea fan) was mostly deposited over an area with no (or very thin) salt and therefore argue that the salt squeeze-out model is inapplicable for most of the CNDB. An exception is the Temsah valley toward the Levant Basin, where the NDSF prograded over and passed the salt pinch-out line (Fig. 1C). In this location, a few hundred meters of thick salt is covered by ~3-km-thick overburden.

The top salt pressure map (Fig. 1D) shows the pressure exerted on the salt jointly by the rock and seawater column. This joint pressure map indicates that, unlike the PQ thickness, which significantly changes from the delta (3–4 km) to the Herodotus Basin (~2 km), when the water column is added, pressure in both areas is quite similar and relatively high (70–80 MPa). Nonetheless, the pattern of the pressure map does not correlate with the pattern of the CNDB. On the contrary, the contraction belt in the Herodotus Basin (green lines) crosscuts the high-pressure zone (Fig. 1D). The only place on this map where a large pressure gradient (50 MPa over a distance of 100 km) almost perfectly coincides with the extension-to-contraction transition is the easternmost side of the NDSF; i.e., toward the Levant Basin.

DISCUSSION

Our analysis shows that the salt squeeze-out model fits observations well only in the easternmost part of the CNDB, where salt spreads out from under the thick (~3 km) overburden toward an area with a much thinner (<1 km) overburden. In other parts of the CNDB, and particularly in the western province of the NDSF, salt simply flows downslope, carrying the overburden with it.

Two cross sections constructed from the Nile Delta outward illustrate the difference between these two regions (Fig. 2). In the Levant Basin, the extension-to-contraction transition coincides with the zone of maximum pressure gradient. Here, salt is forced to flow from high to low pressure, and even upslope against the elevation gradient. As a result, the squeezed-out salt from the Temsah valley forms a small bulge with a local structural maximum.

In the Herodotus Basin, pressure gradient does not explain the extension-to-contraction transition. Here, elevation gradient plays a major role, and both the salt and the overburden glide down toward the deepest point in the basin, where allochthonous rocks reaching from both the NDSF and the Mediterranean Ridge are pushed against local rocks, forming folds and thrusts (Fig. 1B). In this area, downdip uniform gliding over a distance of hundreds of kilometers forms a wide area of translation between the extension and contraction domains (Allen et al., 2016).

Considering the different mechanism controlling salt tectonics in the western (Herodotus) and eastern (Levant) sides of the NDSF, we predict differences in timing. Squeezing of salt toward the Levant Basin could have started only when the edge of the NDSF reached the Temsah valley, which is relatively late in the progradation process. This prediction is consistent with recent observations indicating that folding in the Levant Basin started only ~1.8 m.y. ago; that is, ~3.5 m.y. after salt deposition ended (Ben-Zeev and Gvirtzman, 2019). On the other hand, gliding toward the deep Herodotus Basin should have started earlier, and possibly immediately after salt deposition.

In a wider perspective, the observation that most of the NDSF is located landward of the thick salt is not surprising, because the Messinian salt giant is limited to deep basins (Roveri et al., 2014; Gvirtzman et al., 2017) whereas deltas are formed near shore. Considering these findings, we raise the possibility that the role of differential loading may have been overestimated in other salt basins as well. We further argue that the common scenario for modeling salt flow in response to differential loading along continental margins (Brun and Fort, 2011; Rowan et al., 2012, and references therein) may be unrealistic in many cases, because the overlap between the salt wedge and the sedimentary wedge may be smaller than theoretically considered (Fig. 3). This conclusion is especially valid for young basins, where deltas and shelves have not propagated far enough to reach deep-basin salt (e.g., the Levant shelf; Cartwright and Jackson, 2008; Cartwright et al., 2012; Elfassi et al., 2019). Thus, we recommend precise mapping of

[1]GSA Data Repository item 2020041, data, methods, and enlarged maps, is available online at http://www.geosociety.org/datarepository/2020/, or on request from editing@geosociety.org.

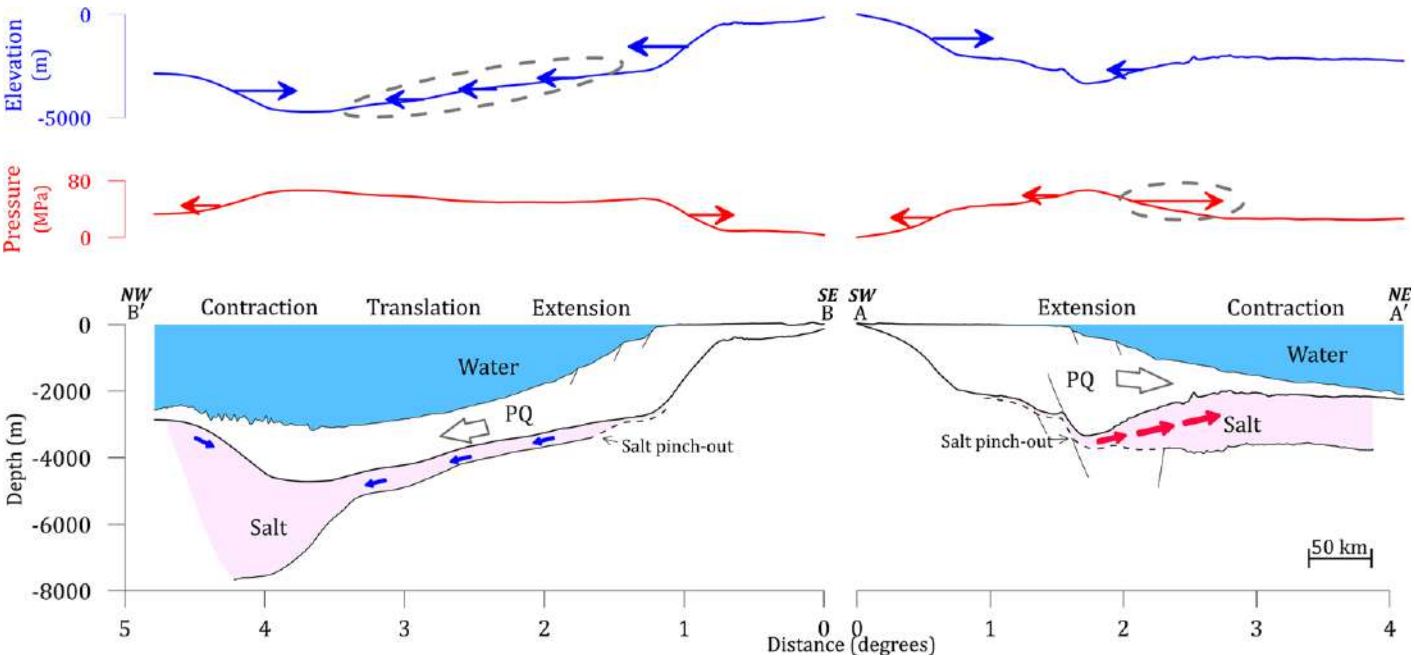

Figure 2. Cross sections illustrating the difference between forces driving salt tectonics in the Levant (AA′) and Herodotus (BB′) Basins (see Fig. 1D for location). Base of salt and faults are after Loncke et al. (2006) and Allen et al. (2016). Red curve is the pressure operating on the top salt surface as a result of sediment and seawater overburden. Blue curve is elevation of the top salt surface. Red and blue arrows emphasize pressure and elevation gradients, respectively (arrow length schematically represents amplitude). Note that elevation and pressure gradients are not relevant in areas with no salt. Gradients dominating salt flow are marked by dashed gray ellipses. PQ—Pliocene–Quaternary sediments.

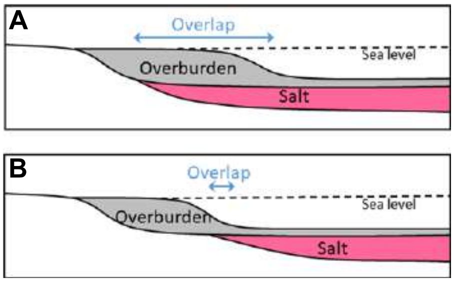

Figure 3. (A) Sketch of commonly used model for salt flow in response to differential loading along continental margins (after Brun and Fort, 2011). (B) Our suggested model, demonstrating overlap between the salt wedge and sedimentary wedge that is smaller than theoretically considered in previous studies.

the salt boundary and the sedimentary overburden before attempting to model their interaction.

CONCLUSIONS

(1) The circum-Nile deformation belt is asymmetric around the Nile Delta and the PQ depocenter.

(2) In most of the study area, the salt below the thickest PQ depocenter is rather thin (<150 m) or completely absent; thus, its squeezing cannot explain the formation of the CNDB.

(3) Throughout the western side of the Nile Delta, toward the deep Herodotus Basin, an elevation gradient causes gliding of the entire salt-overburden sequence downslope. This motion produces updip extension, translation along the slope, and contraction in the deep Herodotus Basin.

(4) Toward the Levant Basin, the propagating front of the Nile Delta was deposited over a thick salt body that had filled the ancient tectonic Temsah valley. This delta front is associated with a steep pressure gradient that causes salt flow northeastward toward the Levant Basin, producing updip extension and downdip contraction.

(5) Previous studies of salt tectonics in the Eastern Mediterranean overestimated the role of differential loading and salt squeezing compared to tilting and gliding.

ACKNOWLEDGMENTS

We are grateful to the editor James Schmitt and reviewers Andrew S. Madof, Christopher Kirkham, and Oliver Duffy for their insightful comments that led to improvements in the manuscript. This study was supported by the Israeli Ministry of National Infrastructures, Energy and Water Resources and by the Mediterranean Research Center of Israel (MERCI). The article is further based upon work of the European Cooperation in Science and Technology (COST) Action "Uncovering the Mediterranean salt giant" (MEDSALT).

REFERENCES CITED

Aal, A.A., El Barkooky, A., Gerrits, M., Meyer, H., Schwander, M., and Zaki, H., 2000, Tectonic evolution of the Eastern Mediterranean Basin and its significance for hydrocarbon prospectivity in the ultradeepwater of the Nile Delta: The Leading Edge, v. 19, p. 1086–1102, https://doi.org/10.1190/1.1438485.

Allen, H., Jackson, C.A.-L., and Fraser, A.J., 2016, Gravity-driven deformation of a youthful saline giant: The interplay between gliding and spreading in the Messinian basins of the Eastern Mediterranean: Petroleum Geoscience, v. 22, p. 340–356, https://doi.org/10.1144/petgeo2016-034.

Ben-Zeev, Y., and Gvirtzman, Z., 2019, When two salt tectonic systems meet: Gliding downslope the Levant Margin and salt-squeezing from under the Nile Delta: Jerusalem, The Hebrew University of Jerusalem, 42 p.

Bertoni, C., and Cartwright, J.A., 2006, Controls on the basinwide architecture of late Miocene (Messinian) evaporites on the Levant margin (Eastern Mediterranean): Sedimentary Geology, v. 188–189, p. 93–114, https://doi.org/10.1016/j.sedgeo.2006.03.019.

Brun, J.-P., and Fort, X., 2011, Salt tectonics at passive margins: Geology versus models: Marine and Petroleum Geology, v. 28, p. 1123–1145, https://doi.org/10.1016/j.marpetgeo.2011.03.004.

Cartwright, J.A., and Jackson, M.P.A., 2008, Initiation of gravitational collapse of an evaporite basin margin: The Messinian saline giant, Levant Basin, eastern Mediterranean: Geological Society of America Bulletin, v. 120, p. 399–413, https://doi.org/10.1130/B26081X.1.

Cartwright, J., Jackson, M., Dooley, T., and Higgins, S., 2012, Strain partitioning in gravity-driven shortening of a thick, multilayered evaporite sequence, *in* Alsop, G.I., et al., eds., Salt Tectonics, Sediments, and Prospectivity: Geological Society [London] Special Publication 363, p. 449–470, https://doi.org/10.1144/SP363.21.

Costa, E., Camerlenghi, A., Polonia, A., Cooper, C., Fabretti, P., Mosconi, A., Murelli, P., Romanelli, M., Sormani, L., and Wardell, N., 2004, Modeling deformation and salt tectonics in the eastern Mediterranean Ridge accretionary wedge: Geological Society of America Bulletin, v. 116, p. 880–894, https://doi.org/10.1130/B25309.1.

Dolson, J.C., Boucher, P.J., Siok, J., and Heppard, P.D., 2005, Key challenges to realizing full potential in an emerging giant gas province: Nile Delta/Mediterranean offshore, deep water, Egypt, *in* Doré, A.G., and Vining, B.A., eds., Petroleum

Geology: North-West Europe and Global Perspectives: Geological Society [London] Petroleum Geology Conference Series 6, p. 607–624, https://doi.org/10.1144/0060607.
Elfassi, Y., Gvirtzman, Z., Katz, O., and Aharonov, E., 2019, Chronology of post-Messinian faulting along the Levant continental margin and its implications for salt tectonics: Marine and Petroleum Geology, v. 109, p. 574–588, https://doi.org/10.1016/j.marpetgeo.2019.05.032.
Gaullier, V., Mart, Y., Bellaiche, G., Mascle, J., Vendeville, B.C., Zitter, T., and Second Leg PRISMED II Scientific Party, 2000, Salt tectonics in and around the Nile deep-sea fan: Insights from the PRISMED II cruise, *in* Vendeville, B.C., et al., eds., Salt, Shale and Igneous Diapirs in and around Europe: Geological Society [London] Special Publication 174, p. 111–129, https://doi.org/10.1144/GSL.SP.1999.174.01.07.
Gemmer, L., Ings, S.J., Medvedev, S., and Beaumont, C., 2004, Salt tectonics driven by differential sediment loading: Stability analysis and finite-element experiments: Basin Research, v. 16, p. 199–218, https://doi.org/10.1111/j.1365-2117.2004.00229.x.
Gennesseaux, M., Burollet, P., and Winnock, E., 1998, Thickness of the Plio-Quaternary sediments (IBCM-PQ): Bollettino di Geofisica Teorica ed Applicata, v. 39, p. 243–284.
Granot, R., 2016, Palaeozoic oceanic crust preserved beneath the eastern Mediterranean: Nature Geoscience, v. 9, p. 701–705, https://doi.org/10.1038/ngeo2784.
Gvirtzman, Z., Reshef, M., Buch-Leviatan, O., and Ben-Avraham, Z., 2013, Intense salt deformation in the Levant Basin in the middle of the Messinian Salinity Crisis: Earth and Planetary Science Letters, v. 379, p. 108–119, https://doi.org/10.1016/j.epsl.2013.07.018.
Gvirtzman, Z., Reshef, M., Buch-Leviatan, O., Groves-Gidney, G., Karcz, Z., Makovsky, Y., and Ben-Avraham, Z., 2015, Bathymetry of the Levant basin: Interaction of salt-tectonics and surficial mass movements: Marine Geology, v. 360, p. 25–39, https://doi.org/10.1016/j.margeo.2014.12.001.
Gvirtzman, Z., Manzi, V., Calvo, R., Gavrieli, I., Gennari, R., Lugli, S., Reghizzi, M., and Roveri, M., 2017, Intra-Messinian truncation surface in the Levant Basin explained by subaqueous dissolution: Geology, v. 45, p. 915–918, https://doi.org/10.1130/G39113.1.
Hall, J.K., Krasheninnikov, V.A., Hirsch, F., Benjamini, C., and Flexer, A., 2005, Geological Framework of the Levant, Volume II: The Levantine Basin and Israel: Jerusalem, Historical Productions-Hall Ltd., 826 p.
Hübscher, C., Cartwright, J., Cypionka, H., DeLange, G.J., Robertson, A., Suc, J.-P., and Urai, J.L., 2007, Global look at salt giants: Eos (Transactions, American Geophysical Union), v. 88, p. 177–179, https://doi.org/10.1029/2007EO160002.
Hübscher, C., Tahchi, E., Klaucke, I., Maillard, A., and Sahling, H., 2009, Salt tectonics and mud volcanism in the Latakia and Cyprus Basins, eastern Mediterranean: Tectonophysics, v. 470, p. 173–182, https://doi.org/10.1016/j.tecto.2008.08.019.
Hudec, M.R., and Jackson, M.P.A., 2007, Terra infirma: Understanding salt tectonics: Earth-Science Reviews, v. 82, p. 1–28, https://doi.org/10.1016/j.earscirev.2007.01.001.
Jackson, M.P.A., 1995, Retrospective salt tectonics, *in* Jackson, M.P.A., et al., eds., Salt Tectonics: A Global Perspective: American Association of Petroleum Geologists Memoir 65, p. 1–28.
Jackson, M.P.A., and Hudec, M.R., 2017, Salt Tectonics: Principles and Practice: Cambridge, UK, Cambridge University Press, 498 p., https://doi.org/10.1017/9781139003988.
Jackson, M.P.A., and Talbot, C.J., 1991, A Glossary of Salt Tectonics: Austin, Texas, University of Texas at Austin, Bureau of Economic Geology Geological Circular 91-4, 44 p., https://doi.org/10.23867/GC9104D.
Loncke, L., Gaullier, V., Mascle, J., Vendeville, B., and Camera, L., 2006, The Nile deep-sea fan: An example of interacting sedimentation, salt tectonics, and inherited subsalt paleotopographic features: Marine and Petroleum Geology, v. 23, p. 297–315, https://doi.org/10.1016/j.marpetgeo.2006.01.001.
Loncke, L., Vendeville, B.C., Gaullier, V., and Mascle, J., 2010, Respective contributions of tectonic and gravity-driven processes on the structural pattern in the Eastern Nile deep-sea fan: Insights from physical experiments: Basin Research, v. 22, p. 765–782, https://doi.org/10.1111/j.1365-2117.2009.00436.x.
Macgregor, D.S., 2012, The development of the Nile drainage system: Integration of onshore and offshore evidence: Petroleum Geoscience, v. 18, p. 417–431, https://doi.org/10.1144/petgeo2011-074.
Maillard, A., Hübscher, C., Benkhelil, J., and Tahchi, E., 2011, Deformed Messinian markers in the Cyprus Arc: Tectonic and/or Messinian Salinity Crisis indicators?: Basin Research, v. 23, p. 146–170, https://doi.org/10.1111/j.1365-2117.2010.00464.x.
Mascle, J., Benkhelil, J., Bellaiche, G., Zitter, T., Woodside, J., Loncke, L., and Prismed II Scientific Pary, 2000, Marine geologic evidence for a Levantine-Sinai plate, a new piece of the Mediterranean puzzle: Geology, v. 28, p. 779–782, https://doi.org/10.1130/0091-7613(2000)28<779:MGEFAL>2.0.CO;2.
Nashaat, M., 1998, Abnormally high formation pressure and seal impacts on hydrocarbon accumulations in the Nile Delta and North Sinai Basins, Egypt, *in* Law, B.E., et al., eds., Abnormal Pressures in Hydrocarbon Environments: American Association of Petroleum Geologists Memoir 70, p. 161–180.
Neev, D., 1977, The Pelusium Line—A major transcontinental shear: Tectonophysics, v. 38, p. T1–T8, https://doi.org/10.1016/0040-1951(77)90207-4.
Netzeband, G.L., Hübscher, C.P., and Gajewski, D., 2006, The structural evolution of the Messinian evaporites in the Levantine Basin: Marine Geology, v. 230, p. 249–273, https://doi.org/10.1016/j.margeo.2006.05.004.
Peel, F.J., 2014, The engines of gravity-driven movement on passive margins: Quantifying the relative contribution of spreading vs. gravity sliding mechanisms: Tectonophysics, v. 633, p. 126–142, https://doi.org/10.1016/j.tecto.2014.06.023.
Peel, F.J., Travis, C.J., and Hossack, J.R., 1995, Genetic structural provinces and salt tectonics of the Cenozoic offshore U.S. Gulf of Mexico: A preliminary analysis, *in* Jackson, M.P.A., et al., eds., Salt Tectonics: A Global Perspective: American Association of Petroleum Geologists Memoir 65, p. 153–175.
Roveri, M., Manzi, V., Bergamasco, A., Falcieri, F.M., Gennari, R., Lugli, S., and Schreiber, B.C., 2014, Dense shelf water cascading and Messinian Canyons: A new scenario for the Mediterranean salinity crisis: American Journal of Science, v. 314, p. 751–784, https://doi.org/10.2475/05.2014.03.
Rowan, M.G., Peel, F.J., Vendeville, B.C., and Gaullier, V., 2012, Salt tectonics at passive margins: Geology versus models—Discussion: Marine and Petroleum Geology, v. 37, p. 184–194, d https://doi.org/10.1016/j.marpetgeo.2012.04.007.
Sagy, Y., Gvirtzman, Z., Reshef, M., and Makovsky, Y., 2015, The enigma of the Jonah high in the middle of the Levant basin and its significance to the history of rifting: Tectonophysics, v. 665, p. 186–198, https://doi.org/10.1016/j.tecto.2015.09.037.
Schultz-Ela, D.D., 2001, Excursus on gravity gliding and gravity spreading: Journal of Structural Geology, v. 23, p. 725–731, https://doi.org/10.1016/S0191-8141(01)00004-9.
Segev, A., Rybakov, M., Lyakhovsky, V., Hofstetter, A., Tibor, G., Goldshmidt, V., and Ben Avraham, Z., 2006, The structure, isostasy and gravity field of the Levant continental margin and the southeast Mediterranean area: Tectonophysics, v. 425, p. 137–157, https://doi.org/10.1016/j.tecto.2006.07.010.
Sestini, G., 1989, Nile Delta: A review of depositional environments and geological history, *in* Whateley, M.K.G., and Pickering, K.T., eds., Deltas: Sites and Traps for Fossil Fuels: Geological Society [London] Special Publication 41, p. 99–127, https://doi.org/10.1144/GSL.SP.1989.041.01.09.
Steinberg, J., Roberts, A.M., Kusznir, N.J., Schafer, K., and Karcz, Z., 2018, Crustal structure and post-rift evolution of the Levant Basin: Marine and Petroleum Geology, v. 96, p. 522–543, https://doi.org/10.1016/j.marpetgeo.2018.05.006.
Vendeville, B.C., 2005, Salt tectonics driven by sediment progradation: Part I—Mechanics and kinematics: American Association of Petroleum Geologists Bulletin, v. 89, p. 1071–1079, https://doi.org/10.1306/03310503063.
Wu, S., Bally, A.W., and Cramez, C., 1990, Allochthonous salt, structure and stratigraphy of the northeastern Gulf of Mexico, Part II: Structure: Marine and Petroleum Geology, v. 7, p. 334–370, https://doi.org/10.1016/0264-8172(90)90014-8.
Zucker, E., Gvirtzman, Z., Steinberg, J., and Enzel, Y., 2017, Diversion and morphology of submarine channels in response to regional slopes and localized salt tectonics, Levant Basin: Marine and Petroleum Geology, v. 81, p. 98–111, https://doi.org/10.1016/j.marpetgeo.2017.01.002.

Printed in USA

GSA Data Repository 2020041

Supplementary material for:

Salt tectonics in the Eastern Mediterranean Sea: Where a giant delta meets a salt giant

Elchanan Zucker [1,2], Zohar Gvirtzman [1,2], Josh Steinberg [3], Yehouda Enzel[1]

[1] *The Fredy and Nadine Herrmann Institute of Earth Sciences, The Hebrew University of Jerusalem, Jerusalem 91904, Israel*

[2] *Geological Survey of Israel, Yesha'yahu Leibowitz 32, Jerusalem, Israel*

[3] *Ratio Oil Exploration, Tel Aviv, Israel*

DATA AND METHODS

Previous regional compilations of the Pliocene-Quaternary section in the Mediterranean presented sediment thickness data (Morelli, 1988; Morelli and Val'chuk, 1988; Gennesseaux et al., 1998; Nashaat, 1998; Hall et al., 2005; Segev et al., 2006; Macgregor, 2012). For the purpose of this study we compiled a base Pliocene (~top salt) structural map. Our compilation (Figure DR1) is based on published and unpublished seismic and well data. The "International Bathymetric Chart of the Mediterranean" (Gennesseaux et al., 1998) is a compilation of the Pliocene-Quaternary sediment "thickness" in two way time (TWT) for the entire Mediterranean Sea, produced by the Intergovernmental Oceanographic Commission. We used this compilation wherever newer data is unavailable. For the Nile deep sea fan (NDSF), the Eratosthenes Seamount, and the Herodotus basin we use various sources that are detailed in table DR1. For Israel's exclusive economic zone we used Steinberg et al. (2011) and Sagy et al. (2015). In addition, we used local structural and thickness maps and many cross sections, some in TWT and some in length units. All sources used for our compilation are listed in table DR1.

The top salt pressure map is calculated by the equation: $p = \rho g h$, where p is pressure at top salt surface, g – gravity constant, ρ - density, h - layer thickness. Using a density of 2200 kg/m^3 for Pliocene-Quaternary layer and 1030 kg/m^3 for seawater layer, we added the effect of the two layers. The result expresses the vertical present-day pressure (MPa) applied on the top of the salt layer highlighting areas with pressure gradients.

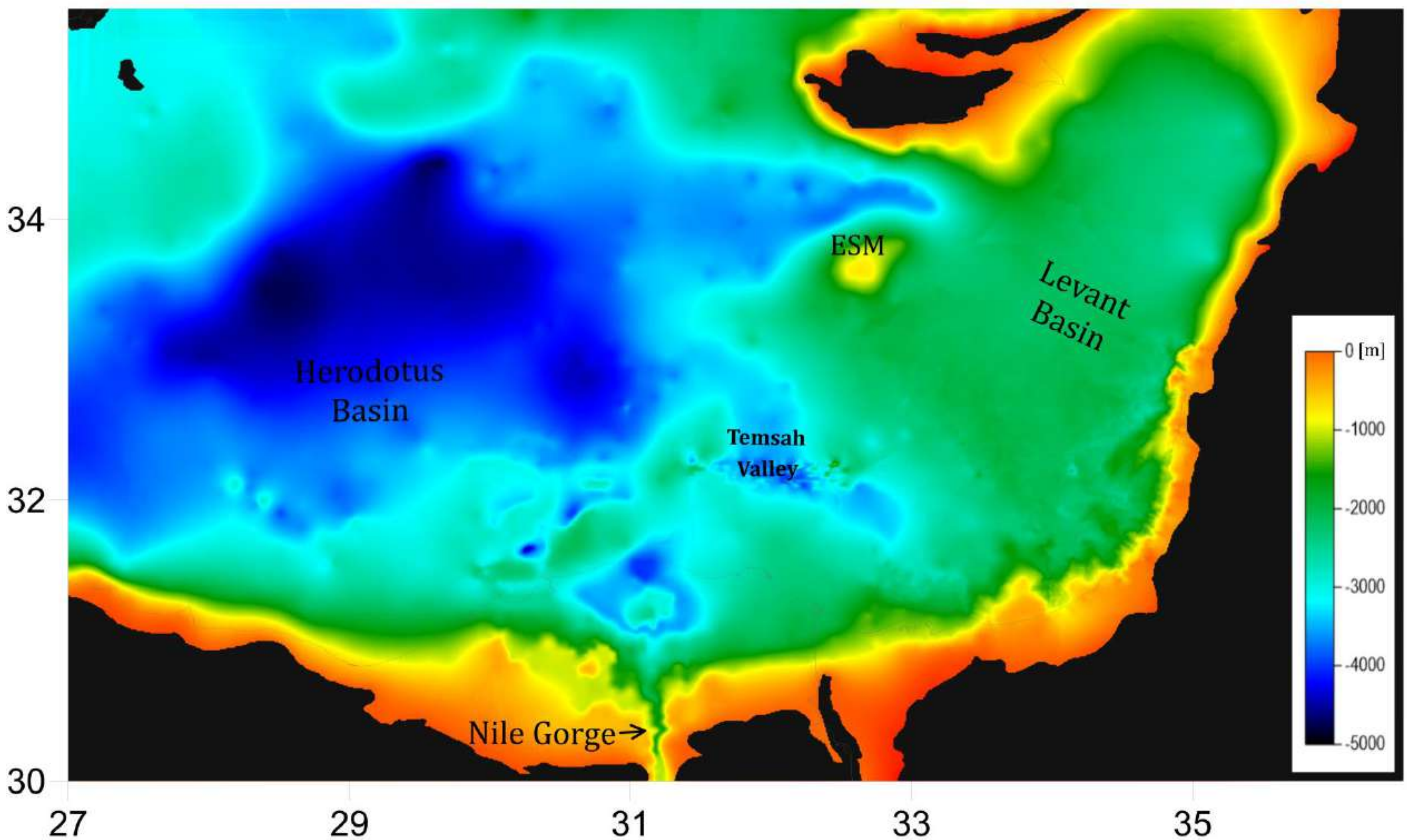

Figure DR1: Base Pliocene (~top Messinian Evaporites) structural map. Black area denotes no Pliocene-Quaternary section. Present-day coastline (gray) is shown for reference.

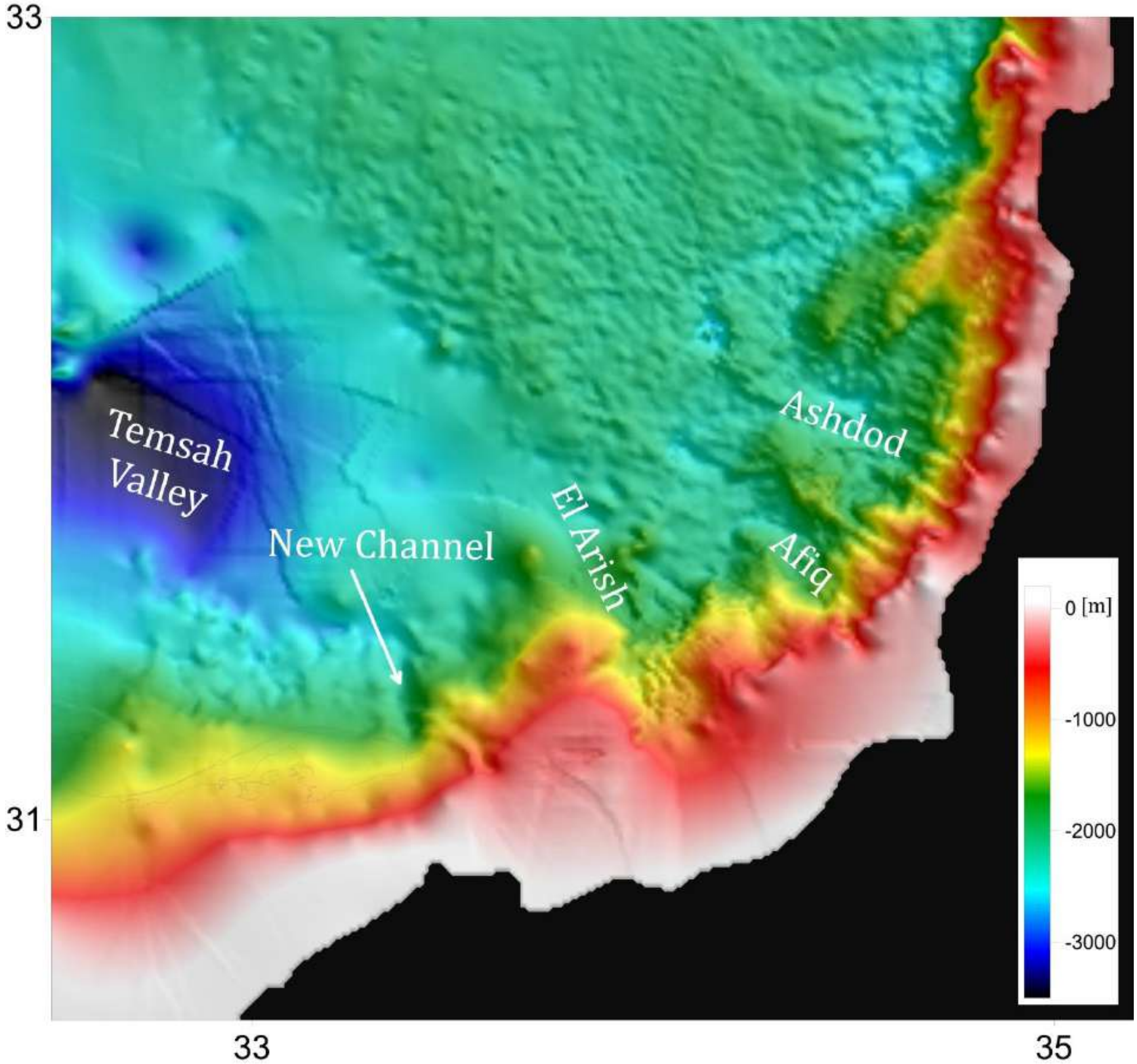

Figure DR2: Base Pliocene structural map showing in detail the steep incised relief left after the Messinian Salinity Crisis offshore Israel and Sinai. Most canyons incised across the continental margin were previously described in the literature (e.g., Druckman et al., 1995; Bar et al., 2013, 2016). However the canyon west of the El Arish Canyon (white arrow) is presented here for the first time (New Channel). This canyon indicates that the Temsah Valley already existed by the end of salt deposition.

TABLE DR1. DATA SOURCES FOR BASE PLIOCENE MAP

#	Source	Depth or Thickness	Sysmic data map / Cross section / Drill hole data	Units
1	Abd-Allah et al., 2012	Depth to Top Salt	Seismic cross section + map	TWT [sec]
2	Barber, 1981	Depth to Top Salt	Seismic map	meters
3	Base Pliocene of the Israeli Exclusive Economic Zone (Sources from steinberg et al., 2011 and Sagy et al., 2015)	Depth to Top Salt & PQ Thickness	Seismic cross section + map	TWT [sec] & meters
4	Came'ra et al., 2010	Depth to Top Salt	Seismic cross section	meters
5	Carton et al., 2009	Depth to Top Salt & PQ Thickness	Seismic cross section + map	TWT [sec] & [msec]
6	Ducassou et al., 2007	Depth to Top Salt	Drill hole data	meters
7	Ducassou et al., 2009	Depth to Top Salt	Drill hole data	meters
8	Garziglia et al., 2008	Depth to Top Salt	Seismic cross section	TWT [sec]
9	Gaullier et al., 2000	Depth to Top Salt	Seismic cross section	TWT [sec]
10	Gennesseaux et al., 1998	PQ Thickness	Seismic map	TWT [msec]
11	Hanafy et al., 2016	PQ Thickness	Seismic map	meters
12	Kellner et al., 2009	Depth to Top Salt	Seismic map	TWT [sec]
13	Loncke et al., 2002; 2006	Depth to Top Salt & PQ Thickness	Seismic cross section + map	TWT [sec] & meters
14	MIDBAR	Depth to Top Salt	Seismic map	TWT [msec]
15	Sarhan et al., 2014	Depth to Top Salt	Seismic cross section	TWT [sec]
16	Shaaban et al., 2006	Depth to Top Salt	Seismic map & Drill hole data	meters

Table DR1: Data sources for the compiled base Pliocene structural map (Figure DR1). Location of each source number can be found in the source location map (Figure DR3).

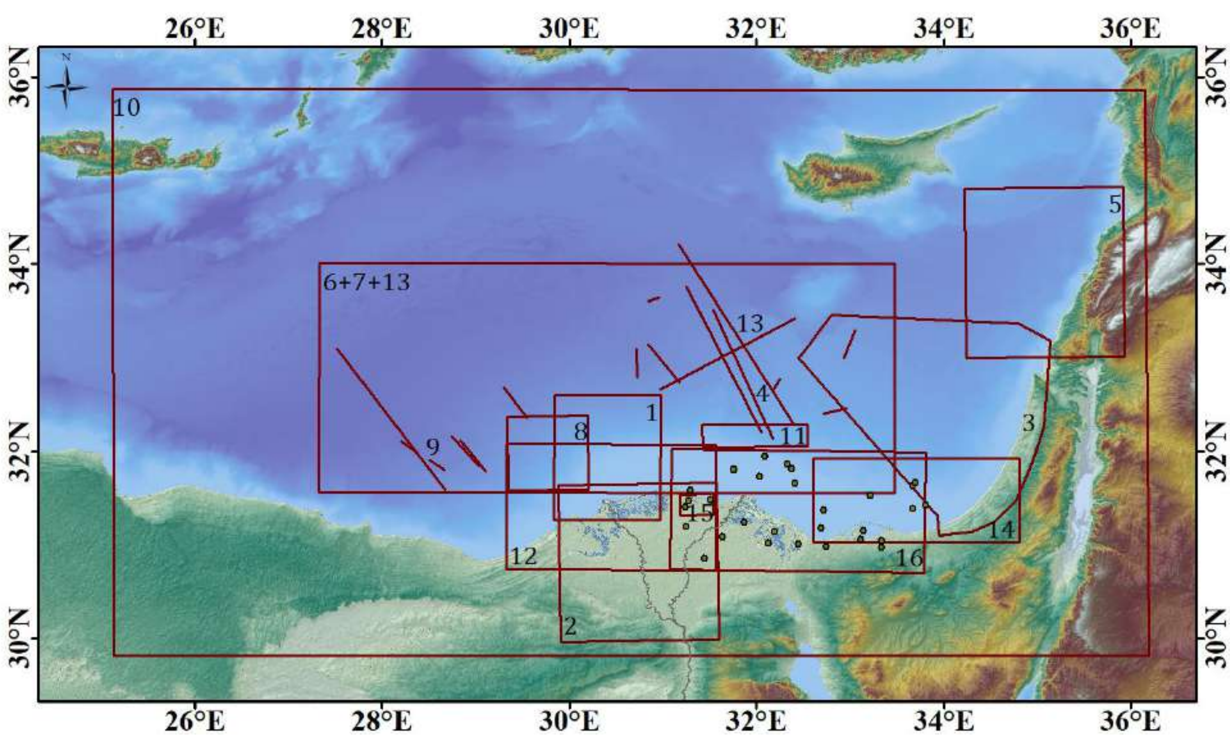

Figure DR3: Location of studies used for compilation. Numbers correspond to Table DR1.

Salt migration

To reconstruct the original boundary of the salt basin prior to its basinward flow, we examine salt rollers, welds, and normal faults. These structures are formed as response to salt withdrawal (Rowan et al., 1999; Wagner and Jackson, 2011; Allen et al., 2016) and thus mark the salt evacuation zone (SEZ, Fig. 1c). Figure DR4 (modified after Allen et al., 2016) demonstrates that the width of the SEZ is <30 km. We, therefore, conclude that the difference between the present-day salt pinch-out line and the original boundary of the salt wedge is quite narrow in terms of the PQ depocenter, which was originally deposited landward of the thick (>150 m) salt layer.

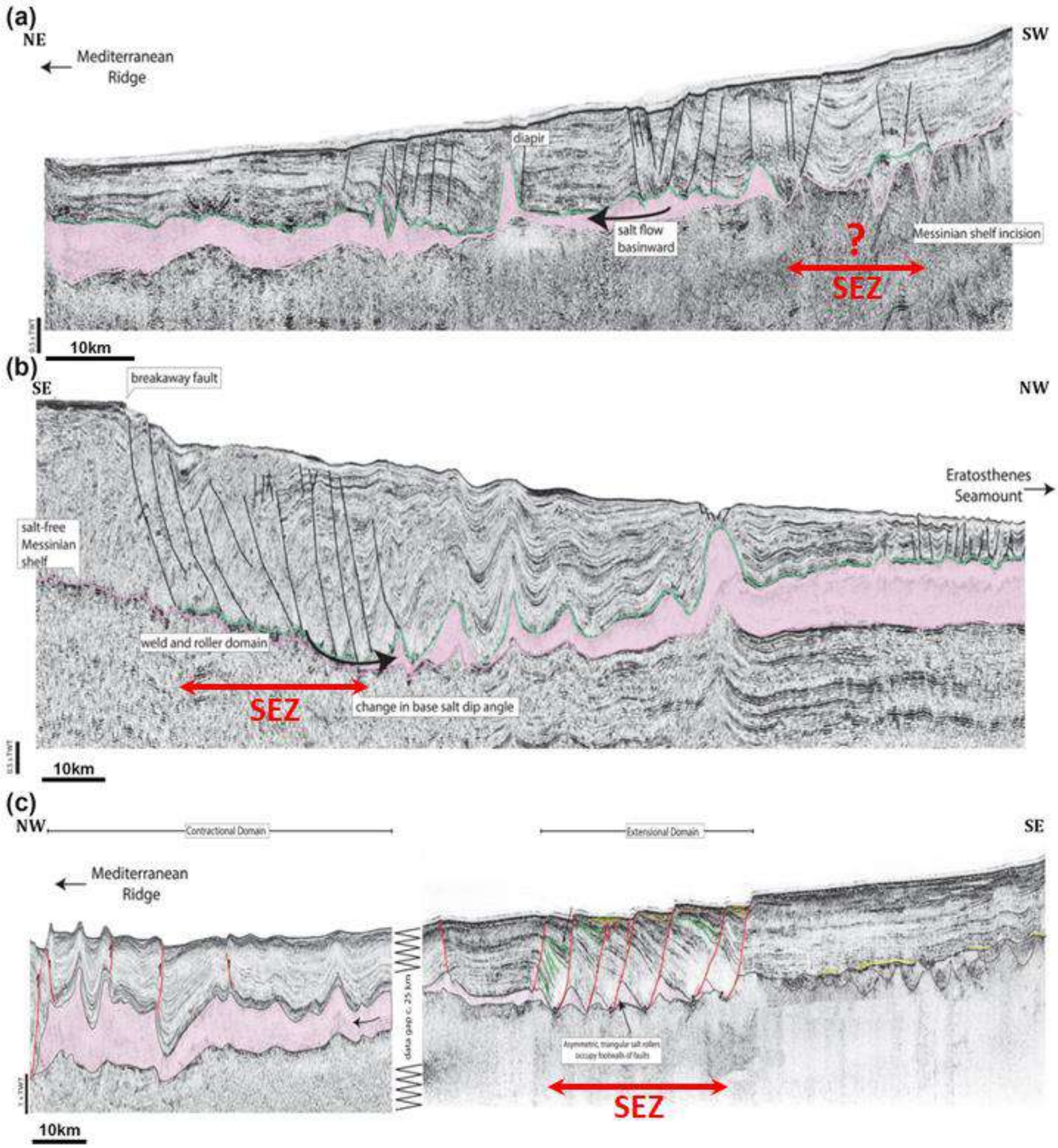

Figure DR4: Seismic cross sections (modified after Allen et al., 2016) showing the distribution of salt rollers, welds, and normal faults. The area marked by a red arrow indicates the salt evacuation zone (SEZ), which is narrower than 30 km. Section's location in Fig. 1c.

REFERENCES

Allen, H., Jackson, C.A.-L., and Fraser, A.J., 2016, Gravity-driven deformation of a youthful saline giant: the interplay between gliding and spreading in the Messinian basins of the Eastern Mediterranean: Petroleum Geoscience, v. 22, p. 340–356, doi:10.1144/petgeo2016-034.

Bar, O., Gvirtzman, Z., Feinstein, S., and Zilberman, E., 2013, Accelerated subsidence and sedimentation in the levant basin during the late tertiary and concurrent uplift of the arabian platform: Tectonic versus counteracting sedimentary loading effects: Tectonics, v. 32, p. 334–350, doi:10.1002/tect.20026.

Bar, O., Zilberman, E., Feinstein, S., Calvo, R., and Gvirtzman, Z., 2016, The uplift history of the Arabian Plateau as inferred from geomorphologic analysis of its northwestern edge: Tectonophysics, v. 671, p. 9–23, doi:10.1016/j.tecto.2016.01.004.

Druckman, Y., Buchbinder, B., Martinotti, G.M., Siman Tov, R., and Aharon, P., 1995, The buried Afiq Canyon (eastern Mediterranean, Israel): a case study of a Tertiary submarine canyon exposed in Late Messinian times: Marine Geology, v. 123, p. 167–185, doi:10.1016/0025-3227(94)00127-7.

Gennesseaux, M., Burollet, P., and Winnock, E., 1998, Thickness of the Plio-Quaternary sediments (IBCM-PQ): Boll. Geofis. Teor. Appl, v. 39, p. 243–284.

Hall, J.K., Krasheninnikov, V.A., Hirsch, F., Benjamini, C., and Flexer, A., 2005, Geological framework of the Levant. Volume II: the Levantine Basin and Israel: Jerusalem, 826 p.

Macgregor, D.S., 2012, The development of the Nile drainage system: integration of onshore and offshore evidence: Petroleum Geoscience, v. 18, p. 417–431, doi:10.1144/petgeo2011-074.

Morelli, C., 1988, International bathymetric chart of the Mediterranean (IBCM) published by the Intergovernmental Oceanographic Commission of UNESCO: AAPG Bulletin, v. 72.

Morelli, C., and Val'chuk, S., 1988, The international bathymetric chart of the Mediterranean (IBCM): published under the authority of the Intergovernmental Oceanographic Commission of Unesco:

Nashaat, M., 1998, Abnormally high Formation pressure and seal impacts on hydrocarbon accumulations in the Nile Delta and North Sinai Basins, Egypt: AAPG Memoir, v. 70, p. 161–180.

Rowan, M.G., Jackson, M.P.A., and Trudgill, B.D., 1999, Salt-related fault families and fault welds in the northern Gulf of Mexico: AAPG Bulletin, v. 83, p. 1454–1484.

Sagy, Y., Gvirtzman, Z., Reshef, M., and Makovsky, Y., 2015, The enigma of the Jonah high in the middle of the Levant basin and its significance to the history of rifting: Tectonophysics, v. 665, p. 186–198, doi:10.1016/j.tecto.2015.09.037.

Segev, A., Rybakov, M., Lyakhovsky, V., Hofstetter, A., Tibor, G., Goldshmidt, V., and Ben Avraham, Z., 2006, The structure, isostasy and gravity field of the Levant continental margin and the southeast Mediterranean area: Tectonophysics, v. 425, p. 137–157, doi:10.1016/J.TECTO.2006.07.010.

Steinberg, J., Gvirtzman, Z., Folkman, Y., and Garfunkel, Z., 2011, Origin and nature of the rapid late Tertiary filling of the Levant Basin: Geology, v. 39, p. 355–358, doi:10.1130/G31615.1.

Wagner, B.H., and Jackson, M.P.A., 2011, Viscous flow during salt welding: Tectonophysics, v. 510, p. 309–326, doi:10.1016/J.TECTO.2011.07.012.

Chapter 4

Diversion and morphology of submarine channels in response to regional slopes and localized salt tectonics, Levant Basin

Published in Marine and Petroleum Geology

Zucker, E., Gvirtzman, Z., Steinberg, J., and Enzel, Y., 2017, Diversion and morphology of submarine channels in response to regional slopes and localized salt tectonics, Levant Basin: Marine and Petroleum Geology, v. 81, p. 98–111, doi:10.1016/j.marpetgeo.2017.01.002

Marine and Petroleum Geology 81 (2017) 98–111

Contents lists available at ScienceDirect

Marine and Petroleum Geology

journal homepage: www.elsevier.com/locate/marpetgeo

Research paper

Diversion and morphology of submarine channels in response to regional slopes and localized salt tectonics, Levant Basin

E. Zucker [a, b, *], Z. Gvirtzman [a, b], J. Steinberg [c], Y. Enzel [a]

[a] *The Fredy and Nadine Herrmann Institute of Earth Sciences, The Hebrew University of Jerusalem, Jerusalem 91904, Israel*
[b] *Geological Survey of Israel, 30 Malkhe Israel, Jerusalem 95501, Israel*
[c] *Ratio Oil Exploration, Tel Aviv, Israel*

A R T I C L E I N F O

Article history:
Received 29 June 2016
Received in revised form
31 December 2016
Accepted 4 January 2017
Available online 5 January 2017

Keywords:
Submarine channels
Sinuosity
Geomorphology
Salt tectonics
Levant basin
Nile delta
Turbidites

A B S T R A C T

In the Levant Basin, submarine channels are abundant around the Nile deep-sea fan (NDSF), an area which is also affected by salt tectonics related to the Messinian salt giant. Here we focus on the relationship between submarine channels and obstacles formed by salt tectonics. Initially, we use methods developed for terrestrial morphological analysis and quantify channel sinuosity, width and slope in search for consistent relationships between morphometric parameters and channel response to obstacles. However, this traditional analysis did not yield robust conclusions. Then, we apply two new morphometric parameters suggested here to express the distortion of channels by obstacles: incident angle (α), defined as the acute angle between the regionally influenced channel direction and the strike of the tectonic obstacle and diversion angle (Ω), defined as the angle between the direction of the regional bathymetric slope and the average direction of the channel. These parameters illustrate the influence of the regional-scale basin geometry and the superimposed tectonic-influenced seabed patterns, on channel development. We found hyperbolic relationships between incident angle (α) and diversion angle (Ω) in which channels flowing approximately parallel ($\alpha \approx 0^\circ$) to tectonic folds are (obviously) not diverted; channels nearly orthogonal ($\alpha \approx 90^\circ$) to obstacles, crosscut them right through and, again, not diverted much. In contrast, channels with a general direction diagonal to the obstacles ($\alpha \approx 40^\circ$), are diverted by ten degrees ($\Omega \approx 10^\circ$). This diversion accumulates along large distances and significantly influences the regional development of channels around the NDSF. Noteworthy, this phenomenon of channel diversion, indirectly deteriorate normal slope-sinuosity relationships known from terrestrial studies. In light of these findings, we suggest that these new parameters can be applied to other basins, where submarine channels interact with seabed obstacles.

© 2017 Elsevier Ltd. All rights reserved.

1. Introduction

While submarine channels are quite abundant along the present-day seafloor, these deposits are rarely exposed on land, and hence, not sufficiently understood (Peakall et al., 2000; Weimer et al., 2006). In recent years, the need to study submarine channel systems has increased for basic understanding of their evolution but also for practical reasons: (1) assessing the geo-hazard risks associated with industrial infrastructure laid on the sea floors (pipelines, cables, facilities); and (2) for tracking and characterizing ancient and buried turbidite units that may contain hydrocarbons. Therefore, it is important to study modern submarine channel systems, assess how active they are, and use them to better understand ancient, buried systems that are not imaged at similar details. This study focuses on the Levant Basin, where recent prolific gas discoveries have enhanced the need for a deeper understanding of the submarine system of the Eastern Mediterranean Sea and its relations to the adjacent Nile deep sea fan (NDSF).

Submarine channels as a part of Turbidite Systems around the western and northern slopes of NDSF (Fig. 1a) were documented in a series of studies (Gaullier et al., 2000; Loncke et al., 2002, 2006, 2009; Ducassou et al., 2008, 2009). The western province of the NDSF is probably the best-documented and the most active part of the Nile fan in terms of turbidite deposition, at least over the past 130,000 years (Maldonado and Stanley, 1979; Bellaiche et al., 2001; Loncke et al., 2002; Ducassou et al., 2007). In that area, where the

* Corresponding author. The Fredy and Nadine Herrmann Institute of Earth Sciences, The Hebrew University of Jerusalem, Jerusalem 91904, Israel.
E-mail address: elchanan.zucker@mail.huji.ac.il (E. Zucker).

http://dx.doi.org/10.1016/j.marpetgeo.2017.01.002
0264-8172/© 2017 Elsevier Ltd. All rights reserved.

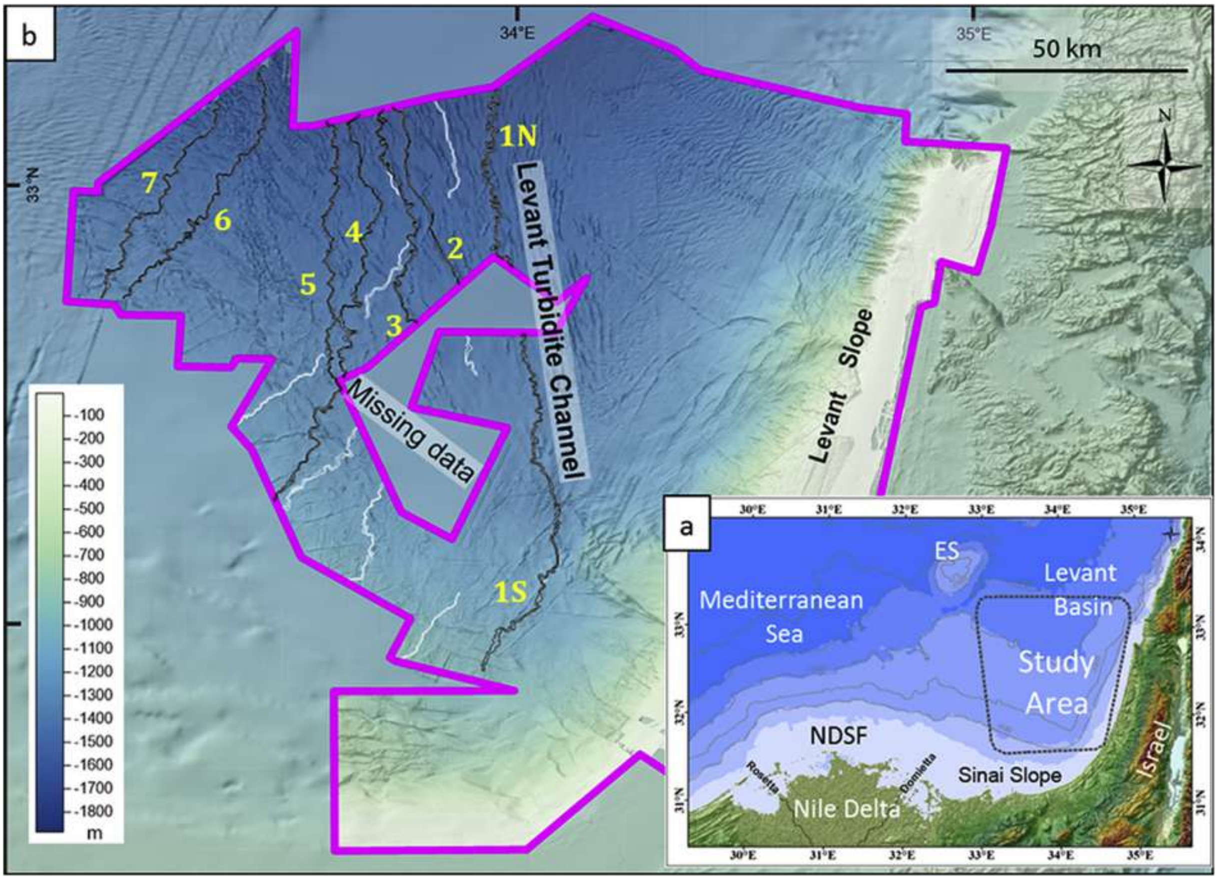

Fig. 1. a) Location map and bathymetry of the southeastern Mediterranean with contour intervals = 500 m. ES = Eratosthenes Seamount. NDSF = Nile deep-sea fan. b) The study area in the southern Levant Basin. Submarine channels 1–7 analyzed in this study. Map prepared based on data from Gvirtzman et al., 2015.

Rosetta canyon is directly connected to the deep sea fan, a series of active well-ramified channel–levee systems have been identified. Turbidite sediments are currently transported through this system ~300 km from the shelf edge (Huguen, 2001; Loncke et al., 2002; Ducassou et al., 2013) confirming earlier suggestions (e.g., Normark et al., 1993) stating that gravity flows are remarkably mobile and can travel long distances via submarine channels until settling at distal submarine fans. In the eastern province of the NDSF (Levant Basin), where evidence for turbidite flow have yet to have been documented, we use the term 'submarine channel' to describe incised conduits for downslope sediment transport, without any implication for process or flow type.

The southern part of the Levant Basin was recently described by Gvirtzman et al. (2015), who showed that the off-Sinai slope contains a net of submarine channels similar to those described north and west of the NDSF unlike the nearby Levant slope, which does not present any channels (Fig. 1b). The width of the off Sinai channels (labelled 2–7) range between 200 and 700 m and their depth relative to respective shoulders is 10–40 m. Wider and more sinusoidal (Fig. 1b) than these channels is the 270–km-long Levant turbidite channel (Gvirtzman et al., 2015), which runs along the lowest points in the valley formed between the Sinai and Levant slopes.

Salt tectonics significantly deforms the Levant Basin shaping the seafloor morphology (e.g. Garfunkel, 1984; Garfunkel and Almagor, 1984, 1987; Gradmann et al., 2005; Netzeband et al., 2006; Bertoni and Cartwright, 2006, 2007; Cartwright and Jackson, 2008; Gvirtzman et al., 2015). This study focuses on the relationships between submarine channels and lineaments produced by salt tectonics. Interestingly, a few of the channels in the Levant Basin do not always take the steepest downslope path (i.e. do not follow the maximum slope). Rather, at certain segments they are deflected towards the northwest by elongated tectonic ridges forming a zig-zag channel pattern (Gvirtzman et al., 2015). Therefore, our goal is also to understand how seabed obstacles that originate in salt tectonics influence submarine turbidite channels in the Levant Basin and in general.

To achieve this goal we begin with a classic morphometric analysis measuring channel sinuosity, width, and slope, looking for consistent relationships between these parameters and the channel response to tectonic related obstacles. Then, we introduce a morphometric parameter that expresses the distortion of channels by obstacles. This parameter quantifies and assists in explaining the influence of the regional basin geometry and the superimposed tectonic influenced seabed pattern on channel development.

We conclude this study with insight and implications derived from our research; comparing channel flow direction to the regional basin architecture allows for the immediate identification of regions in which channel morphology is affected by tectonics. This is done by demonstrating the potential applicability of our new analysis method in our neighboring region; The analysis presented here demonstrates how channel morphology can be used to trace areas with very gentle tectonic elements that cannot be traced without high resolution bathymetry data by emphasizing the differences between the western province off the NDSF and the Levant basin in the east. To give this new method an even broader applicability, we present several examples from different basins around the world and discuss how tectonic obstacles may affect channels

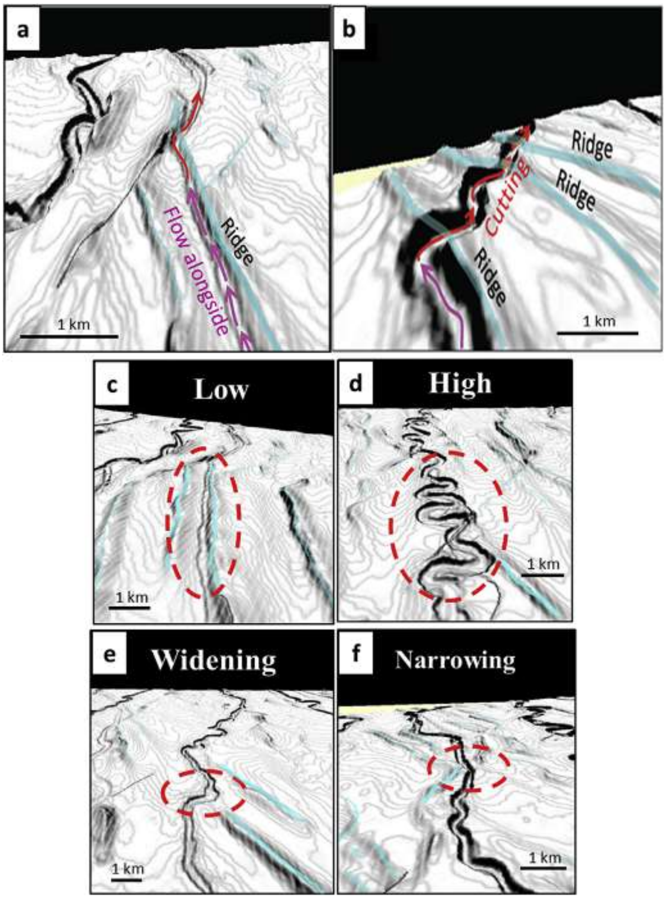

Fig. 2. 3D-bathymetry images of two types of interactions observed in the southern Levant Basin between submarine channels and seabed obstacles: a) Channel flowing alongside an obstacle. b) Channel cuts through an obstacle. c) and d) display channel-obstacles interactions that affect channel sinuosity. e) and f) display channel-obstacle interactions that affect channel width. Blue lines represent ridges. Vertical exaggeration is ×3. (For interpretation of the references to colour in this figure legend, the reader is referred to the web version of this article.)

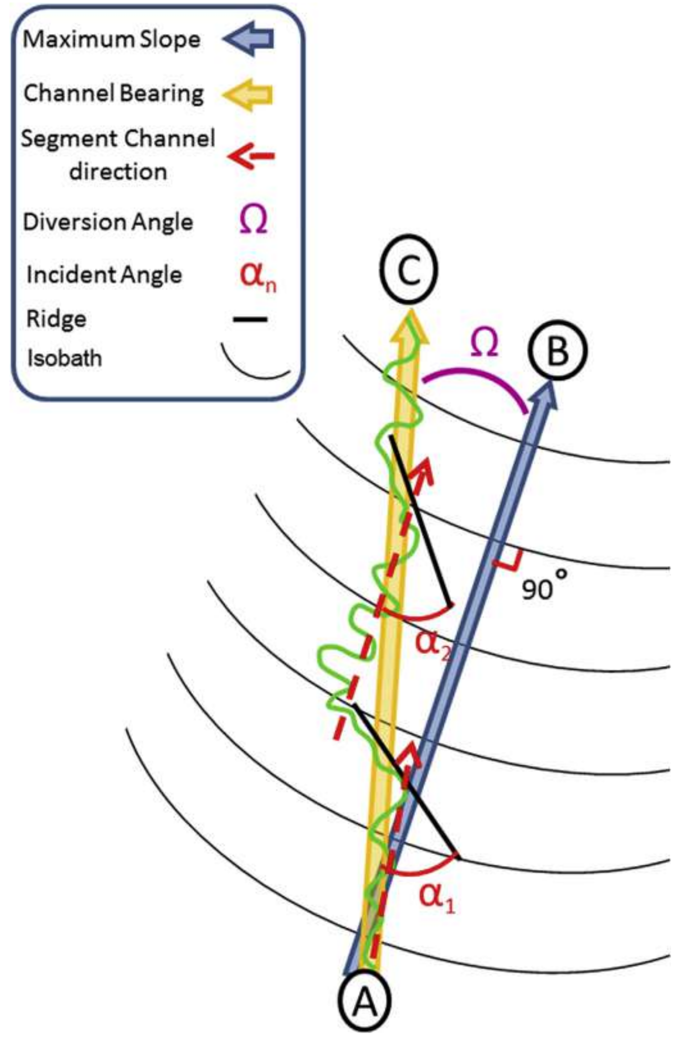

Fig. 3. Method for determining the morphometric parameters, suitable for the channel-obstacle analysis: Diversion angle (Ω) and incident angle (α). The arrow A-B is the direction of the maximum downstream slope in the channel flowing area. Arrow A-C is the actual general channel bearing. Angle BAC is the diversion angle (Ω).

and how they respond morphometrically. We further offer the method presented here when analyzing the effect of tectonic obstacles on the regional channel systems.

2. Geologic setting

The Levant Basin (Fig. 1a), located in the southeastern most corner of the Mediterranean Sea, is an extensional basin formed at the margins of the Neotethys Ocean during the late Paleozoic and early Mesozoic (Garfunkel, 1998; Robertson, 1998). About 6 million years ago, towards the end of the Miocene (Messinian), the Mediterranean transformed into a giant saline basin and ~2 km-thick salt layer was deposited on its seafloor (Hsü et al., 1973; Ryan, 1973; reviewed by Ryan, 2009). This short event in the history of the Earth is termed the Messinian Salinity Crisis (MSC, for overall review see Roveri et al., 2014 and references therein). In the Levant Basin, the MSC and the deformation caused later by subsurface salt motion was documented and studied by numerous works over the past four decades (e.g. Neev et al., 1976; Ryan and Cita, 1978; Ben-Avraham, 1978; Almagor and Hall, 1983; Mart and Ben-Gai, 1982; Tibor et al., 1992; Martinez et al., 2005; Huebscher et al., 2008; Cartwright et al., 2012; Gvirtzman et al., 2013). This sequence wedges out to a few tens of meters at the basin margins.

Following the MSC, when normal marine conditions resumed, sediment supply from the Nile River produced a giant delta with a well-developed deep sea fan (NDSF). Unlike the Oligo-Miocene deposits that are thick in the deep Levant Basin and thin along the Levant continental margin (Steinberg et al., 2011; Macgregor, 2012), the Plio-Quaternary section is thick along the continental margin and thin in the deep basin. The thickness of the Plio-Quaternary section in the deep basin is only 400–500 m whereas below the NDSF it reaches ~4 km (Said, 1981; Mascle et al., 2006; Segev et al., 2006; Loncke et al., 2006; Gvirtzman et al., 2008; Steinberg et al., 2011). These Plio-Pleistocene deposits, overlying the Messinian evaporites, consist of Nile-derived clay-rich siliciclastic sediments (Gvirtzman and Buchbinder, 1978; Mart and Ben-Gai, 1982; Ben-Gai et al., 2005) unconformably overlying and leveling the rough Messinian relief (Gvirtzman and Buchbinder, 1978; Bertoni and Cartwright, 2006; Steinberg et al., 2011). Offshore Israel, Nile-derived sediments have produced a wide shelf that had propagated about 20 km westwards since the early Pliocene (e.g. Gvirtzman and Buchbinder, 1978; Mart et al., 1978; Almagor and Garfunkel, 1979; Buchbinder and Zilberman, 1997; Goldsmith and Golik, 1980; Ben-Avraham and Mart, 1981; Mart, 1982; Ben-Gai et al., 2005).

At the end of the Pliocene, about 2.5 million years after the end of the MSC and about 2.5 Ma before present, significant deformation related to subsurface salt motion has begun (Almagor, 1984; Garfunkel and Almagor, 1984; Cartwright et al., 2012). Salt motion, over the past 2.5 million years, developed into a complex circum-Nile radial contraction domain of folds and faults. The surface expression of folds is quite subtle; tens of meters high, hundreds of meters wide, and a few kilometers long, forming a pattern of elongated obstacles with spacing of 1.5–6 km. In the subsurface, fold amplitudes increase and frequently overlay thrust faults with vertical displacement of a few hundreds of meters. The radial system of folds and thrust faults is accompanied by a nearly perpendicular swarm of strike-slip faults and a fringing belt where shortening is accommodated by conjugate sets of strike-slip faults. The surface expression of strike slip faults is quite narrow forming a

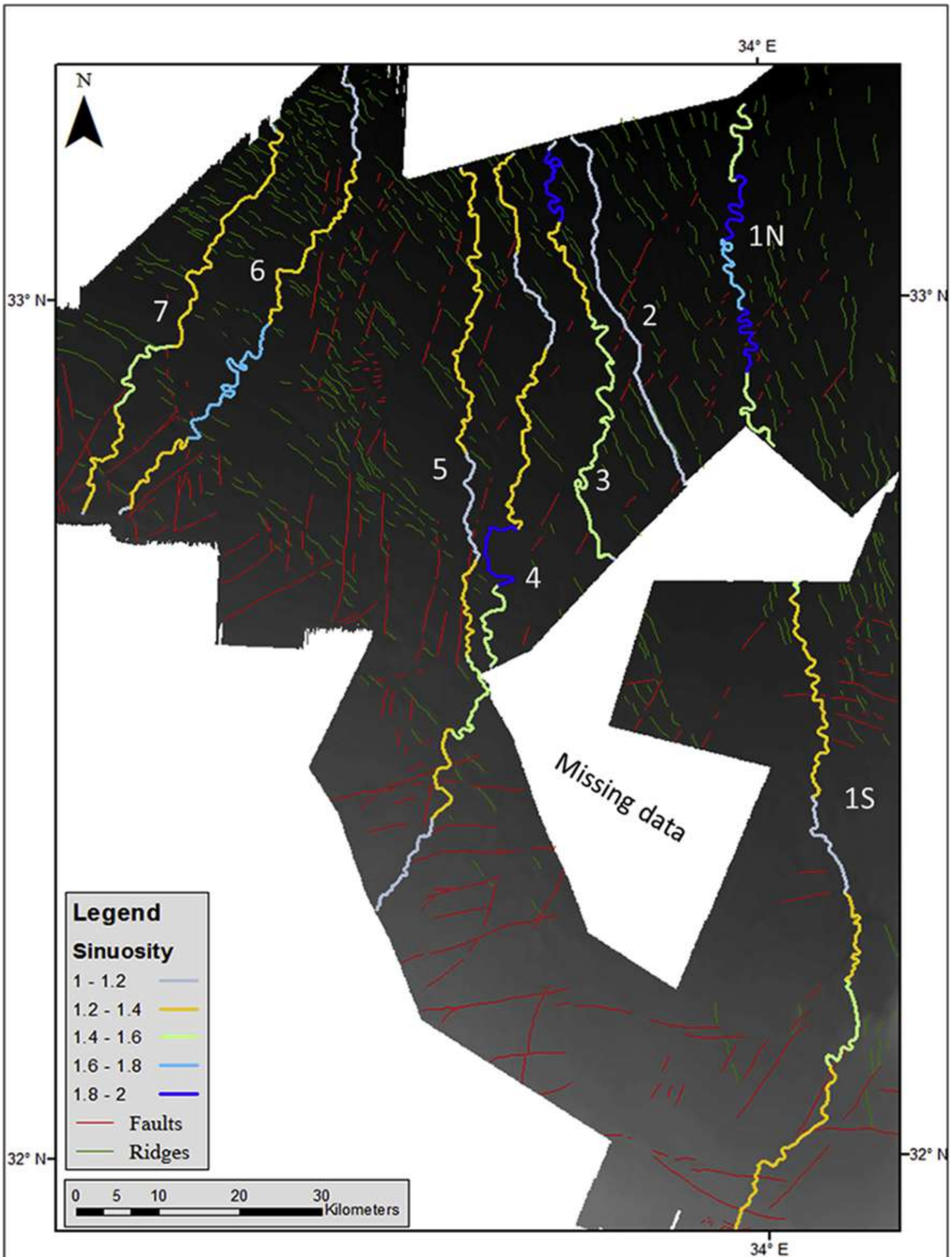

Fig. 4. Sinuosity of channels determined for 15 km long segments. Location in Fig. 1.

few meter high step or fissure (Gvirtzman et al., 2013, 2015). Updip, towards both the Nile River in the south and towards the Israeli slope to the east, the contraction domain is accompanied by an extensional domain of normal faults (Almagor and Hall, 1983; Garfunkel, 1984; Gradmann et al., 2005; Cartwright and Jackson, 2008).

At present the seafloor is shaped by two synchronous processes (Gvirtzman et al., 2015): 1) Salt tectonics that produces faults and folds (references above) and 2) various processes of sediment transport and deposition such as landslides along the upper continental slope (Martinez et al., 2005; Mart and Ryan, 2007; Katz et al., 2015) and turbidite channels in the deeper basin (e.g. Pratson et al., 2000; Peakall et al., 2000; Bellaiche et al., 2001; Mayall et al., 2006; Folkman and Mart, 2008; Garziglia et al., 2008; Kane et al., 2008; Gvirtzman et al., 2015).

3. Data and methods

To perform the morphometric analysis we first prepared a 10 × 10 m digital elevation model (DEM) of the study area by

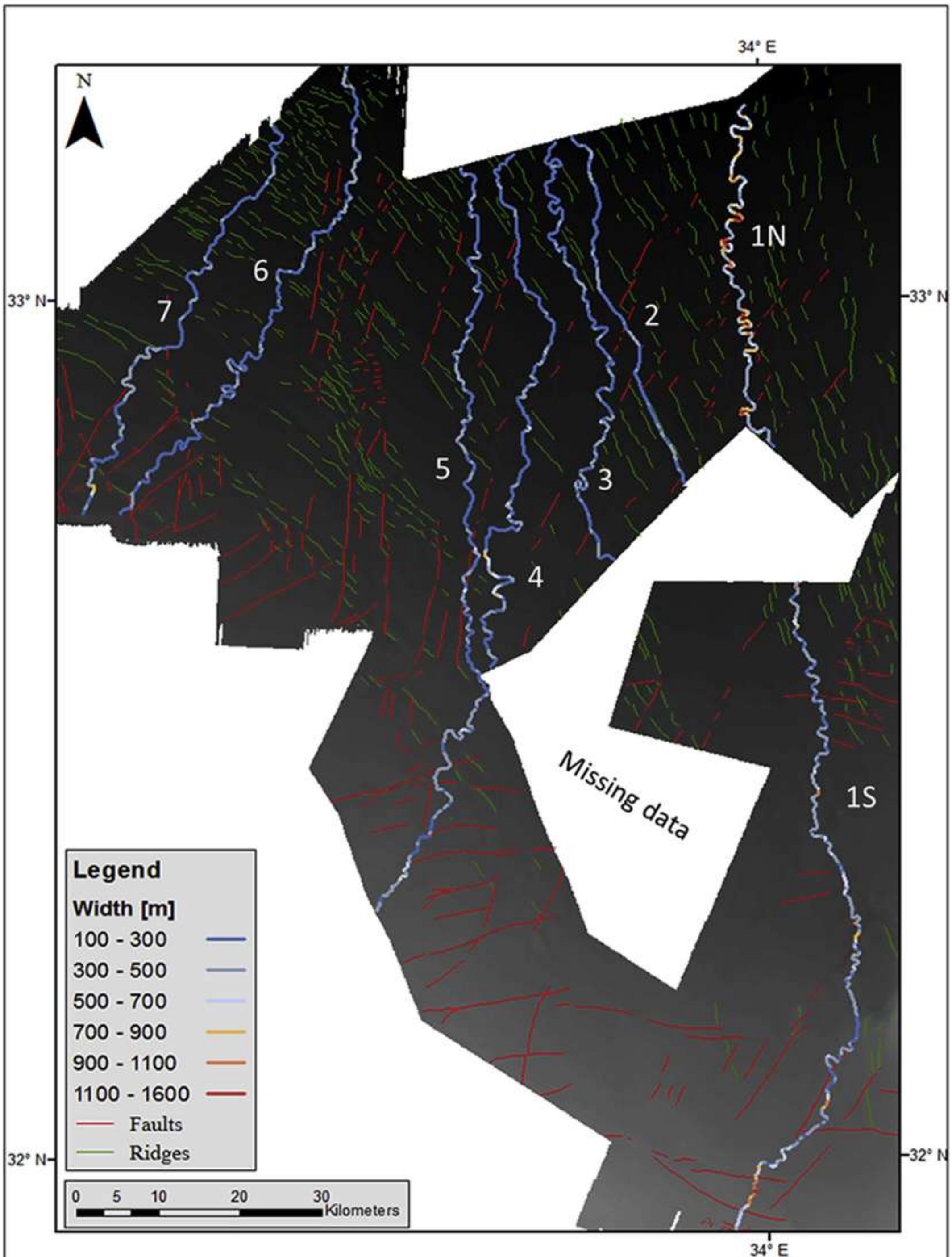

Fig. 5. Width of the channels, analyzed in ~100 m long segments. Location in Fig. 1.

integrating grids taken from Gvirtzman et al. (2015). These grids were acquired from various commercial ventures either ready-to-use seismic data grids, or seismic data from which seafloor was independently interpreted. To obtain water depth values using time grids, two way travel time (TWT) values were multiplied by a constant velocity of 755 m/sec (corresponding to a water acoustic velocity of 1510 m/sec; see Table 1 of Gvirtzman et al., 2015 and references therein). Then, we accurately mapped seven submarine channels employing an ArcGIS hydrological model, commonly used for analyzing continental drainage networks and channels together with several other ArcGIS tools that enhance channel outline. This procedure follows many studies assuming that morphology of deep-water channels can be observed similarly to terrestrial fluvial channels (Flood and Damuth, 1987; Clark et al., 1992; Shanmugam, 1996; Imran et al., 1999; Babonneau et al., 2002; Kolla et al., 2007). The data generated by this algorithm-based mapping (Fig. 1b) are more accurate than the manually digitized channels of Gvirtzman et al. (2015) and set the basis for quantitative morphometric analysis of the marine channels.

Morphometric analysis is useful in quantifying morphologic

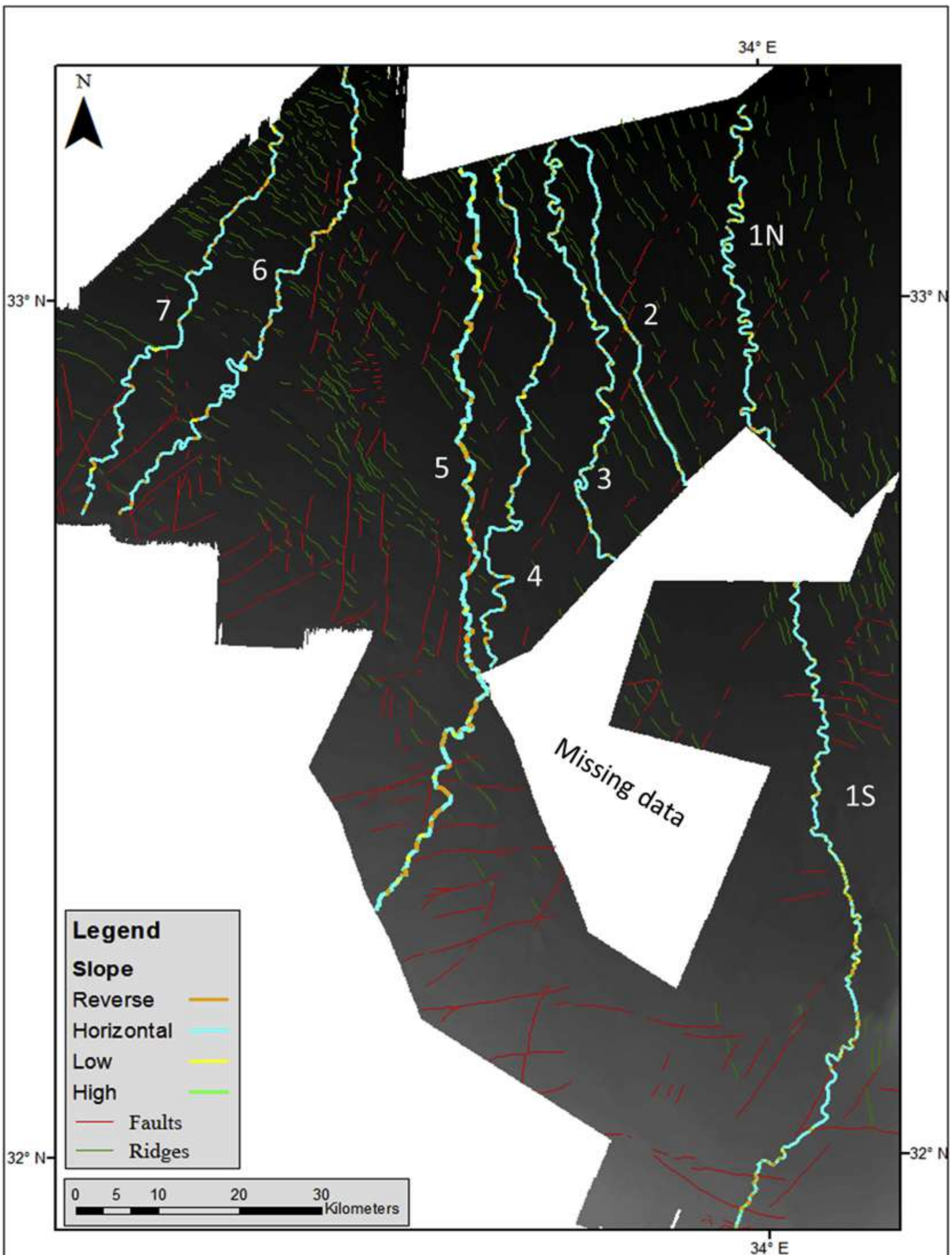

Fig. 6. Slopes of the channels, analyzed for ~100 m long segments. Location in Fig. 1.

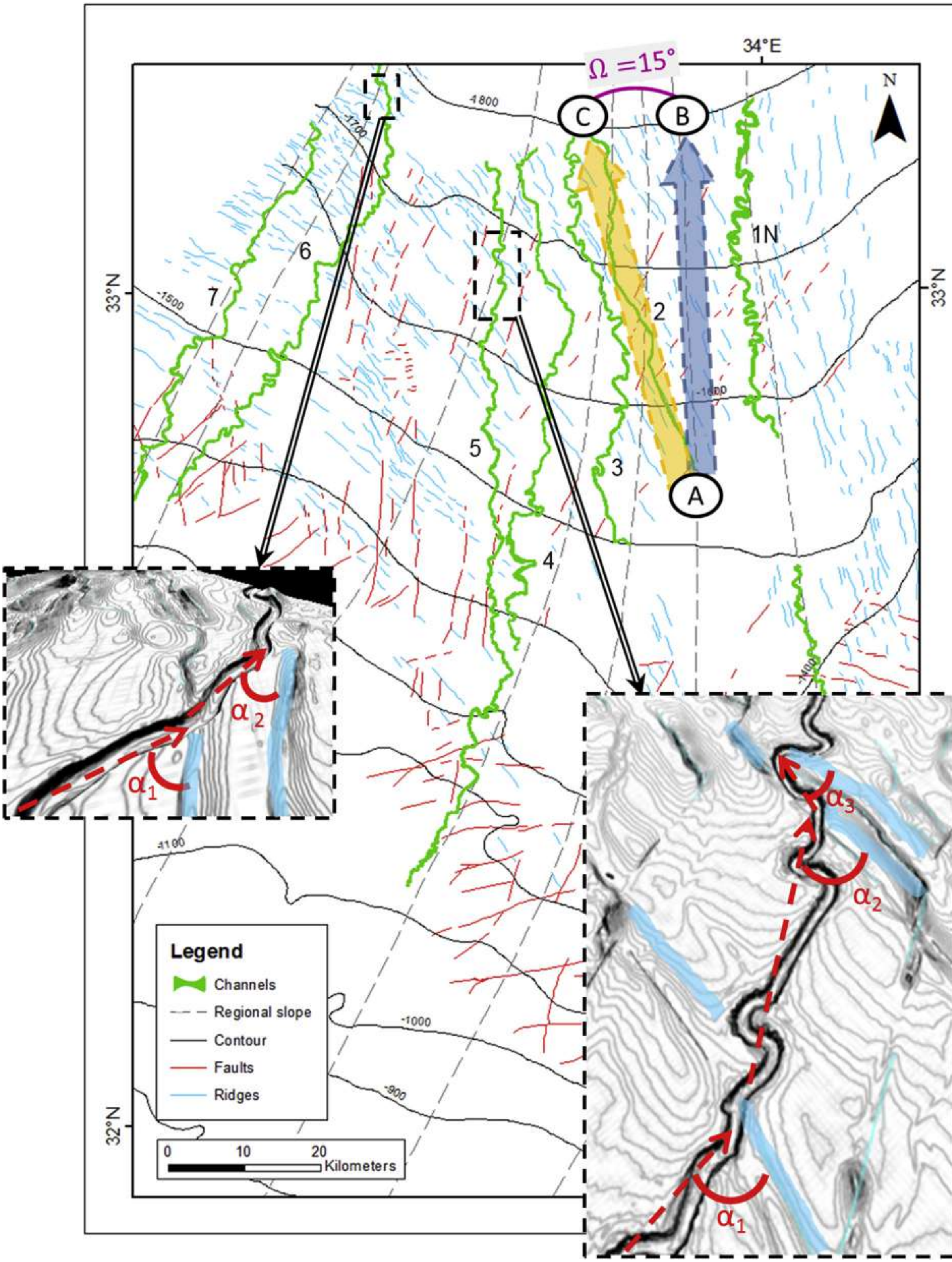

Fig. 7. A map showing channel 2 diversion (as defined in Fig. 3). 3D-bathymetry images show the different incident angels (Red dashed arrows) for each segment. Vertical exaggeration is ×3. (For interpretation of the references to colour in this figure legend, the reader is referred to the web version of this article.)

parameters such as width, sinuosity, and slope. It is based on the assumption that noticeable, systematic changes in these measurable characteristics are caused by primarily tectonic and lithologic impacts (e.g. Schumm, 1977; Schumm, 1986; Wells et al., 1988) on streams. Systematic morphometric changes between channels or between different reaches of the same channel are therefore used in evaluation of local and regional tectonics. Previous studies have used morphometric analyses, amongst others, to identify and classify sediment transport systems worldwide (Schumm, 1986; references therein; Clark et al., 1992; Normark et al., 1993; Broucke et al., 2004; Weimer et al., 2006; Mayall et al., 2006; Deptuck et al., 2007).

In the southeastern Levant Basin we observed two main types of interactions between submarine channels and seabed obstacles: a) Flowing alongside the obstacle (Fig. 2a), which is similar to what Clark and Cartwright (2009) termed “confinement”, and b) cutting right through the obstacle (Fig. 2b). These interactions may occur one right after the other, for example: a channel will flow alongside an obstacle till it reaches a weaker or lower relief that enables cutting through. When a channel flows alongside a fold (or confined by a syncline; i.e. two sub-paralleling folds) it frequently decreases its sinuosity (Fig. 2c). When the channel crosses faults it frequently increases its meanders (Fig. 2d). Similarly, at some distance from obstacles channels widen (Fig. 2e); at other points they may show narrowing (Fig. 2f). Here we examine, define, and quantify such consistent relationships, if and where they exist, for channel-obstacle interactions.

We begin with a common morphometric analysis measuring sinuosity (the ratio of channel length to direct distance from start point to end point), width, and slope employing self-developed ArcGIS and Global Mapper models. Initially, a centerline is produced along each channel (i.e., the GIS-generated thalweg). Then, the channel slope, sinuosity, and width are calculated along it. Sinuosity of each channel was characterized in two scales: a) A single number that expresses the total sinuosity of the channel within the studied area, and b) sinuosity measured continuously for 15-km-long segments along the thalweg. In our exploration for the best scale to represent sinuosity changes along channel, we

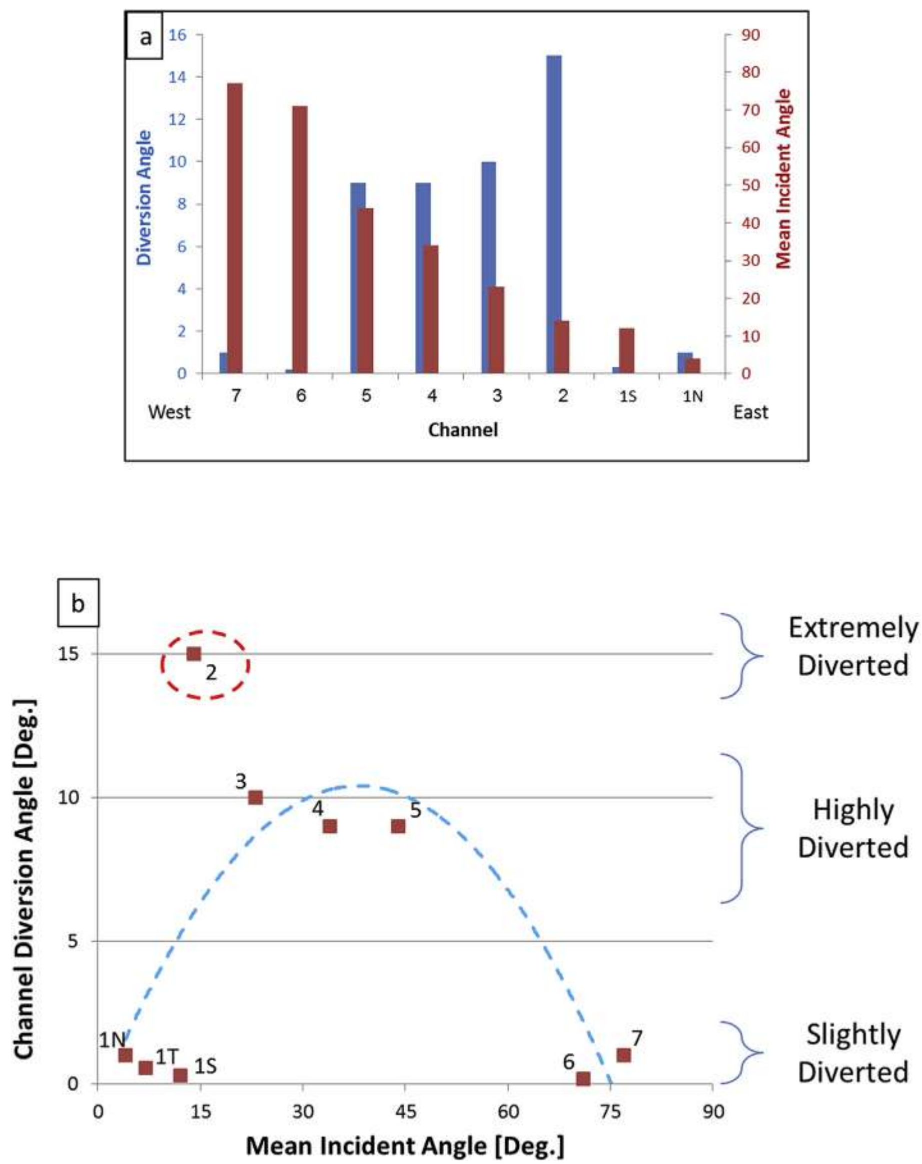

Fig. 8. a) The channel diversion VS incident angles for all channels. b) The hyperbolic relationship observed between incident angle and diversion angle. Channel 2 deviates from this behavior. 1T is the combination of 1N and 1S.

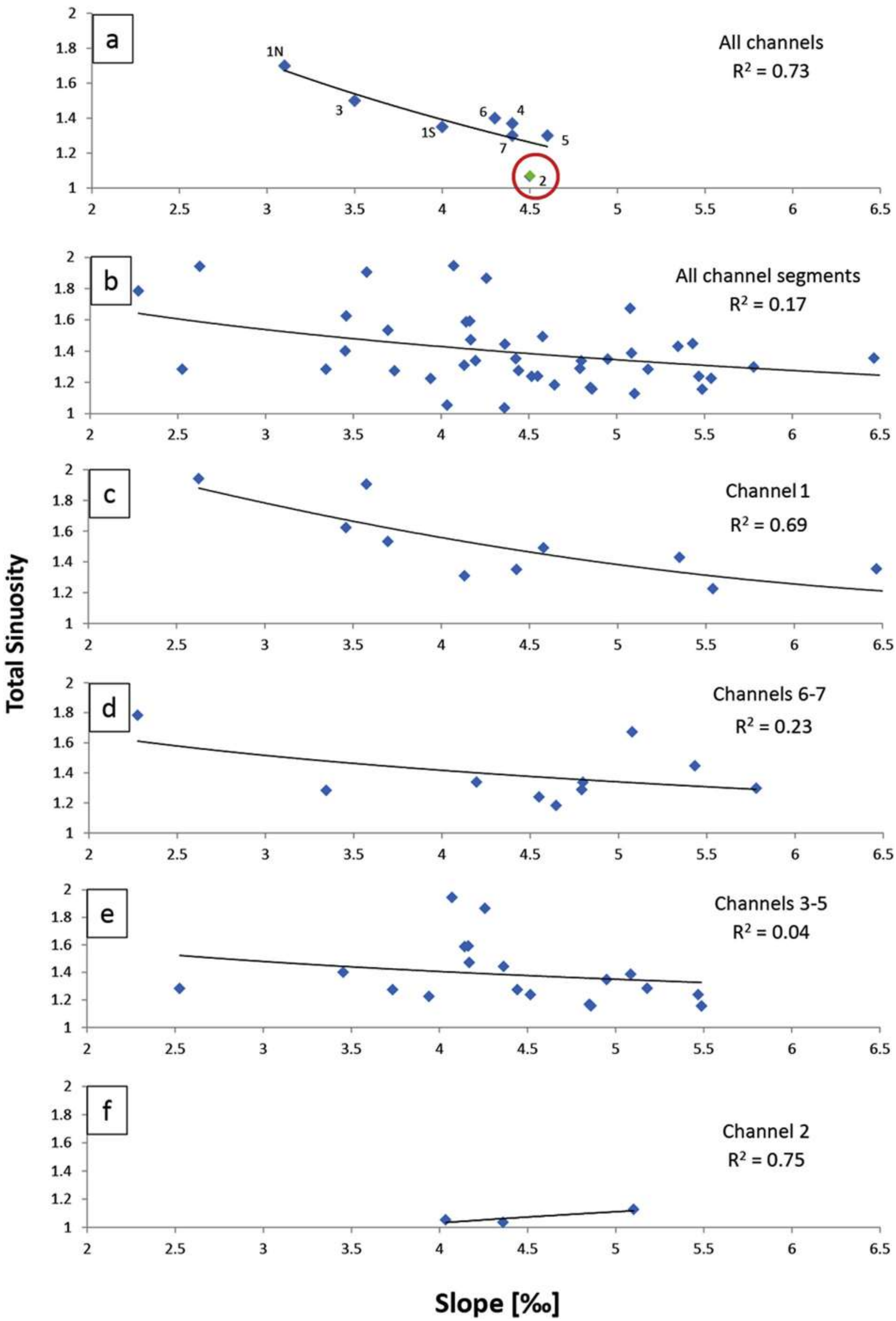
a
All channels
R² = 0.73
1N
3
1S
6
4
7
5
2
b
All channel segments
R² = 0.17
c
Channel 1
R² = 0.69
d
Channels 6-7
R² = 0.23
e
Channels 3-5
R² = 0.04
f
Channel 2
R² = 0.75
Total Sinuosity
Slope [‰]

identified this 15 km "window" as most suitable (discussed more below). Unlike sinuosity, channel width (bank-to-bank, normal to channel direction) and thalweg slope were measured at ~100-m long windows to catch smaller changes. In addition, a single average slope was calculated for the entire studied length of each channel.

Besides sinuosity, width, and slope, we applied two new morphometric parameters suitable for the channel-obstacle analysis: diversion angle (Ω) and incident angle (α) (Fig. 3). Without interfering by any obstacle or tectonics, it is expected that a channel beginning at any point (e.g., point A in Fig. 3) will take the steepest route (the direction of maximum slope; blue arrow in Fig. 3) downstream. In reality, preexisting or coeval elongated obstacles may divert the channel by an angle (α), which is the acute angle between the regionally influenced channel direction and the strike of the tectonic obstacle. After several incidences each causing a local diversion, a channel that had started at point A reaches point C (orange arrow in Fig. 3) rather than point B and the angle Ω = BAC is termed channel diversion.

4. Results

We analyzed seven submarine channels (black lines in Fig. 1b, annotated 1–7). Due to a gap in the bathymetric data, the Levant Turbidite Channel of Gvirtzman et al. (2015) we split it into north and south segments (1N and 1S, respectively). Discontinuous channels (gray lines in Fig. 1b) are not considered here further.

Sinuosity generally changes along the studied channels between 1.2 and 1.4 (orange segments, Fig. 4). Two exceptions to this relatively narrow range are channels 1N and 2 where sinuosity is higher and lower, respectively. The maximal measured sinuosity in the studied channels and in the entire area is 1.8–2 (dark blue), which indicates doubling of channel length vs. Valley length. Obviously, sinuosity depends on the length of segments chosen for analysis (e.g., for segment length close to zero sinuosity approaches 1; i.e. a straight line) as discussed by Ferry et al. (2005) and Clark and Cartwright (2009, 2011). To examine the dependence of our results on segment length, we prepared sinuosity maps for 0.4, 2.5, 5, 10, 15, and 20 km long segments (not shown here). We realized that a length of 0.4 km is too short to catch common meanders in the study area that are considerably longer. Fifteen-km long segments seem to be the most informative. Regardless of the precise length, the use of segment lengths of 10 and 20 km, do not alter the main outcome of the results presented below.

The most frequent channel widths in the study area ranges between 100 and 500 m (colder shades in Fig. 5). The wider channels in the northern part of channel 1 are the exception and reach 900–1600 m (hotter colors). In addition, at specific locations width changes near faults or folds (Fig. 2e and f). However, we did not identify a simple rule associating changes in channel width to locations of obstacles, as was demonstrated in several terrestrial cases (Schumm, 1986).

Fig. 6 presents four ranges of channel slope: high (50‰–100‰), low (15‰–50‰), sub-horizontal (15‰ to −15‰), and negative sub-horizontal (<-15‰). Negative (or reverse) slope means that locally the thalweg is going upwards while advancing in the general flow direction, indicating either post-flow deformation with some uplift component of the channel thalweg or a depositional process that leaves a negative slope when sediments settle down after a flow event (examples in Weimer et al., 2006, Chapter 6, and references therein). The most frequent channel slope in the study area is sub-horizontal (−15‰–15‰), but low (15‰–50‰) and high (50‰–100‰) slopes are recognized as well. Again, a simple rule relating changes in slope to interference with obstacles is difficult to identify.

The channel bearing diversions from the steepest slope direction are emphasized in Fig. 7. A comparison between channels and maximum slope directions (Fig. 7, dashed black boxes) demonstrates that the directions of channel 1 and channel 6 and 7 approximately coincide with the regional slope, whereas other channels are diverted to the northwest. A detailed numeric example for such an analysis is presented in Fig. 8a (and in appendix A) with an average incidence $\alpha = 14^\circ$, and divergence $\Omega = 15^\circ$. This figure also demonstrates that for very low (1°–5°) and very high (70°–80°) incident angles, diversion is very small (Ω~0°). For intermediate incidence angles, diversion is relatively high (10°–15°). The explanation for this is that when a channel reaches a barrier orthogonal to flow direction (α~90°), channels cut right through without a diversion. Similarly, when a channel is approximately sub-parallel to obstacle, channels will flow alongside obstacles without diversion. Only when the channel flow direction is approximately diagonal (α~45°) to obstacles, channels are diverted significantly until finding a point where they can crosscut the obstacle or a point where the obstacle ends and returning to the regional slope direction is possible (Fig. 2b).

5. Discussion

5.1. Morphometry of submarine channels

The first order responses of channels to active salt tectonics in the southeastern Levant Basin are either (a) bypassing of the obstacles or (b) cutting them through weaker or lower zones or during initial stages of formation. Often, these responses are associated with changes in morphometric attributes, but no consistent behavior is identified. Upon encountering an obstacle, channel sinuosity sometimes increases and sometimes decreases, whereas channel width and slope generally do not change much (Appendix B). Hence, we conclude that the classic approach of analyzing sinuosity, width, and slope, do not provide much insight to channel-tectonic interaction in the area studied.

In contrast, the diversion analysis proposed in this study, shows hyperbolic relationships (Fig. 8b) between incident angle (α) and diversion angle (Ω). Channel 1 flows parallel to tectonic folds (α~0°) and is not diverted. Channels 6 and 7 crosscut folds at nearly orthogonal (α~80°) direction and therefore are considered as non-diverted. Channels 3, 4, and 5 are diverted by ~10° as a result of incidence with many small folds with an average incidence angle of about 40°. Channel 2 presents the highest diversion with a divergence angle of 15°, despite its relatively small average incidence angle (14°). This high diversion of channel 2 from the regional slope is forced by its confinement both along several relatively long submarine synclines and in-between two obstacles. These two types of tectonic features are in affect ~70% of the total length of channel 2. The confinement prevents the channel from meandering by creating barriers that define the path of channel flow (Fig. 2a).

Regardless of channel-tectonic interaction, slope and sinuosity of the entire channel lengths are reversely well correlated (Fig. 9a

Fig. 9. Sinuosity-slope relationships. Figures a) and b) are sinuosity of all channels using their entire length and of their 15 km long segments, respectively. Channel 2 (marked in red) deviates from the general trend of channel sinuosity. Removing it, increase the correlation between slope and sinuosity r2 = 0.86. See Table 1 for data. Figures c–f present the slope-sinuosity relationships for the individual channels using sinuosity determination for 15 km long segments. (For interpretation of the references to colour in this figure legend, the reader is referred to the web version of this article.)

Table 1
Sinuosity and slope for the entire length of each channel.

Channel	Total sinuosity	[‰]Average slope
1N	1.7	3.1
1S	1.35	4
2	1.07	4.5
3	1.5	3.5
4	1.37	4.4
5	1.3	4.6
6	1.4	4.3
7	1.3	4.4

and Table 1). This is consistent with observations from continental rivers that cut their way through steep landscape and meander in low relief terrains, a general observation that begun with Leopold and Wolman (1957). For instance, the Levant Turbidite Channel (channel 1) is less sinusoidal at its southern segment (1S) and presents numerous meanders in the gently sloping deeper basin (1N). Interestingly, channel 2 is, again, an exception to this rule; removing it from the regression analysis increases the correlation to 0.86. In other words, channel 2 is diverted, straight, and does not fit the general slope-sinuosity trend observed in the southeastern Levant Basin channels.

Sinuosity-slope relationships using many 15-km-long segments (Fig. 9b–f), instead of considering each channel as a whole (Fig. 9a), indicates that sinuosity-slope relationships are more complex when splitting the channels to segments. On the same sinuosity-slope axes, segments from all the channels show large scattering and poor correlation of $R^2 \sim 0.2$ (Fig. 9b). Separating this large number of segments according to their respective incidence angle reveals significant differences. All segments of channel 1 that are parallel to tectonic folds yield well correlation ($R^2 \sim 0.7$, Fig. 9c), whereas channels 6 and 7, which are orthogonal to folds show poor correlation ($R^2 \sim 0.2$, Fig. 9d). In channels 3, 4, and 5, which flow diagonally to folds there is no correlation ($R^2 \sim 0.05$, Fig. 9e) between sinuosity and slope. Overall In channel 1, the normal slope-sinuosity behavior remains; in channels 6 and 7, it is completely disordered and in channels 3, 4, and 5, it is slightly disturbed. These observations are consistent with the diversion analysis, indicating that tectonic elements within the basin not only affect channel diversion, but also improve or deteriorate slope-sinuosity relationship. Channel 2 is an exception with an opposite slope-sinuosity trend and relatively high correlation ($R^2 \sim 0.8$, Fig. 9f) between slope and sinuosity.

These slope-sinuosity results are consistent with variations along the Levant Turbidite Channel (channel 1) that is wider and more sinusoidal in its distal northern part, which is less steep. Gvirtzman et al. (2015) has raised the question of its sources arguing that it may be fed by the NDSF sediments just like the rest of the submarine channels in the Levant Basin or by a combination of the El-Arish and Ha-Bsor rivers as an alternative source. Our results indicate that the high sinuosity of this channel 1 is well explained by its relatively low slope (e.g., Leopold and Wolman, 1957). Unfortunately, its morphology attributes do not shed new light on its sources.

5.2. Regional implications

Studying the local channel evolution around individual structures in southern Levant basin, Clark and Cartwright (2011) presented a local scale “Diversion” as a type of interaction between submarine channels and underlying deformation. From their work it can be concluded that even on that localized scale, submarine channel deformation is controlled by the frequency and scale of the structures. This emphasizes that the morphology of submarine channels is controlled directly by the regional style of deformation.

Fig. 10 shows that the channels we mapped (green) in the southern Levant basin are a part of a larger channel system (blue) surrounding the NDSF (Loncke et al., 2006, 2009). Interestingly, comparing channel direction to the shape of isobaths allows immediate identification of regions with channel diversion. For instance, in the northern part of the Levant basin (approximately between lat. 33°-34° and long. 33°-34°) channels are not orthogonal to isobaths, but divert westwards similar to what we described in detail, south of this region. In contrast, in the western province of the NDSF (facing the Rosetta branch of the Nile River) the channel system is quite orthogonal to isobaths fitting the regional slope.

Consistent with our analysis is the circum-Nile fold belt mapped and described by Loncke et al. (2006) and later by Gvirtzman et al. (2015), which crosses the Levant basin in the region where we identify channel diversion, but it does not cross the Rosetta channel system in the west (i.e. in the western province area where channels flow perpendicular to the isobaths, the fold belt are further north). This quick analysis of Fig. 10 demonstrates how channel diversion can be used to trace areas with very gentle tectonic elements that cannot be traced without high resolution bathymetry data.

5.3. Implications to other basins

The analysis of channels in the Levant Basin illustrates that diversion is strongly dependent on incidence angle [α], which in turn, depends on the basin geometry and the tectonic pattern. In the area studied here, folding axis direction varies from NNW in the east (near channel 1) to NW in the central area (channels 3, 4, and 5) to WNW in the west (channels 6 and 7). This pattern is not random, but is the outcome of the salt tectonics that forms the circum-Nile delta radial system (Loncke et al., 2006, 2009; Gvirtzman et al., 2015).

The exceptional behavior of channel 2 further indicates that the length of the tectonic segment confining and bounding the channel is also important. With the same line of reasoning, we hypothesize that the spacing between tectonic elements is of vast importance; large spacing allows long segments to flow without disturbance in the direction of the regional slope. As a generalized prediction that may be tested in other basins, we suggest that $\Omega = f(L, D, \alpha)$, where L is the length of obstacles and D is typical distance between obstacles. We hypothesize that Ω will increase with increasing L, decrease with increasing D, and will show hyperbolic relationship with α, as in the Levant basin (Fig. 11).

Can this analysis be applied for other basins in the world? In what follows we bring some examples of different basins around the world describing how obstacles affect channels and how they respond morphometrically.

In the southeastern corner of Iran, the Indus Valley and the Mississippi Valley, diversion was described for fluvial rivers upon encountering tectonic obstacles (Schumm, 1986).

The migration and aggradation of submarine channels in the western Niger Delta were seismically analyzed (Deptuck et al., 2007). The results show that in many cases, the thalweg of the submarine channel is confined due to “local factors” that shape the channel morphology, consistent with our results. The same channel-levee system was seismically interpreted further down dip (Tripsanas et al., 2012). These seismic sections of the Niger Delta display a 50–100 m deep and 500–1000 m wide channel climbing over a 19 km long and 5 km wide ridge that present a 20–70 m tall obstacle across the channels path.

Offshore Angola, Gee and Gawthorpe, 2006 use seismic data to demonstrate how submarine channels react to obstacles generated around salt diapirs. The diapirs offshore Angola are 3–6 km wide at

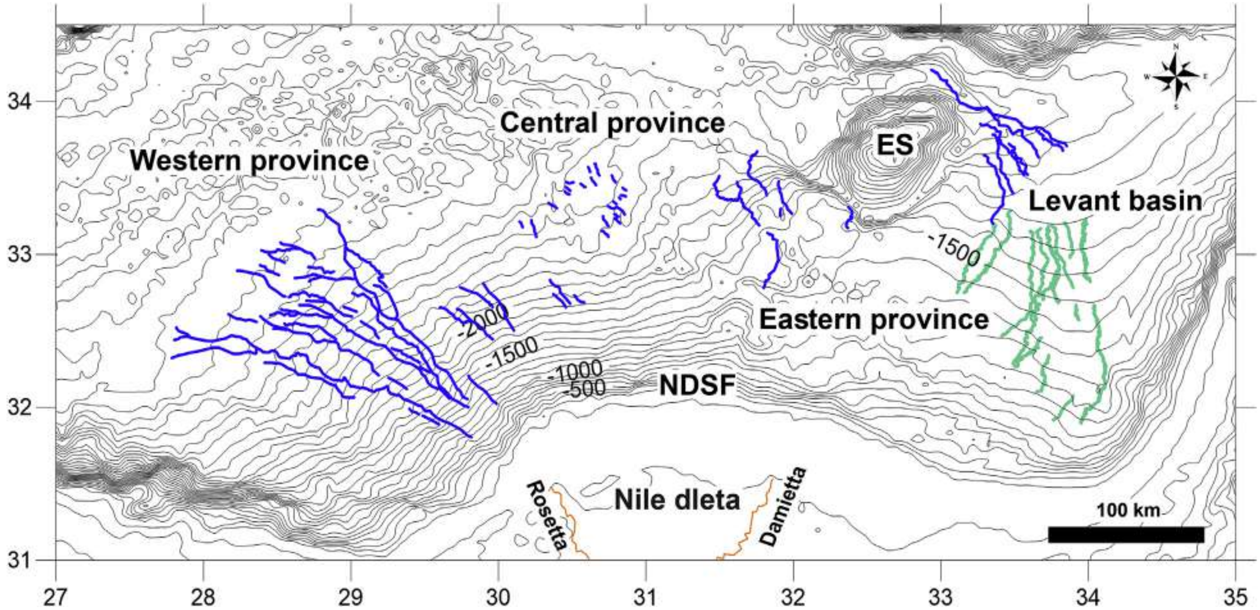

Fig. 10. The different provinces of the eastern Mediterranean Sea as divided by Loncke et al. (2006). Blue lines indicate channels mapped by Loncke et al. (2006). Green lines are channels mapped in this study. ES = Eratosthenes Seamount. NDSF = Nile deep-sea fan. (For interpretation of the references to colour in this figure legend, the reader is referred to the web version of this article.)

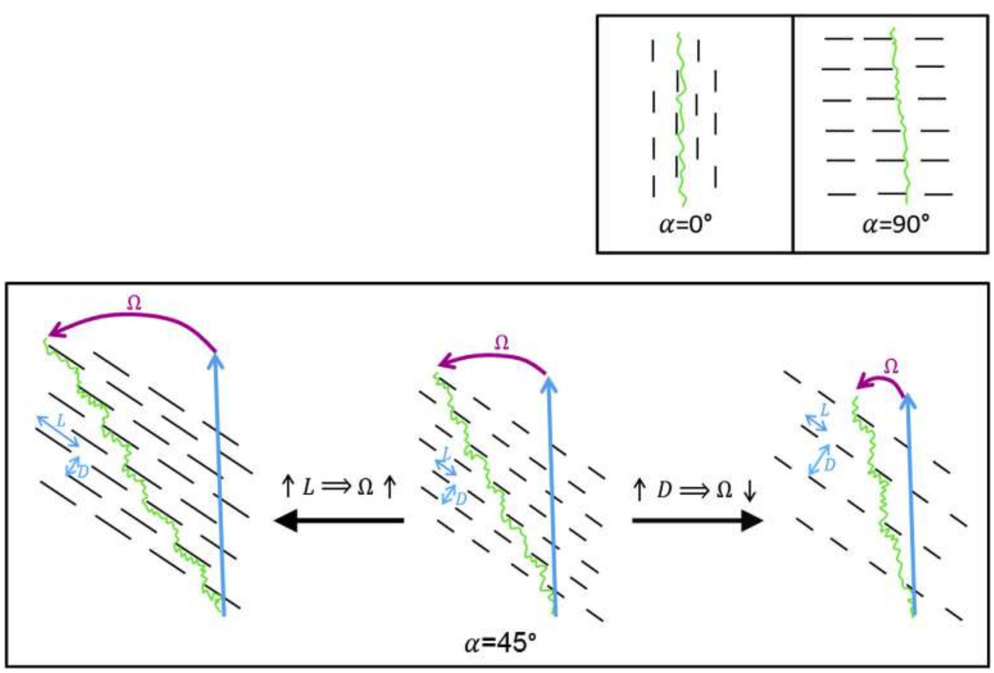

Fig. 11. Illustration of the parameters documenting channel diversion; $\Omega=(L,D,\alpha)$. Ω = diversion angle; α = incident angle; L = segment length; D = distance between obstacles; blue arrow = regional slope. Incident angles that are parallel or perpendicular ($\alpha = 90^\circ$ or 0°) do not affect channel flow direction (top). If incident angle $\approx 45^\circ$, segment length and distance between obstacles have opposite effects on diversion (bottom). An increase in segment length increases the diversion and an increase in distance between obstacles decreases the diversion. (For interpretation of the references to colour in this figure legend, the reader is referred to the web version of this article.)

the subsurface forming a twice as wide deformation zone on the seafloor with a radial system of arcuate faults and folds >200 m high. These channels, upon encountering obstacles, are shifted laterally and vertically.

In the Sao Tomé system in the southern Brazil Basin, Viana et al. (2003) focused on causes of changes in sediment volume delivered by submarine channels. They demonstrate that, amongst other variables such as sea level and volcanic activity, salt diapirisim shifts the course of a submarine channel, affecting the final sediment volume delivered.

Regional diversion can be applied in other salt-tectonic affected submarine basins such as other Brazil basins (Rohais et al., 2010), the southern Bering Sea, the Gulf of Mexico (Nelson et al., 2011), and the Congo Fan (Kolla et al., 2001).

These previously studied basins have been morphometrically studied to a great extent, mostly focusing on local affects.

Understanding the regional effect of tectonic obstacles on submarine channels, as sediment suppliers, can further explain different depositional settings not yet understood. Therefore, while analyzing different submarine channel systems and basins the method presented above should be taken into consideration when analyzing the effect of tectonic obstacles on the regional channel systems.

6. Conclusions

Submarine channels are abundant features in the eastern Mediterranean Sea with sinuosity, width and slope characteristics that vary significantly downstream. The bathymetry data show how geomorphology of channels responds and is tightly related to obstacles created by salt tectonics (i.e. faults and folds) on the sea floor of the basin (Gvirtzman et al., 2014, 2015). To measure the impact of tectonics on the basin-scale morphology of the submarine channels, two new geomorphic parameters, termed Channel Diversion and Incident Angle, were developed. These new parameters determine (a) whether a submarine channel is morphologically affected upon encountering obstacles, (b) how this channel morphology is affected by the tectonic obstacle in a regional point of view, and (c) which other parameters affect these observations. In our basin, submarine channels that encounter obstacles on a near parallel or near perpendicular angle on average, are mildly or not diverted. On contrary, if this channel-obstacle incident occurs on a ~45° angle, the channel will be highly diverted.

Furthermore, sinuosity-slope relations demonstrate that submarine channels have similar behavior to fluvial channels. This study demonstrates that tectonic elements within a basin not only affect channel diversion, but also slope-sinuosity relationship.

Acknowledgments

We are much grateful to E. Dente for helping with the ArcGIS models, comments and advice. This study was supported by the Israeli Ministry of National Infrastructures, Energy and Water Resources.

Appendix A. Supplementary data

Supplementary data related to this article can be found at http://dx.doi.org/10.1016/j.marpetgeo.2017.01.002.

References

Almagor, G., 1984. Salt-controlled slumping on the Mediterranean slope of central Israel. Mar. Geophys. Res. 6, 227–243.

Almagor, G., Garfunkel, Z., 1979. Submarine slumping in continental margin of Israel and northern Sinai. AAPG Bull. 63, 324–340.

Almagor, G., Hall, J.K., 1983. Morphology of the continental margin off north-central Israel. Israel J. Earth Sci. 32, 75–82.

Babonneau, N., Savoye, B., Cremer, M., Klein, B., 2002. Morphology and architecture of the present canyon and channel system of the Zaire deep-sea fan. Mar. Pet. Geol. 19, 445–467. http://dx.doi.org/10.1016/S0264-8172(02)00009-0.

Bellaiche, G., Loncke, L., Gaullier, V., Mascle, J., Courp, T., Moreau, A., Radan, S., Sardou, O., 2001. Le cône sous-marin du Nil et son réseau de chenaux profonds : nouveaux résultats (campagne Fanil). Comptes Rendus l'Académie des Sci. - ser. IIA - Earth Planet. Sci. 333, 399–404. http://dx.doi.org/10.1016/S1251-8050(01)01645-7.

Ben-Avraham, Z., 1978. The structure and tectonic setting of the levant continental margin, Eastern Mediterranean. Tectonophysics 46, 313–331. http://dx.doi.org/10.1016/0040-1951(78)90210-X.

Ben-Avraham, Z., Mart, Y., 1981. Late Tertiary structure and stratigraphy of north Sinai continental margin. AAPG Bull. 65, 1135–1145.

Ben-Gai, Y., Ben-Avraham, Z., Buchbinder, B., Kendall, C.G.S.C., 2005. Post-Messinian evolution of the Southeastern Levant Basin based on two-dimensional stratigraphic simulation. Mar. Geol. 221, 359–379. http://dx.doi.org/10.1016/j.margeo.2005.03.003.

Bertoni, C., Cartwright, J.A., 2006. Controls on the basinwide architecture of late Miocene (messinian) evaporites on the levant margin (eastern mediterranean). Sediment. Geol. 188–189, 93–114. http://dx.doi.org/10.1016/j.sedgeo.2006.03.019.

Bertoni, C., Cartwright, J.A., 2007. Major erosion at the end of the messinian salinity crisis: evidence from the Levant basin, eastern mediterranean. Basin Res. 19, 1–18. http://dx.doi.org/10.1111/j.1365-2117.2006.00309.x.

Broucke, O., Temple, F., Rouby, D., Robin, C., Calassou, S., Nalpas, T., Guillocheau, F., 2004. The role of deformation processes on the geometry of mud-dominated turbiditic systems, Oligocene and Lower–Middle Miocene of the Lower Congo basin (West African Margin). Mar. Pet. Geol. 21, 327–348. http://dx.doi.org/10.1016/j.marpetgeo.2003.11.013.

Buchbinder, B., Zilberman, E., 1997. Sequence stratigraphy of Miocene-Pliocene carbonate-siliciclastic shelf deposits in the eastern Mediterraneanmargin (Israel): ef- fects of eustasy and tectonics. Sediment. Geol. 112, 7–32.

Cartwright, J.A., Jackson, M.P.A., 2008. Initiation of gravitational collapse of an evaporite basin margin: the Messinian saline giant. Levant. Basin, East. Mediterr. Geol. Soc. Am. Bull. 120, 399–413. http://dx.doi.org/10.1130/B26081X.1.

Cartwright, J., Jackson, M., Dooley, T., Higgins, S., 2012. Strain partitioning in gravity-driven shortening of a thick, multilayered evaporite sequence. Geol. Soc. London. Spec. Publ. 363, 449–470. http://dx.doi.org/10.1144/SP363.21.

Clark, J.D., Kenyon, N.H., Pickering, K.T., 1992. Quantitative analysis of the geometry of submarine channels: implications for the classification of submarine fans. Geology. http://dx.doi.org/10.1130/0091-7613(1992)020<0633:QAOTGO>2.3.CO.

Clark, I.R., Cartwright, J.A., 2009. Interactions between submarine channel systems and deformation in deepwater fold belts: examples from the Levant Basin, Eastern Mediterranean sea. Mar. Pet. Geol. 26, 1465–1482. http://dx.doi.org/10.1016/j.marpetgeo.2009.05.004.

Clark, I.R., Cartwright, J.A., 2011. Key controls on submarine channel development in structurally active settings. Mar. Pet. Geol. 28, 1333–1349. http://dx.doi.org/10.1016/j.marpetgeo.2011.02.001.

Deptuck, M.E., Sylvester, Z., Pirmez, C., O'Byrne, C., 2007. Migration–aggradation history and 3-D seismic geomorphology of submarine channels in the Pleistocene Benin-major Canyon, western Niger Delta slope. Mar. Pet. Geol. 24, 406–433. http://dx.doi.org/10.1016/j.marpetgeo.2007.01.005.

Ducassou, E., Capotondi, L., Murat, A., Bernasconi, S.M., Mulder, T., Gonthier, E., Migeon, S., Duprat, J., Giraudeau, J., Mascle, J., 2007. Multiproxy Late Quaternary stratigraphy of the Nile deep-sea turbidite system — towards a chronology of deep-sea terrigeneous systems. Sediment. Geol. 200, 1–13. http://dx.doi.org/10.1016/j.sedgeo.2007.01.023.

Ducassou, E., Mulder, T., Migeon, S., Gonthier, E., Murat, A., Revel, M., Capotondi, L., Bernasconi, S.M., Mascle, J., Zaragosi, S., 2008. Nile floods recorded in deep Mediterranean sediments. Quat. Res. 70, 382–391. http://dx.doi.org/10.1016/j.yqres.2008.02.011.

Ducassou, E., Migeon, S., Mulder, T., Murat, A., Capotondi, L., Bernasconi, S.M., Mascle, J., 2009. Evolution of the Nile deep-sea turbidite system during the Late Quaternary: influence of climate change on fan sedimentation. Sedimentology 56, 2061–2090. http://dx.doi.org/10.1111/j.1365-3091.2009.01070.x.

Ducassou, E., Migeon, S., Capotondi, L., Mascle, J., 2013. Run-out distance and erosion of debris-flows in the Nile deep-sea fan system: evidence from lithofacies and micropalaeontological analyses. Mar. Pet. Geol. 39, 102–123. http://dx.doi.org/10.1016/j.marpetgeo.2012.09.006.

Ferry, J., Mulder, T., Parize, O., Raillard, S., 2005. Concept of equilibrium profile in deep-water turbidite system: effects of local physiographic changes on the nature of sedimentary process and the geometries of deposits. Geol. Soc. Lond. Spec. Publ. 244, 181–193. http://dx.doi.org/10.1144/GSL.SP.2005.244.01.11.

Flood, R.D., Damuth, J.E., 1987. Quantitative characteristics of sinuous distributary channels on the Amazon Deep-Sea Fan. Geol. Soc. Am. Bull. http://dx.doi.org/10.1130/0016-7606(1987)98<728:QCOSDC>2.0.CO;2.

Folkman, Y., Mart, Y., 2008. Newly recognized eastern extension of the Nile deep-sea fan. Geology 36, 939. http://dx.doi.org/10.1130/G24995A.1.

Garfunkel, Z., 1984. Large-scale submarine rotational slumps and growth faults in the Eastern Mediterranean. Mar. Geol. 55, 305–324. http://dx.doi.org/10.1016/0025-3227(84)90074-4.

Garfunkel, Z., 1998. Constrains on the origin and history of the Eastern Mediterranean basin. Tectonophysics 298, 5–35. http://dx.doi.org/10.1016/S0040-1951(98)00176-0.

Garfunkel, Z., Almagor, G., 1984. Geology and structure of the continental margin off northern Israel and the adjacent part of the Levantine Basin. Mar. Geol. 62, 105–131. http://dx.doi.org/10.1016/0025-3227(84)90057-4.

Garfunkel, Z., Almagor, G., 1987. Active salt dome development in the Levant Basin, southeast Mediterranean. In: Dynamical Geology of Salt and Related Structures, pp. 263–300. http://dx.doi.org/10.1016/B978-0-12-444170-5.50011-7.

Garziglia, S., Migeon, S., Ducassou, E., Loncke, L., Mascle, J., 2008. Mass-transport deposits on the Rosetta province (NW Nile deep-sea turbidite system, Egyptian margin): characteristics, distribution, and potential causal processes. Mar. Geol. 250, 180–198. http://dx.doi.org/10.1016/j.margeo.2008.01.016.

Gaullier, V., Mart, Y., Bellaiche, G., Mascle, J., Vendeville, B.C., Zitter, T., 2000. Salt tectonics in and around the Nile deep-sea fan: insights from the PRISMED II cruise. Geol. Soc. Lond. Spec. Publ. 174, 111–129. http://dx.doi.org/10.1144/GSL.SP.1999.174.01.07.

Gee, M.J.R., Gawthorpe, R.L., 2006. Submarine channels controlled by salt tectonics: examples from 3D seismic data offshore Angola. Mar. Pet. Geol. 23, 443–458. http://dx.doi.org/10.1016/j.marpetgeo.2006.01.002.

Goldsmith, V., Golik, A., 1980. Sediment transport model of the southeastern

Mediterranean coast. Mar. Geol. 37, 147–175. http://dx.doi.org/10.1016/0025-3227(80)90015-8.

Gradmann, S., Hübscher, C., Ben-Avraham, Z., Gajewski, D., Netzeband, G., 2005. Salt tectonics off northern Israel. Mar. Pet. Geol. 22, 597–611. http://dx.doi.org/10.1016/j.marpetgeo.2005.02.001.

Gvirtzman, G., Buchbinder, B., 1978. The late tertiary of the coastal plain and continental shelf of Israel and its bearing of the history of the Eastern Mediterranean. In: Ross, D.H., Neprochnov, Y.P. (Eds.), Initial Reports of the Deep Sea Drilling Project. US Government Printing Office, Washington, pp. 1195–1222.

Gvirtzman, Z., Zilberman, E., Folkman, Y., 2008. Reactivation of the Levant passive margin during the late Tertiary and formation of the Jaffa Basin offshore central Israel. J. Geol. Soc. Lond. 165, 563–578. http://dx.doi.org/10.1144/0016-76492006-200.

Gvirtzman, Z., Reshef, M., Buch-Leviatan, O., Ben-Avraham, Z., 2013. Intense salt deformation in the Levant basin in the middle of the messinian salinity crisis. Earth Planet. Sci. Lett. 379, 108–119. http://dx.doi.org/10.1016/j.epsl.2013.07.018.

Gvirtzman, Z., Csato, I., Granjeon, D., 2014. Constraining sediment transport to deep marine basins through submarine channels : the Levant margin in the Late Cenozoic. Mar. Geol. 347, 12–26.

Gvirtzman, Z., Reshef, M., Buch-Leviatan, O., Groves-Gidney, G., Karcz, Z., Makovsky, Y., Ben-Avraham, Z., 2015. Bathymetry of the Levant basin: interaction of salt-tectonics and surficial mass movements. Mar. Geol. 360, 25–39. http://dx.doi.org/10.1016/j.margeo.2014.12.001.

Hsü, K.J., Ryan, W.B.F., Cita, M.B., 1973. Late Miocene Desiccation of the Mediterranean. Nature. ISSN: 0028-0836 242 (5395), 240–244. ISBN: 0028-0836, http://dx.doi.org/10.1038/242240a0.

Huebscher, C., Beitz, M., Dummong, S., Gradmann, S., Meier, K., Netzband, G., 2008. Startigraphy, fluid dynamics and structural evolution of the messinian evaporites in the Levant basin, eastern mediterranean sea. In: Briand, F. (Ed.), The Messinian Salinity Crisis from Mega-deposits to Microbiology - a Consensus Report. CIESM, p. 168.

Imran, J., Parker, G., Pirmez, C., 1999. A nonlinear model of flow in meandering submarine and subaerial channels. J. Fluid Mech. http://dx.doi.org/10.1017/S0022112099006515.

Kane, I.A., McCaffrey, W.D., Peakall, J., 2008. Controls on sinuosity evolution within submarine channels. Geology 36, 287. http://dx.doi.org/10.1130/G24588A.1.

Katz, O., Reuven, E., Aharonov, E., 2015. Submarine landslides and fault scarps along the eastern Mediterranean Israeli continental-slope. Mar. Geol. 369, 100–115.

Kolla, V., Bourges, P., Urruty, J.M., Safa, P., 2001. Evolution of deep-water Tertiary sinuous channels offshore Angola (west Africa) and implications for reservoir architecture. Am. Assoc. Pet. Geol. Bull. 85, 1373–1405. http://dx.doi.org/10.1306/8626CAC3-173B-11D7-8645000102C1865D.

Kolla, V., Posamentier, H.W., Wood, L.J., 2007. Deep-water and fluvial sinuous channels—characteristics, similarities and dissimilarities, and modes of formation. Mar. Pet. Geol. 24, 388–405. http://dx.doi.org/10.1016/j.marpetgeo.2007.01.007.

Leopold, L.B., Wolman, M.G., 1957. River channel patterns. U.S. Geol. Surv. Prof. Pap. 282-B, 39–59.

Loncke, L., Gaullier, V., Bellaiche, G., Mascle, J., 2002. Recent depositional patterns of the nile deep-sea fan from echo-character mapping. Am. Assoc. Pet. Geol. Bull. 86.

Loncke, L., Gaullier, V., Mascle, J., Vendeville, B., Camera, L., 2006. The Nile deep-sea fan: an example of interacting sedimentation, salt tectonics, and inherited subsalt paleotopographic features. Mar. Pet. Geol. 23, 297–315. http://dx.doi.org/10.1016/j.marpetgeo.2006.01.001.

Loncke, L., Gaullier, V., Droz, L., Ducassou, E., Migeon, S., Mascle, J., 2009. Multi-scale slope instabilities along the Nile deep-sea fan, Egyptian margin: a general overview. Mar. Pet. Geol. 26, 633–646. http://dx.doi.org/10.1016/j.marpetgeo.2008.03.010.

Macgregor, D.S., 2012. The development of the Nile drainage system: integration of onshore and offshore evidence. Pet. Geosci. 18, 417–431. http://dx.doi.org/10.1144/petgeo2011-074.

Maldonado, A., Stanley, D.J., 1979. Depositional patterns and Late Quaternary evolution of two Mediterranean submarine fans: a comparison. Mar. Geol. 31, 215–250.

Mart, Y., 1982. Quaternary tectonic pattern along the continental margin of the northeastern Mediterranean. Mar. Geol. 49, 327–344.

Mart, Y., Eisin, B., Folkman, Y., 1978. The Palmahim Structure - a model of contineous tectonic activity since the upper Miocene in the southeastern Mediterranean off Israel. Earth Planet. Sci. Lett. 39, 328–334.

Mart, Y., Ben-Gai, Y., 1982. Some depositional patterns at continental margin of southeaster Mediterranean Sea. AAPG Bulletin-American Assoc. Petrol. Geol. 66, 460–470.

Mart, Y., Ryan, W., 2007. The Levant slumps and the Phoenician structures: collapse fea- tures along the continental margin of the southeastern Mediterranean Sea. Mar. Geophys. Res. 28, 297–307.

Martinez, J.F., Cartwright, J., Hall, B., 2005. 3D seismic interpretation of slump complexes: examples from the continental margin of Israel. Basin Res. 17, 83–108. http://dx.doi.org/10.1111/j.1365-2117.2005.00255.x.

Mascle, J., Sardou, O., Loncke, L., Migeon, S., Caméra, L., Gaullier, V., 2006. Morphostructure of the egyptian continental margin: insights from swath bathymetry surveys. Mar. Geophys. Res. 27, 49–59. http://dx.doi.org/10.1007/s11001-005-1559-x.

Mayall, M., Jones, E., Casey, M., 2006. Turbidite channel reservoirs—key elements in facies prediction and effective development. Mar. Pet. Geol. 23, 821–841. http://dx.doi.org/10.1016/j.marpetgeo.2006.08.001.

Neev, D., Almagor, G., Arad, A., Ginzburg, A., Hall, J., 1976. The geology of the southeastern Mediterranean Sea. Geol. Survery Isr. 51.

Nelson, C.H., Escutia, C., Damuth, J.E., Twichell, D.C., 2011. Interplay of mass-transport and turbidite-system deposits in different active tectonic and passive continental margin Settings : external and local controlling factors. SEPM Spec. Publ. 39–66.

Netzeband, G.L., Hübscher, C.P., Gajewski, D., 2006. The structural evolution of the Messinian evaporites in the Levantine Basin. Mar. Geol. 230, 249–273. http://dx.doi.org/10.1016/j.margeo.2006.05.004.

Normark, W.R., Posamentier, H., Mutti, E., 1993. Turbidite systems: state of the art and future directions. Rev. Geophys. 31, 91. http://dx.doi.org/10.1029/93RG02832.

Peakall, J., McCaffrey, B., Kneller, B., 2000. A process model for the evolution, morphology, and architecture of sinuous submarine channels. J. Sediment. Res. 70, 434–448. http://dx.doi.org/10.1306/2DC4091C-0E47-11D7-8643000102C1865D.

Pratson, L., Imran, J., Parker, G., Syvitski, J., Hutton, E., 2000. AAPG Memoir 72/SEPM Special Publication No. 68, Chapter 6: Debris Flows Vs. Turbidity Currents: a Modeling Comparison of Their Dynamics and Deposits.

Robertson, A., 1998. Mesozoic-Tertiary tectonic evolution of the easternmost Mediterranean area: integration of marine and land evidence. Proc. Ocean. Drill. Program, Sci. results 160, 723–782.

Rohais, S., Granjeon, D., Robin, C., Richardeau, M.A., 2010. 3D stratigraphic modelling of the syn-rift and sag deposits in the Campos basin (Brazil): implication for its structural evolution. In: 18th International Sedimentological Congress.

Roveri, M., Flecker, R., Krijgsman, W., Lofi, J., Lugli, S., Manzi, V., Sierro, F.J., Bertini, A., Camerlenghi, A., De Lange, G., Govers, R., Hilgen, F.J., Hübscher, C., Meijer, P.T., Stoica, M., 2014. The Messinian Salinity Crisis: past and future of a great challenge for marine sciences. Mar. Geol. 352, 25–58. http://dx.doi.org/10.1016/j.margeo.2014.02.002.

Ryan, W.B.F., 1973. Geodynamic implications of the Messinian crisis of salinity. In: Messinian Events in the Mediterranean, pp. 26–38.

Ryan, W.B.F., 2009. Decoding the mediterranean salinity crisis. Sedimentology 56, 95–136. http://dx.doi.org/10.1111/j.1365-3091.2008.01031.x.

Ryan, W.B.F., Cita, M.B., 1978. The nature and distribution of Messinian erosional surfaces — indicators of a several-kilometer-deep Mediterranean in the Miocene. Mar. Geol. 27, 193–230. http://dx.doi.org/10.1016/0025-3227(78)90032-4.

Said, R., 1981. Introduction. In: The GEOLOGICAL EVOLUTION of the RIVER NILE. Springer New York, New York, NY, pp. 1–11. http://dx.doi.org/10.1007/978-1-4612-5841-4_1.

Schumm, S.A., 1977. The Fluvial System.

Schumm, S.A., 1986. Alluvial river response to active tectonics. Act. Tect. 80–94.

Segev, A., Rybakov, M., Lyakhovsky, V., Hofstetter, A., Tibor, G., Goldshmidt, V., Ben Avraham, Z., 2006. The structure, isostasy and gravity field of the Levant continental margin and the southeast Mediterranean area. Tectonophysics 425, 137–157. http://dx.doi.org/10.1016/j.tecto.2006.07.010.

Shanmugam, G., 1996. High-density turbidity currents: are they sandy debris Flows?: PERSPECTIVES. J. Sediment. Res. 66.

Steinberg, J., Gvirtzman, Z., Folkman, Y., Garfunkel, Z., 2011. Origin and nature of the rapid late Tertiary filling of the Levant Basin. Geology 39, 355–358. http://dx.doi.org/10.1130/G31615.1.

Tibor, G., Ben-Avraham, Z., Steckler, I.M., Fligelman, H., 1992. Late tertiary subsidence history of the southern levant margin, eastern mediterranean sea, and its implications to the understanding of the messinian event. J. Geophys. Res. 97614, 593–617. http://dx.doi.org/10.1029/92JB00978.

Tripsanas, E.K., Lee, E., Hack, W., Shipp, R.C., 2012. Architectural changes and preferential sand deposition in a confined channel–levee system forced to surmount a ridge crest efthymios. SEPM Spec. Publ. 269–277. http://dx.doi.org/10.2110/pec.12.99.0243.

Viana, A., Figueiredo, A., Faugères, J.-C., Lima, A., Gonthier, E., Brehme, I., Zaragosi, S., 2003. The Sao Tomé deep-sea turbidite system (southern Brazil Basin): cenozoic seismic stratigraphy and sedimentary processes. Am. Assoc. Pet. Geol. Bull. 87, 873–894. http://dx.doi.org/10.1306/12100201048.

Weimer, P., Slatt, R.M., Bouroullec, R., Fillon, R., Pettingill, H., Pranter, M., Tari, G., 2006. Introduction to the petroleum geology of deepwater setting. GSW Books. http://dx.doi.org/10.1306/St571314.

Wells, S.G., Bullard, T.F., Menges, C.M., Drake, P.G., Karas, P.A., Kelson, K.I., Ritter, J.B., Wesling, J.R., 1988. Regional variations in tectonic geomorphology along a segmented convergent plate boundary pacific coast of Costa Rica. Geomorphology 1, 239–265. http://dx.doi.org/10.1016/0169-555X(88)90016-5.

Chapter 5

Synthesis and Conclusions

Synthesis and Conclusions

Chapters 2-4 have contributed to the understanding of the (a) sedimentary processes involved in forming the Nile Delta/cone and the accretion of the eastern Mediterranean shelf during the late Cenozoic (b) mutual relationships of the delta and the Messinian salt giant, and (c) sediment distributary channels and their large-and local-scale interactions with the deforming evaporites. I presented my multiple-methods study of the Eastern Mediterranean basins including seismic stratigraphy, stratigraphic modeling, salt tectonic analysis, and bathymetric and submarine geomorphologic analyses. All these analyses were conducted within the unique setting of mutually affecting giant delta atop a salt giant; together, they have a large impact on the evolving basins of the Eastern Mediterranean.

Below, I first present and shortly summarize the highlights and the main contributions from each chapter. Then a list of conclusions is drawn.

The Nile Delta and the continental shelf of the Levant

The Nile Delta, one of the largest deltas in the world, is a globally unique feature controlling the sedimentary and morphologically of the Eastern Mediterranean. Numerous studies (e.g., Schumm, 1969; Salem, 1976; Summerhayes et al., 1978; Barber, 1981; Said, 1981; Sestini, 1989; Stanley, 1990, 1996; Stanley and Warne, 1993, 1998; Dolson et al., 2000; Gaullier et al., 2000; Loncke et al., 2002, 2006; Goudie, 2005; Mascle et al., 2006; Segev et al., 2006; Ducassou et al., 2008; Kellner et al., 2009; Macgregor, 2012; Abdelsalam, 2018; Be'eri-Shlevin et al., 2018) have focused on the evolution of this delta, its feeding river, the channels that distribute sediments into the deeper basins around the delta, and the evolution of the Levant continental shelf. The Nile River has been shown as the source of sediments not only of the delta, but also of the abyssal plains of the Eastern Mediterranean and the continental shelf of the Levant. The sediments from the Nile were transported alongshore and margin-parallel, within the Nile littoral cell, deposited eastward along the southern Levant shoreline and eventually progradated north forming the Levant continental shelf. The evolution of the Levant shelf began relatively late, 2-3 million years after the MSC (Ben-Zeev et al., 2019). Modeling the evolution of the Levant continental shelf indicates (Chapter 2) that only after the formation of a shallow submarine structural connection between the NDSF and the northern shoreline of the Sinai Peninsula due to margin-parallel sediment transport, sediments can begin accreting and initiating the continental shelf of the Levant. Due to the understanding that margin-parallel sediment transport is a strong depth-dependent process, initially, shales were transported and deposited to construct the shale base of the shelf. These shale basal units build up to forming a base for the shelf shallow enough (up to 50 m depth) so sandy sediments can be transported on, and eventually deposited to form the continental shelf of the Levant.

These insights from Chapter 2 contribute two fundamental understandings to the margin-parallel sediment transport and shelf formation:

(1) Alongshore sand transport is a part of a much broader process that is termed here margin-parallel sediment transport. Sand is transported in a nearshore shallow water belt where margin-parallel current energy is high. Shale transport occurs at greater depths over the deeper shelf and the continental slope. Shales are the first sediment to be transported and deposited to create a base on top of which later sandy sediments can be transported and form the sedimentary body and its internal structures observed today.

(2) The formation of the continental shelf of the Levant became possible only after a morpho-sedimentary connection was established between the NDSF and the

southern shores of Israel. We propose this as the reason for the 2-3 My delay observed in the shelf formation relative to the initial stages of the main deposition of the NDSF, almost immediately after the MSC.

Salt tectonics

Salt tectonics in the Eastern Mediterranean has been a highly researched topic by academics, gas and oil industries and different countries for many years (Neev et al., 1976; Ben-Avraham, 1978; Ryan and Cita, 1978; Said, 1981; Mart, 1982; Almagor and Hall, 1983; Almagor, 1984; Garfunkel and Almagor, 1984; Tibor et al., 1992; Gaullier et al., 2000; Gradmann et al., 2005; Frey Martinez et al., 2005; Loncke et al., 2006, 2009, 2010; Mascle et al., 2006; Netzeband et al., 2006; Hübscher et al., 2007, 2009; Cartwright and Jackson, 2008; Kellner et al., 2009; Cartwright et al., 2012; Gvirtzman et al., 2015, 2013). Many of these studies focused on local phenomenon and were site specific. Here, I focused on the broader region by asking what the main drivers of the regional patterns in salt tectonics are. Unlike the 'common knowledge' that the sedimentary load of the thick Nile deep sea fan squeezed out the underlying salt (Loncke et al., 2006, 2010; Netzeband et al., 2006; Cartwright et al., 2012; Gvirtzman et al., 2013, 2015), my results demonstrate that for most of its special extent, this load does not even overly the salt layer. Therefore, the load cannot be considered as the regional salt tectonic driving force. The only area, where such a squeeze-out mechanism works, is towards the Levant Basin. There, the relatively thick NDSF sediment overburden squeezes out the salt trapped in the Temsah valley (Chapter 3, Fig. 1). The rest of the deformation around the NDSF is driven by salt moving towards the deepest part of the basin by elevation-head gradient. I conclude that most probably, salt squeezing by differential loading was overestimated as the main driving force in the Eastern Mediterranean. This may have been the case in other salt basins as well as delta cones accumulate at margins of depositional basins and the thick-enough salt sequences most commonly form at their centers. This work also emphasizes the importance of high-accuracy separate mapping of the spatial distribution and thickness of the siliclastic and other sedimentary sequences and of the salt layers; only then can the regional driving forces be proposed or determined. The very long time I invested in such mapping and the final maps were highly beneficial in the understanding sediment thickness, salt tectonics, and the potential driving forces throughout the Eastern Mediterranean.

Submarine channel geomorphology response to salt tectonics

Submarine channels act as conduits of sediment into the deep basins all over continental margins. Such submarine channels are the main source-to-sink sediment conduits to the deep Eastern Mediterranean basins (e.g., Maldonado and Stanley, 1979; Peakall et al., 2000; Pratson et al., 2000; Gaullier et al., 2000; Bellaiche et al., 2001; Huguen, 2001; Loncke et al., 2002, 2006, 2009; Mayall et al., 2006; Ducassou et al., 2007, 2008, 2009, 2013; Garziglia et al., 2008; Kane et al., 2008; Yehoshua and Yossi, 2008; Gvirtzman et al., 2015). Due to active salt tectonics in this region over the past ~5 Ma, submarine channels have been affected by the salt tectonics (Almagor and Hall, 1983; Almagor, 1984; Garfunkel and Almagor, 1984; Garfunkel, 1984; Gradmann et al., 2005; Cartwright and Jackson, 2008; Cartwright et al., 2012; Gvirtzman et al., 2013, 2015). In order to express semi-quantitatively how seabed obstacles influence the morphology of submarine channels, I first used the common geomorphic/morphometric methods including changes of channel width, sinuosity, and slope in searching for a systematic relationship. In other words, the goal was to characterize how width, sinuosity, and slope of submarine channels change when facing obstacles formed and forming by salt tectonic on the sea floor; do these interactions form systematic patterns in the channel morphology.

These classic analyses did not produce a systematic rule for the local interactions of channels and obstacles. I have shown, however, that at the wider-scale of the entire length of the channels, there is a substantial effect of the obstacles on the direction of the submarine channels and they are deflected from the direction of the regional slope. I incorporated a new morphometric analysis that quantifies how and when the channel flow direction is diverted by salt tectonics (Chapter 4). These results can be applied for the entire Eastern Mediterranean and elsewhere in the world. This contribution can assist in detecting courses and in determining deviations of buried paleo-channels that are important targets for sediment conduits and exploration in the gas and oil industry.

Contributing to the evolution of the post-Messinian Eastern Mediterranean

This dissertation displays a geologic evolution that focuses on a unique opportunity where an evolving basin comprises of a giant delta atop a salt giant. The three previous chapters show how sedimentation and salt tectonics are two processes in the geological record that have a mutual effect on each other and on the evolving basin they both lay in, and that effect leaves its morphological mark on the present-day bathymetry. A deeper understanding of the broader process termed margin-parallel sediment transport and the evolution of the Levant continental shelf in the past 5 My enables the deeper understanding of the main sedimentary features that evolved in this geologic time. Likewise, the discovery and the disproof of common approaches enabled a deeper understanding and clarification of the existing driving forces that form the present-day morphology. Finally, the innovation of a new method was invented when no existing method could describe the morphological effect that salt tectonic obstacles have on submarine channels. All these discovery's and inventions demonstrate that by using many different disciplines of geological research it is possible to piece together different parts of the geological history and understand the relation and affect a salt giant and a giant delta have on each other and on an evolving geologic region. This study contributes to the creation of a regional synthesis demonstrating mutual sedimentation and salt tectonics impacts and assists in understanding the evolution of the Eastern Mediterranean since the Messinian salinity crisis.

Conclusions

The main conclusions of this thesis are:

(1) The margin-parallel sediment transport has a great impact and is crucial for the evolution of the Levant continental margin. The process of margin-parallel currents first transporting shaly sediments to create a marginal foot for sandy sediments to be transported and deposited on. In time, this builds a continental shelf connection that enables the formation of the Levant continental shelf.

(2) In the Eastern Mediterranean the forces that govern salt tectonics are two: in the Levant salt tectonics is governed by differential loading whereas towards the Herodotus Basin salt tectonics is governed by elevation gradient. This conclusion proves that previous studies of salt tectonics in this region have overestimated the role of salt squeezing compared to tilting and gliding.

(3) Measuring the impact of tectonics on the basin-scale morphology of the submarine channels that exist within can be done only by the new method I have proposed. In order to do so, two new geomorphic parameters, termed Channel Diversion and Incident Angle, were developed. These new

parameters determine (a) whether a submarine channel is morphologically affected upon encountering obstacles, (b) how this channel morphology is affected by the tectonic obstacle in a regional point of view, and (c) which other parameters affect these observations. In the Levant Basin, submarine channels that encounter obstacles on a near parallel or near perpendicular angle on average, are mildly or not diverted. On contrary, if this channel-obstacle incident occurs on a ~45° angle, the channel will be highly diverted.

References

Abdelsalam, M.G., 2018, The Nile's journey through space and time: A geological perspective: Earth-Science Reviews, v. 177, p. 742–773, doi:10.1016/J.EARSCIREV.2018.01.010.

Almagor, G., 1984, Salt-controlled slumping on the Mediterranean slope of central Israel: Marine Geophysical Researches, v. 6, p. 227–243, doi:10.1007/BF00286527.

Almagor, G., and Hall, J.K., 1983, Morphology of the continental margin off north central Israel: Israel Journal of Earth Sciences, v. 32, p. 75–82.

Barber, P.M., 1981, Messinian subaerial erosion of the proto-Nile Delta: Marine Geology, v. 44, p. 253–272, doi:10.1016/0025-3227(81)90053-0.

Be'eri-Shlevin, Y., Avigad, D., and Gerdes, A., 2018, The White Nile as a source for Nile sediments: Assessment using U-Pb geochronology of detrital rutile and monazite: Journal of African Earth Sciences, v. 140, p. 1–8, doi:10.1016/J.JAFREARSCI.2017.12.032.

Bellaiche, G., Loncke, L., Gaullier, V., Mascle, J., Courp, T., Moreau, A., Radan, S., and Sardou, O., 2001, The Nile Cone and its channel system: New results after the Fanil cruise: Comptes Rendus de l'Academie de Sciences - Serie IIa:

Sciences de la Terre et des Planetes, v. 333, p. 399–404, doi:10.1016/S1251-8050(01)01645-7.

Ben-Avraham, Z., 1978, The structure and tectonic setting of the levant continental margin, Eastern Mediterranean: Tectonophysics, v. 46, p. 313–331, doi:10.1016/0040-1951(78)90210-X.

Cartwright, J.A., and Jackson, M.P.A., 2008, Initiation of gravitational collapse of an evaporite basin margin: The Messinian saline giant, Levant Basin, eastern Mediterranean: Geological Society of America Bulletin, v. 120, p. 399–413, doi:10.1130/B26081X.1.

Cartwright, J., Jackson, M.P.A., Dooley, T., and Higgins, S., 2012, Strain partitioning in gravity-driven shortening of a thick, multilayered evaporite sequence: Geological Society, London, Special Publications, v. 363, p. 449–470, doi:10.1144/SP363.21.

Dolson, J.C., Shann, M. V, Hammouda, D.H., Rashed, R., and Matbouly, D.S., 2000, THE PETROLEUM POTENTIAL OF EGYPT, *in* Second Wallace E. Pratt memorial Conference on Petroleum Provinces of the 21st Century, p. 37, http://archives.datapages.com/data/bulletns/1999/12dec/2033/images/dolson.pdf.

Ducassou, E., Capotondi, L., Murat, A., Bernasconi, S.M., Mulder, T., Gonthier, E., Migeon, S., Duprat, J., Giraudeau, J., and Mascle, J., 2007, Multiproxy Late Quaternary stratigraphy of the Nile deep-sea turbidite system — Towards a chronology of deep-sea terrigeneous systems: Sedimentary Geology, v. 200, p. 1–13, doi:10.1016/j.sedgeo.2007.01.023.

Ducassou, E., Migeon, S., Capotondi, L., and Mascle, J., 2013, Run-out distance and erosion of debris-flows in the Nile deep-sea fan system: Evidence from lithofacies and micropalaeontological analyses: Marine and Petroleum Geology, v. 39, p. 102–123, doi:10.1016/j.marpetgeo.2012.09.006.

Ducassou, E., Migeon, S., Mulder, T., Murat, A., Capotondi, L., Bernasconi, S.M., and Mascle, J., 2009, Evolution of the Nile deep-sea turbidite system during the Late Quaternary: influence of climate change on fan sedimentation: Sedimentology, v. 56, p. 2061–2090, doi:10.1111/j.1365-3091.2009.01070.x.

Ducassou, E., Mulder, T., Migeon, S., Gonthier, E., Murat, A., Revel, M., Capotondi, L., Bernasconi, S.M., Mascle, J., and Zaragosi, S., 2008, Nile floods recorded in deep Mediterranean sediments: Quaternary Research, v. 70, p. 382–391, doi:10.1016/j.yqres.2008.02.011.

Frey Martinez, J., Cartwright, J., and Hall, B., 2005, 3D seismic interpretation of slump complexes: examples from the continental margin of Israel: Basin Research, v. 17, p. 83–108, doi:10.1111/j.1365-2117.2005.00255.x.

Garfunkel, Z., 1984, Large-scale submarine rotational slumps and growth faults in the Eastern Mediterranean: Marine Geology, v. 55, p. 305–324, doi:10.1016/0025-3227(84)90074-4.

Garfunkel, Z., and Almagor, G., 1984, Geology and structure of the continental margin off northern Israel and the adjacent part of the Levantine Basin: Marine Geology, v. 62, p. 105–131, doi:10.1016/0025-3227(84)90057-4.

Garziglia, S., Migeon, S., Ducassou, E., Loncke, L., and Mascle, J., 2008, Mass-transport deposits on the Rosetta province (NW Nile deep-sea turbidite system, Egyptian margin): Characteristics, distribution, and potential causal processes: Marine Geology, v. 250, p. 180–198, doi:10.1016/j.margeo.2008.01.016.

Gaullier, V., Mart, Y., Bellaiche, G., Mascle, J., Vendeville, B.C., and Zitter, T., 2000, Salt tectonics in and around the Nile deep-sea fan: insights from the PRISMED II cruise: Geological Society, London, Special Publications, v. 174, p. 111–129, doi:10.1144/GSL.SP.1999.174.01.07.

Goudie, A.S., 2005, The drainage of Africa since the Cretaceous: Geomorphology, v. 67, p. 437–456, doi:10.1016/j.geomorph.2004.11.008.

Gradmann, S., Hübscher, C., Ben-Avraham, Z., Gajewski, D., and Netzeband, G., 2005, Salt tectonics off northern Israel: Marine and Petroleum Geology, v. 22, p. 597–611, doi:10.1016/j.marpetgeo.2005.02.001.

Gvirtzman, Z., Reshef, M., Buch-Leviatan, O., and Ben-Avraham, Z., 2013, Intense salt deformation in the Levant Basin in the middle of the Messinian Salinity Crisis: Earth and Planetary Science Letters, v. 379, p. 108–119, doi:10.1016/j.epsl.2013.07.018.

Gvirtzman, Z., Reshef, M., Buch-Leviatan, O., Groves-Gidney, G., Karcz, Z., Makovsky, Y., and Ben-Avraham, Z., 2015, Bathymetry of the Levant basin: interaction of salt-tectonics and surficial mass movements: Marine Geology, v. 360, p. 25–39, doi:10.1016/j.margeo.2014.12.001.

Hübscher, C., Cartwright, J., Cypionka, H., DeLange, G.J., Robertson, A., Suc, J.-P., and Urai, J.L., 2007, Global look at salt giants: Eos, Transactions American Geophysical Union, v. 88, p. 177–179, doi:10.1029/2007EO160002.

Hübscher, C., Tahchi, E., Klaucke, I., Maillard, A., and Sahling, H., 2009, Salt tectonics and mud volcanism in the Latakia and Cyprus Basins, eastern Mediterranean: Tectonophysics, v. 470, p. 173–182, doi:10.1016/J.TECTO.2008.08.019.

Huguen, C., 2001, Déformation récente à actuelle et argilo-cinèse associée au sein de la Ride Méditerranéenne (Méditerranée orientale):, http://www.theses.fr/2001PA066439 (accessed November 2016).

Kane, I.A., McCaffrey, W.D., and Peakall, J., 2008, Controls on sinuosity evolution within submarine channels: Geology, v. 36, p. 287, doi:10.1130/G24588A.1.

Kellner, A., Khawaga, H. El, Brink, G., Brink-larsen, S., Hesham, M., Abu, H., Saad, E., Atef, A., Young, H., and Finlayson, B., 2009, Depositional History of the West Nile Delta – Upper Oligocene to Upper Pliocene, *in* AAPG International Conference and Exhibition, Cape Town, South Africa, v. 30092.

Loncke, L., Droz, L., Ducassou, E., Migeon, S., Mascle, J., Gaullier, V., Droz, L., Ducassou, E., Migeon, S., and Mascle, J., 2009, Multi-scale slope instabilities along the Nile deep-sea fan, Egyptian margin: A general overview: Marine and Petroleum Geology, v. 26, p. 633–646, doi:10.1016/j.marpetgeo.2008.03.010.

Loncke, L., Gaullier, V., Bellaiche, G., and Mascle, J., 2002, Recent depositional Patterns of the Nile deep-sea fan from Echo-character Mapping: AAPG Bulletin, v. 86.

Loncke, L., Gaullier, V., Mascle, J., Vendeville, B., and Camera, L., 2006, The Nile deep-sea fan: An example of interacting sedimentation, salt tectonics, and inherited subsalt paleotopographic features: Marine and Petroleum Geology, v. 23, p. 297–315, doi:10.1016/j.marpetgeo.2006.01.001.

Loncke, L., Vendeville, B.C., Gaullier, V., and Mascle, J., 2010, Respective contributions of tectonic and gravity-driven processes on the structural pattern in the Eastern Nile deep-sea fan: insights from physical experiments: Basin Research, v. 22, p. 765–782, doi:10.1111/j.1365-2117.2009.00436.x.

Macgregor, D.S., 2012, The development of the Nile drainage system: integration of onshore and offshore evidence: Petroleum Geoscience, v. 18, p. 417–431, doi:10.1144/petgeo2011-074.

Maldonado, A., and Stanley, D.J., 1979, DEPOSITIONAL PATTERNS AND LATE QUATERNARY EVOLUTION OF TWO MEDITERRANEAN SUBMARINE FANS: A COMPARISON: Marine Geology, v. 31, p. 215–250.

Mart, Y., 1982, Quaternary tectonic patterns along the continental margin of the southeastern Mediterranean: Marine Geology, v. 49, p. 327–344, doi:10.1016/0025-3227(82)90047-0.

Mascle, J., Sardou, O., Loncke, L., Migeon, S., Caméra, L., and Gaullier, V., 2006, Morphostructure of the Egyptian Continental Margin: Insights from Swath Bathymetry Surveys: Marine Geophysical Researches, v. 27, p. 49–59, doi:10.1007/s11001-005-1559-x.

Mayall, M., Jones, E., and Casey, M., 2006, Turbidite channel reservoirs—Key elements in facies prediction and effective development: Marine and Petroleum Geology, v. 23, p. 821–841, doi:10.1016/j.marpetgeo.2006.08.001.

Neev, D., Almagor, G., Arad, A., Ginzburg, A., and Hall, J., 1976, The geology of the southeastern Mediterranean Sea: Geological Survery of Israel, p. 51, http://www.getcited.org/pub/101826857.

Netzeband, G.L., Hübscher, C.P., and Gajewski, D., 2006, The structural evolution of the Messinian evaporites in the Levantine Basin: Marine Geology, v. 230, p. 249–273, doi:10.1016/j.margeo.2006.05.004.

Peakall, J., McCaffrey, B., and Kneller, B., 2000, A Process Model for the Evolution, Morphology, and Architecture of Sinuous Submarine Channels: Journal of

Sedimentary Research, v. 70, p. 434–448, doi:10.1306/2DC4091C-0E47-11D7-8643000102C1865D.

Pratson, L., Imran, J., Parker, G., Syvitski, J., and Hutton, E., 2000, AAPG Memoir 72/SEPM Special Publication No. 68, Chapter 6: Debris Flows vs. Turbidity Currents: a Modeling Comparison of Their Dynamics and Deposits:, http://archives.datapages.com/data/specpubs/memoir72/ch06/mem72ch06.htm.

Ryan, W.B.F., and Cita, M.B., 1978, The nature and distribution of Messinian erosional surfaces — Indicators of a several-kilometer-deep Mediterranean in the Miocene: Marine Geology, v. 27, p. 193–230, doi:10.1016/0025-3227(78)90032-4.

Said, R., 1981, The Geological Evolution of the River Nile: New York, NY, Springer Science & Business Media, 153 p., doi:10.1007/978-1-4612-5841-4_1.

Salem, R., 1976, Evolution of Eocene-Miocene Sedimentation Patterns in Parts of Northern Egypt: AAPG Bulletin, v. 60, p. 34–64, http://archives.datapages.com/data/bulletns/1974-76/data/pg/0060/0001/0000/0034.htm (accessed September 2015).

Schumm, S.A., 1969, River metamorphosis: Journal of the Hydraulics Division, American Society of Civil Engineers, v. 95, p. 255–273.

Segev, A., Rybakov, M., Lyakhovsky, V., Hofstetter, A., Tibor, G., Goldshmidt, V., and Ben Avraham, Z., 2006, The structure, isostasy and gravity field of the Levant continental margin and the southeast Mediterranean area: Tectonophysics, v. 425, p. 137–157, doi:10.1016/J.TECTO.2006.07.010.

Sestini, G., 1989, Nile Delta: a review of depositional environments and geological history: Geological Society, London, Special Publications, v. 41, p. 99–127, doi:10.1144/GSL.SP.1989.041.01.09.

Stanley, D.J., 1996, Nile delta: extreme case of sediment entrapment on a delta plain and consequent coastal land loss: Marine Geology, v. 129, p. 189–195, doi:10.1016/0025-3227(96)83344-5.

Stanley, D.J., 1990, Recent subsidence and northeast tilting of the Nile delta, Egypt: Marine Geology, v. 94, p. 147–154, doi:10.1016/0025-3227(90)90108-V.

Stanley, D.J., and Warne, A.G., 1993, Nile delta: recent geological evolution and human impact.: Science (New York, N.Y.), v. 260, p. 628–34, doi:10.1126/science.260.5108.628.

Stanley, D.J., and Warne, A.G., 1998, Nile Delta in Its Destruction Phase: Journal of Coastal Research, v. 14, p. 794–825, http://www.jstor.org/stable/4298835.

Summerhayes, C.P., Sestini, G., Misdorp, R., and Marks, N., 1978, Nile Delta: Nature and evolution of continental shelf sediments: Marine Geology, v. 27, p. 43–65, doi:10.1016/0025-3227(78)90073-7.

Tibor, G., Ben-Avraham, Z., Steckler, M., and Fligelman, H., 1992, Late Tertiary subsidence history of the southern Levant Margin, eastern Mediterranean Sea, and its implications to the understanding of the Messinian Event: Journal of Geophysical Research, v. 97, p. 17593, doi:10.1029/92JB00978.

Yehoshua, F., and Yossi, M., 2008, Newly recognized eastern extension of the Nile deep-sea fan: Geology, v. 36, p. 939– 942., doi:10.1130/G24995A.1.

הדלתא אינם ממוקמים על גבי ענק המלח, אלא בעיקר בשוליו, באזורים בהם המלח דק יחסית (>200 m). המסקנה הראשונית של ממצא זה היא שסחיטה של מעט המלח הזה, אינה יכולה להסביר את הדגם הסמי-רדיאלי של מערכת הקמטים האזורית. רק באזור המזרחי ביותר של הדלתא הפונה לאגן הלבנט, מודל סחיטת המלח נמצא מתאים. באזור זה, ישנה שכבת מלח עבה המכוסה בסלעים שעוביים משתנה לטרלית והמלח נע מאזור בו הוא נתון בלחץ גבוה לאזור סמוך בו הוא נתון בלחץ נמוך יותר, אפילו כאשר הזרם נאלץ לטפס כלפי מעלה. מודל זה של סחיטת מלח כתוצאה מהפרשי לחצים הינו יוצא מן הכלל ומוגבל לצד המזרחי של הדלתא. בצידה השני של הדלתא זרימת מלח מונעת על ידי הפרשי גבהים סטרוקטורליים, היינו מלח זורם ממקום גבוה (קרבת הדלתא) לאזור הנמוך ביותר במרחב (אגן הרודוטוס).

לאחר הבנת המניע לטקטוניקת מלח, המחקר עבר לעסוק בהשפעה של מכשולים בקרקעית הים (בעיקר קמטי טקטוניקת מלח) על מסלול הזרימה של תעלות טורבידיטיות רצנטיות. התעלות התת-ימיות שנחקרו נמצאות במורדות המזרחיים של מניפת הנילוס לכיוון אגן הלבנט. כדי לכמת את האופן בו תעלה תת-ימית מגיבה למכשול, תחילה מדדתי לאורך מסלול זרימת התעלות פרמטרים מורפומטריים קלאסיים כגון: פיתוליות, רוחב ושיפוע, אבל התוצאות לא הניבו מסקנות ברורות ועקביות. בשלב שני פיתחתי שני פרמטרים המייצגים את ההסטה המצטברת של תעלות בעקבות מפגש עם מכשולים רבים בדרכם. שני הפרמטרים הללו הם זווית הפגיעה אלפא, שמוגדרת כזווית החדה שבין התעלה לסטרייק של המכשול; וזווית ההסטה אומגה, שהינה הזוית שבין כיוון השיפוע האזורי של קרקעית הים (כיוון הזרימה הצפוי ללא הסטה) ובין כיוון הזרימה בפועל. התוצאות מראות שכאשר תעלה פוגשת מכשולים שכיוונם תת-מקביל או תת-ניצב לכיוון התעלה, לא תתרחש הסטה מכיוון שהתעלות לא פוגשות מכשולים או חוצות אותם ישירות. כשהמפגש בין התעלה למכשולים הוא אלכסוני, התעלות מוסטות במצטבר בערך בכ-10° ולאורך מרחקים גדולים הסטה זו משפיעה מאוד על דגם ניקוז התעלות. צורת הניתוח הזו, המשתמשת בפרמטרים החדשים שהוגדרו בעבודה זו, יכולה לסייע בהבנת דגמי ניקוז תת ימיים באגנים אחרים בעולם ובפרט כאלה הנתונים להשפעת טקטוניקה פעילה.

סינתיזה של שלושת חלקי העבודה משפרת את ההבנה של התפתחות החתך הסדימנטרי הפליו-רביעוני במזרח הים התיכון בשלושה אספקטים: א) מנגנוני הובלת סדימנטים שיוצרים דלתאות ומדפי יבשת. ב) הכוחות המניעים את מעוות המלח. ג) השפעת מעוות המלח על הכיסוי הסדימנטרי שמעליו ועל דגם הובלת סדימנטים על גבי קרקעית הים.

תקציר

מתחת לקרקעית הים התיכון מונח לו אחד מענקי המלח הגדולים בכדור הארץ, שהושקע בזמן משבר המליחות המסיני (5.97-5.3 Ma), שהתרחש בסוף המיוקן. מאז הצטברותו, ענק המלח המסיני הולך ונקבר על ידי סדימנטים, אך עדיין בהשוואה לענקי מלח אחרים בעולם, הוא צעיר ורדוד יחסית. נסיבות אלו הפכו את הים התיכון לאזור מועדף לחקר השלב המוקדם של מעוות אגני מלח, שהינו קשה לשחזור באגנים בהם המלח עמוק ומאוד מעוות.

המחקר שלי מתמקד במזרח הים התיכון ובפרט באגן הלבנט, מול חופי ישראל. המטרה היא לחקור את התפתחות האגן במהלך חמישה מיליון השנים האחרונות כדי להבין שלושה תהליכים טקטונו-סטרטיגרפיים: התפתחות מדף יבשת (לבנט) בסמוך לדלתת נהר (נילוס); היחס בין דלתת ענק (נילוס) לבין ענק מלח (המסיני) השוכן תחתיה; השפעת מכשולים שנוצרים בקרקעית הים בגלל טקטוניקת מלח על תעלות טורבידיטיות תת-ימיות. המצב הייחודי של אזור המחקר המכיל ענק מלח, דלתת ענק ומדף יבשת רחוק מאות קילומטרים מהדלתא אך עדין מוזן ממנה, מספק הזדמנות להבין תהליכי יסוד שהינם חשובים גלובלית.

כדי לחקור את בניית מדף היבשת הלבנטיני לצד דלתת הנילוס, השתמשתי בתוכנת סימולציה סטרטיגרפית תלת-מימדית (DionisosFlow) בעלת רכיב חדש שתוכנת במיוחד למחקר זה. אני בוחן מחדש את הפרדיגמה המקובלת בנושא הובלת סדימנטים והקשר דלתא-מדף ומראה כי הובלת חול צמודת חוף הינה חלק קטן ממערכת גדולה יותר אשר קראתי לה פה הובלת סדימנטים מקבילת שולי יבשת. בעבודתי זו אני מבסס מושג זה ומבהיר את רכיביו. חול מובל בצמוד לחוף ברצועה צרה ורדודה איפה שהזרמים הימיים בעלי אנרגיה גבוהה. בו זמנית חרסיות מובלות בעומק על המדף ומעבר לו במדרון העמוק, מקום בו הזרמים בעלי אנרגיה נמוכה יחסית. תוצאות המודל מדגישות שללא זרמים מקבילי יבשת המובילים חרסית וסילט בעומק, השקעת סדימנטים אל מול חופי ישראל ככל הנראה הייתה זניחה ומדף הלבנט לא היה נבנה. יתר על כן, למרות שהובלה מקבילת שוליים מתרחשת בו זמנית ליצירת דלתת הנילוס, התפתחות מדף היבשת הלבנטיני התרחשה ברובה רק לאחר 2-3 מליוני שנה. קודם מדף יבשת נבנה אל מול חופי סיני, לאחר מכן מול חופי ישראל, ורק לאחרונה לאורך חופי לבנון. המודל גם מדגים את ההשתנות הליתולוגית החריפה בין סדימנטציה אל מול שפך נחל וסדימנטציה מקבילת מדרון יבשת. הובלת סדימנטים במורד המדרון אשר מאופיינת באנרגיה גבוהה משקיעה תערובת של חול, סילט וחרסית. לעומת זאת, הובלה מקבילת מדרון, אשר מאופיינת באנרגיה נמוכה, משקיעה בעיקר חרסית וסילט. יוצא מן הכלל היא ההובלה צמודת החוף, שלמרות שהינה מקבילת שוליים היא מאופיינת באנרגיה גבוהה, המסיעה בעיקר חולות. מעניינת במיוחד היא המסקנה שהובלה מקבילת מדרון הינו תהליך יעיל של מיון בין חול לחרסית. תוצאות המודל תורמות להבנה הבסיסית של תהליכי הובלת סדימנט, הפצתם והשקעתם לאורך מדרוני יבשות ובפרט לקשר שבין דלתאות ומדפי יבשות סמוכים.

חלק שני של המחקר עוסק בקשר בין דלתת הנילוס לטקטוניקת המלח היוצרת את מערכת הקמטים הסובבת נילוס. עד היום מקובל היה לחשוב, שמערכת הקמטים הסובבת נילוס הינה תולדה של "סחיטת" מלח החוצה בצורה סמי-רדיאלית ממתחת לדלתא העבה. לאחר איסוף נתונים רבים על עובי הכיסוי הסדימנטרי שמעל המלח, בניתי מפת עובי של הכיסוי בשטח שבין חופי הלבנט ועד לאגן הרודוטוס ובין מצריים וטורקיה-יוון. מפה זו מגלה כי האזורים העבים ביותר של

המכון הגיאולוגי
משרד האנרגיה

ההתפתחות הטקטונו-סטרטגרפית של מזרח הים התיכון לאחר האירוע המסיני: דלתת ענק על ענק מלח

אלחנן צוקר

חיבור לשם קבלת תואר "דוקטור לפילוסופיה" הוגש לסנט האוניברסיטה העברית בירושלים

עבודה זו נעשתה בהדרכתם של:

פרופ' זהר גבירצמן, המכון הגיאולוגי לישראל

פרופ' יהודה אנזל, האוניברסיטה העברית בירושלים

דוח מס' GSI/15/2023

דצמבר 2023